Some Investigations on Performance Evaluation of Compact Circularly Polarized Antennas for 5G Wireless Applications

Submitted in partial fulfilment of the requirements

for the award of the degree of

Doctor of Philosophy

by

Ravikanti Swetha

(Roll No. 716141)

Supervisor

Dr. L. Anjaneyulu

Professor

DEPARTMENT OF ELECTRONICS AND COMMUNICATION ENGINEERING

NATIONAL INSTITUTE OF TECHNOLOGY

WARANGAL – 506004, INDIA.

December 2021

APPROVAL SHEET

This Thesis entitled **"SOME INVESTIGATIONS ON PERFORMANCE EVALUATION OF COMPACT CIRCULARLY POLARIZED ANTENNAS FOR 5G WIRELESS APPLICATIONS"** by **RAVIKANTI SWETHA** is approved for the degree of **Doctor of Philosophy.**

Examiners

Supervisor

Dr. L. Anjaneyulu
Professor, ECE Dept., NIT WARANGAL

Chairman

Prof.C.B.Rama Rao
Professor, ECE
Dept., NIT WARANGAL

Date: 3-12-2021

DECLARATION

I hereby declare that the matter embodied in this thesis entitled "**SOME INVESTIGATIONS ON PERFORMANCE EVALUATION OF COMPACT CIRCULARLY POLARIZED ANTENNAS FOR 5G WIRELESS APPLICATIONS**" is based entirely on the results of the investigations and research work carried out by me under the supervision of **Dr. L. Anjaneyulu**, Professor, Department of Electronics and Communication Engineering, National Institute of Technology Warangal, India. I declare that this work is original and has not been submitted in part or full, for any degree or diploma to this or any other University. and was not submitted elsewhere for the award of any degree.

I declare that this written submission represents my ideas in my own words and where others ideas or words have been included, I have adequately cited and referenced the original sources. I also declare that I have adhered to all principles of academic honesty and integrity and have not misrepresented or fabricated or falsified any idea/date/fact/source in my submission. I understand that any violation of the above will be cause for disciplinary action by the institute and can also evoke penal action from the sources which have thus not been properly cited or from whom proper permission has not been taken when needed.

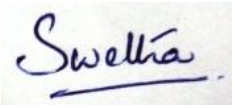

(Ravikanti Swetha)

(Roll No. 716141)

Date: 3-12-2021

Place: Warangal

National Institute of Technology, Warangal

(Deemed University)

CERTIFICATE

This is to certify that the thesis entitled "**SOME INVESTIGATIONS ON PERFORMANCE EVALUATION OF COMPACT CIRCULARLY POLARIZED ANTENNAS FOR 5G WIRELESS APPLICATIONS**" being submitted by **Mrs. Ravikanti Swetha** in partial fulfilment for the award of the degree of *Doctor of Philosophy in Department of Electronics and Communication Engineering* of National Institute of Technology Warangal, is a record of bonafide research work carried out by her under my supervision. To the best of our knowledge, the work incorporated in this thesis has not been submitted elsewhere for the award of any degree.

Dr. L. Anjaneyulu,
(Supervisor)
Dept. of Electronics & Communication Engineering,
National Institute of Technology,
Warangal – 506004, India.

Dedicated to

My Guru and my beloved Husband

ACKNOWLEDGEMENTS

It gives me immense pleasure to express my deep sense of gratitude and sincere thanks to my supervisor and mentor, **Dr.L.Anjaneyulu**, Professor, Department of Electronics & Communication Engineering, National Institute of Technology, Warangal, for his perpetual encouragement, invaluable guidance, and suggestions. His steady influence throughout my Ph.D. career has oriented me in a proper direction and supported me with promptness and care. His knowledge, logical and thought-provoking advice, and discussions both technically and morally helped me to become a capable researcher. He not only gave me the required knowledge to pursue my research through the subjects he taught but also always gave the required moral support during my hard times. He inculcated in me a never-ending motivation and zeal towards my research efforts, as well as encouraged my presentation skills regularly. His encouragement helped me to overcome the difficulties encountered in my research as well as in my personal life.

I wish to express my thanks to **Prof.C.B.Rama Rao** as chairman of the DSC for his kind support. I would like to thank **Prof. N.V.S.N Sharma,** one of my doctoral Scrutiny Committee members, for sharing his extensive experience in Antenna, RF/microwave design and his invaluable assistance in academic work and extend my thanks to **Dr. D. Vakula,** Associate Professor, one of my Doctoral Scrutiny Committee member, for her valuable suggestions throughout my semester presentations. I would like to thank **Dr.Arun Kumar**, one of my doctoral Scrutiny Committee members, for his valuable suggestions throughout my research.

I take this privilege to thank my external Doctoral Scrutiny Committee member, **Prof. D. Srinivasacharya**, Professor of Mathematics Department, for his detailed review, constructive suggestions, and excellent advice during the progress of this research work.

I am thankful to **Dr. T. Kishore Kumar**, former Head, Dept. of E.C.E., for his help and cooperation. I thank all the faculty and non-teaching staff of the Dept. of ECE, especially

Microwave lab assistant T. Venkateshwarluat NIT Warangal, who helped me during the research period.

I thank my nation India, for giving me the opportunity to carry out my research work at the NIT Warangal. A special thanks to **MHRD** for its financial support. I wish to express my sincere thanks to **Prof. N.V. Ramana Rao**, Director, NIT Warangal, for his official support and encouragement.

I want to mention my sincere and special thanks to **Mr. Rakesh Kumar Singh**, Scientist 'E'RCI, DRDO, Hyderabad, and his team of Antenna wing for his continuous support that has helped me so much during this period. Also, I would like to extend my thanks to the team of Cosmic Enterprises, Hyderabad, for supporting the fabrication of Patch antennas.

I take this opportunity to convey my regards to my closest friends for always being next to me. Thanks to Dr. T.Venu Madav, Dr.Ch.Sulakshana, Dr.D.Kiran, Dr.R.Sahoo, Dr.Rahul Singha, Dr.N.Suman, Dr.B.pranitha, M.Sandhya, D.Srinivas, Department of Electronics and Communication Engineering, for their constant motivation throughout the work. With all your support and encouragement, my study life has become happy in all respects!

I acknowledge my gratitude to all my teachers and colleagues at various places for supporting and cooperating with me to complete the work. I'm very grateful to my mother, Anasurya, and father Venkatesham for successfully carrying out my research work.

Finally, I render my respect and acknowledge my biggest debt to my mother-in-law K. Annapurna, who wished to see me as Dr. Swetha, my father-in-law, and my loving sisters-in-law for giving me mental support and inspiration. They have motivated and helped me to complete my research work successfully.

I would like to thank my beloved son’s advait and nixith for their support. Last but not least, I am very much grateful to my dear husband, K.Vinay Kumar, for his support,

encouragement, understanding, and sacrifices, which helped and motivated me a lot throughout the time of my research. I could not have done it without you.

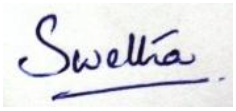

Ravikanti Swetha

ABSTRACT

The evolution of four generations of technology brought enormous changes and growth in the wireless communication system. To overcome the shortcomings of 4Gwireless communication, a new generation is evolved as a 5G wireless communication system. It is expected to fulfill better reliability, better connectivity, lower latency, higher data rate, and better quality. Wideband antenna elements with excellent frequency and time domain characteristics are essential to ensure high-speed, reliable data and video transmission. Therefore, developing low-profile antennas satisfying all the above characteristics simultaneously is a burning topic of current research in microwave techniques, antennas, and radar systems.

The compact microstrip circularly polarized antenna for 5G wireless communication is in high demand since the advances in semiconductor technology for wireless technology have led to a reduction in cost. Federal Communications Commission (FCC) adopted a new regulation in the 5GHz band, with an additional 400 MHz band, which resulted in a standard IEEE 802.11ac for 5G WLAN (Wireless Local Network application).

The 5G wireless communication system adopts wireless services and employs multiple antenna systems. To offer more services, size, cost and complexity play a major role in the 5G wireless communication system. Hence there is a need for adaptability and versatile subsystems that have a broad bandwidth that supports multiple frequency bands. To fulfill some of the needs of these systems and provide a cost-effective solution, a single circularly polarized antenna with possible techniques loaded on its aperture is essential. Hence, we propose the best possible solution of using circularly polarized antennas for 5G wireless communication due to its flexibility in basic electrical and radiating properties.

The key idea of the research work is to focus on developing compact broadband circularly polarized antennas with less complex design and compact size. Circularly polarized antennas are preferred over linearly polarized antennas because irrespective of positioning of antennas, data transmission takes place, and limitations of the use of such technology have been investigated. Four different novel designs of circularly polarized antennas are proposed to be suitable candidates for different 5G wireless applications.

1. A Compact microstrip antenna loaded with asymmetric slits to achieve circular polarization.
2. A new method of exciting the basic square patch with a hook-shaped aperture stacked upon a copper plate with the support of foam achieved a 20dB cross-polarization level.
3. A novel way of designing a triple-band antenna with simple asymmetric circular patches and a superstrate technique to improve the characteristics of the designed antenna.
4. A new prototype is designed to investigate the performance characteristics of the circularly polarized antenna with frequency selective structure as the superstrate.

At first, the prototype antenna models, Method of the moment, and Finite element method are used to fully characterize the functionality and characteristics of the proposed antenna technology through electromagnetic simulations performed using IE3D(Integral equation three-dimensional) and HFSS (High-frequency structure simulator)software. A complete investigation and performance of the proposed antennas are conducted through experimental field measurements that are verified with simulations.

The proposed antennas offer compactness, and constraint size is maintained. The maximum axial ratio bandwidth for circularly polarized antennas is 50%, and a gain of 8dBic are achieved. The proposed antennas are best suitable for WiMAX (Worldwide Interoperability for microwave access), WLAN, C-band, WI-FI (wireless fidelity) and mobile applications, etc. The proposed circularly polarized microstrip antennas can be used for a modern communication system, vehicular applications, air traffic control, defense tracking, modern radars, remote sensing, and WPAN (wireless personal area network), which falls under X-band application.

Contents

LIST OF FIGURES

LIST OF TABLES

LIST OF ABBREVIATIONS

ADS	Advanced Design System
AFSS	Active Frequency Selective Surface
AMPS	Advanced Mobile phone System
AR	Axial Ratio
ASA	Annular Slot Antenna
ASIC	Application Specific Integrated Circuit
AUT	Antenna Under Test
ARBW	Axial ratio bandwidth
BW	Bandwidth
CAD	Computer Aided Design
CCW	Counter Clockwise
CP	Circularly Polarized
CR	Cognitive Radio
CST	Computer Simulation Technology
CW	Clockwise
DARPA	Defence Advanced Research Projects Agency
DBS	Direct Broadcast Satellite
DCS	Distributed Control System
E	Electric field
EBG	Energy band gap
EM	Electromagnetic
FCC	Federal Communications Commission
FDTD	Finite Difference Time Domain

FEM	Finite Element Method
FET	Field Effect Transistor
FOM	Figure of merit
FRMS	Frequency Reconfigurable Metasurface
FSS	Frequency Selective Surface
GPS	Global Positioning System
GSM	Global System for Mobile Communication
H	Magnetic field
HF	High Frequency
HFSS	High Frequency Structure Simulator
HIPERLAN	High Performance Radio Local Area Network
HP	Hewlett Packard
IEEE	Institute of Electrical and Electronics Engineering
IE3D	Integral Equation 3-Dimension
IMT	International Mobile Telecommunications
IOT	Internet of things
ISM	Industrial, Scientific and Medical
LF	Low Frequency
LHCP	Left Hand Circular Polarization
LP	Linear Polarization
LTE	Long Term Evolution
MIC	Microwave Integrated Circuit
MIMO	Multiple-Input Multiple -Output
MMIC	Monolithic Microwave Integrated Circuit
MoM	Method of Moments

MS	Meta Surface
PCB	Printed Circuit Board
PCS	Personal Communication Service
PFSS	Passive frequency Selective Surface
PNA	Performance Network Analyzer
PRS	Partially Reflective Surface
RF	Radio Frequency
RFIC	Radio Frequency Integrated Circuit
RFID	Radio Frequency Identification
RFSR	Reconfigurable Frequency Selective Reflector
RHCP	Right Hand Circular Polarization
RL	Return Loss
RLC	Resistance InductanceCapacitance
RMPA	Rectangular microstrip patch antenna
RFID	Radio frequency identification
EM	Transverse Electromagnetic
VNA	Vector Network Analyzer
VSWR	Voltage Standing Wave Ratio
WLAN	Wireless Local Area Network
Wi-Bro	Wireless Broadband
Wi-Fi	Wireless Fidelity
WiMAX	Worldwide Interoperability Microwave Access
WPAN	wireless personal area network
1G	First generation
2G	Second generation

3G	Third generation
4G	fourth generation
5G	Fifth generation

LIST OF SYMBOLS

B	:	Magnetic flux density
D	:	Electric flux density
ρ	:	Charge density
J	:	Current density
R_r	:	Radiation resistance
P_r	:	Reflected Power
P_i	:	Incident Power
Γ	:	Reflection Coefficient
V_0^-	:	Amplitude of Reflected wave
V_0^+	:	Amplitude of Incident wave
Z_0	:	Characteristic Impedance
Z_L	:	Load impedance
f_u	:	Upper cut-off frequency
f_l	:	Lower cut-off frequency
f_r	:	Resonant frequency
η_0	:	Total Antenna Efficiency
η_r	:	Reflection Efficiency
G	:	Gain
D	:	Directivity
λ_0	:	Free space wavelength
μ_r	:	Relative Permeability
ε_r	:	Relative Permittivity or dielectric constant of the substrate
h	:	thickness of the substrate

E_θ	:	Electric field in Elevation plane
E_φ	:	Electric field in Azimuth plane
Q_d	:	Stored Charge
I_d	:	DC bias current
τ	:	Carrier lifetime
R_S	:	Forward resistance of the diode in ON state
μ_N	:	Electron Mobility
μ_P	:	Hole Mobility
C_T	:	Diode Capacitance
L_s	:	Parasitic Inductance
S_{11}	:	Reflection Coefficient
S_{12}/S_{21}	:	Isolation/Insertion loss
R	:	Resistance
C	:	Capacitance
L	:	Inductance
G	:	Conductance
Z	:	Impedance
Y	:	Admittance
r	:	Radius of the circle
J_n	:	Bessel function of order n
k	:	wave number

Chapter 1

Introduction

The annals of antennas precede James Clerk Maxwell, who combined the theories of electricity and magnetism and expressively represented their associations through a set of reflective equations identified as Maxwell's Equations [1].

$$\nabla \times E = -\frac{\partial B}{\partial t}$$

$$\nabla \times H = J + \frac{\partial D}{\partial t}$$

$$\nabla . D = \rho$$

$$\nabla . B = 0$$

These equations preside over the laws of electromagnetic radiation and eventually rule the world of wireless communication. An antenna is one of the most fundamental elements in a wireless communication system. It is defined as a device that can transmit and receive electromagnetic energy by converting electric current to radio waves and vice versa [2]. Generally, the antenna is fabricated by a conductor, and antennas are also existing which utilize dielectric materials. In many wireless communication systems, an antenna is used for transmitting/receiving devices and integrated with many other devices in the system for better performance.

1.1 Antenna Fundamentals

Any type of antenna is primarily based on the percept of electromagnetic radiation that takes place because of accelerated or decelerated electric charges within an undertaking material. This could be best explained with the assist of a typical radio communication system is illustrated in fig. 1.1. A 50 Ω transmission line is used to connect the generator to an antenna. The message signal is modulated to the carrier and amplified. The amplified signal is sent to the antenna via the transmission line. The receiving antenna collects the radiated signal. The received signal is demodulated to get the original message at the receiver. In this way, the antenna acts as a transducer that transforms electrical signals, i.e., voltages and currents, into

electromagnetic waves or vice versa. An antenna is said to be resonant if its input impedance is entirely real. So, the real part of impedance should be matched at the feed line to transfer a maximum power without reflection. However, the operating frequency decides the size of the antenna [3].

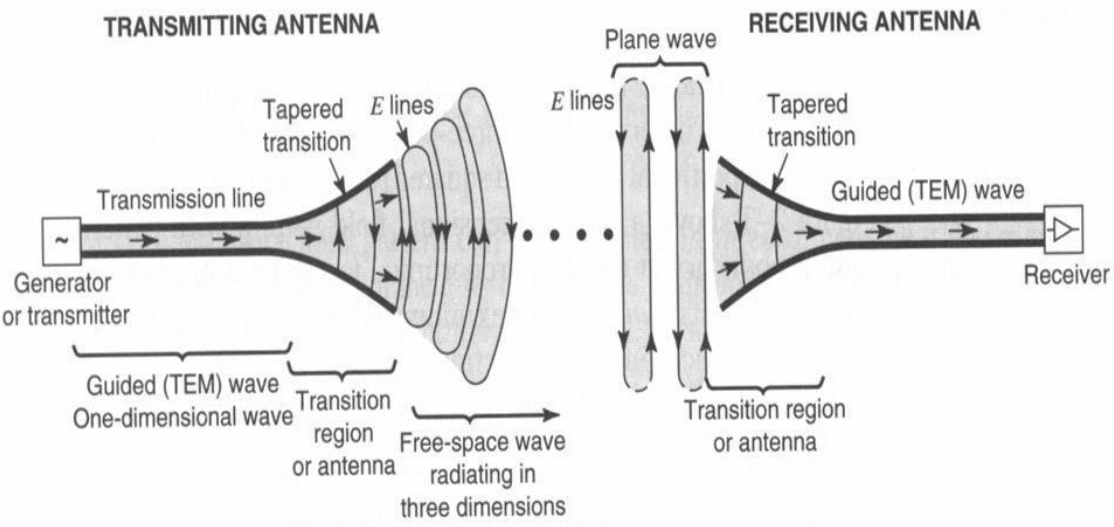

Fig. 1.1 Antenna and Electromagnetic waves generation in a radio system [3]

To apprehend the demanding situations confronted whilst designing antennas and explain the antenna's performance, it's essential to offer a few history statistics on a number of important parameters. There are numerous types of antennas advanced for lots distinctive applications, and they may be classified based on four distinct groups as wire, aperture, reflector, and printed antennas, and that they may be used as single elements or arrays with differing geometry; however, there are certain fundamental parameters which can be used to explain all of them.

1.1.1 Input Impedance

Input impedance is defined as "the impedance presented by an antenna at its terminals or the ratio of the voltage to current at a pair of terminals or the ratio of the appropriate components of the E to H fields at a point." It is shown in Equation 1.1.

$$Z_a = \frac{V(0)}{I} \tag{1.1}$$

$$Z_a = R_a + jX_a$$

where in $R_a=R_l+R_r$ is the antenna resistance,

R_l = ohmic,conductor and dielectric loss

$R_{r=}$ radiation resistance , $X_{a=}$ antenna reactance

$Z_s=R_s+jX_s$.

$$R_r+R_l=R_s \text{ and } X_a= - X_s \tag{1.2}$$

The Thevenin equivalent is shown in fig.1.2.

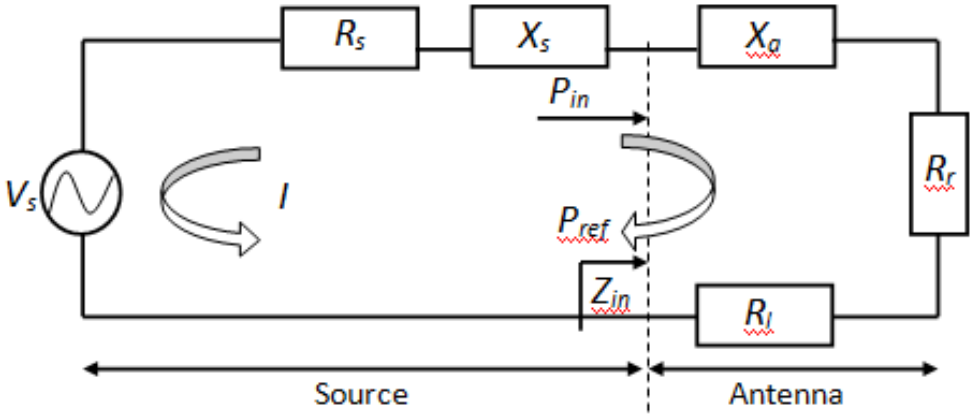

Fig. 1.2 Thevenin Equivalent model for Antenna

When we have conjugate matching in the generator, half of the energy dissipated in the form of internal resistance (R_s), and the other half is delivered to the antenna.

1.1.2 Return loss and Impedance Bandwidth

Return loss is the amount of signal power absorbed by a load when the energy from a source is sent to it. It is usually expressed as the ratio between reflected and incident power expressed in dB.

$$R_L = 10\log_{10}\left(\frac{P_r}{P_i}\right) \tag{1.3}$$

In other words, return loss is the measurement of how well devices or lines are matched. For a well-matched condition, a high return loss is desirable, resulting in a lower insertion loss. Fig.1.3 shows the sample return loss graph. As for the reflection coefficient (Γ), it is the ratio of

the amplitude of the reflected wave (V_0^-) to the amplitude of the incident wave (V_0^+) which is given in the equation below.

$$RL(dB) = -20\log|\Gamma| \tag{1.4}$$

where $$|\Gamma| = \frac{V_0^-}{V_0^+} = \frac{Z_L - Z_0}{Z_L + Z_0}$$

$|\Gamma|$ is Reflection Coefficient

V_0^+ is Incident Wave

V_0^- is Reflected Wave

Z_L and Z_0 are load and characteristic impedances

The return loss of -10dB and VSWR of 2 are generally acceptable. The impedance bandwidth, BW, is defined as,

$$BW = \frac{f_u - f_l}{f_r} \times 100\% \tag{1.5}$$

The bandwidth of an antenna can be defined for *impedance*, *radiation pattern*, and *polarization*. In a wireless communication system, the impedance bandwidth allows most of the power to be transmitted to an antenna from a feed or a transmission system at a transmitter and from an antenna to its load at a receiver or terminal.

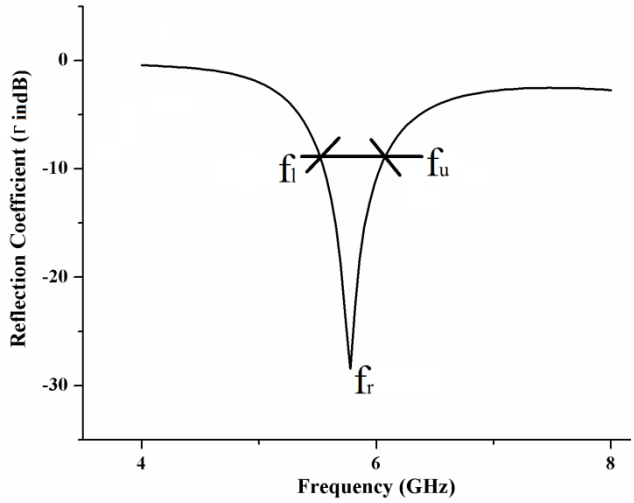

Fig. 1.3 Impedance bandwidth and operating frequency are shown in return loss

1.1.3 Directivity, Gain, and Efficiency

The directivity of an antenna is defined as "the ratio of the radiation intensity in a given direction from the antenna to the radiation intensity averaged over all directions. The average radiation intensity is equal to the total power radiated by the antenna divided by 4π. If the direction is not specified, the direction of maximum radiation intensity is implied [3]."

The antenna efficiency is the amount of losses occurring due to reflection and I^2R losses (ohmic losses that include dielectric and conduction losses) at the terminals of the antenna. The total power delivered to the antenna terminals must be equal to the antenna ohmic losses P_{ohmic} (conduction loss + dielectric loss) plus total power radiated by the antenna P_r.

Antenna radiation efficiency, η_{cd}, is a measure of how efficient the antenna is at radiating the power delivered to its terminals and can be defined as:

$$\eta_{cd} = \frac{P_r}{P_{in}} = \frac{P_r}{P_{ohmic} + P_r} \tag{1.6}$$

Total antenna efficiency,η_0 and reflection efficiency are related by:

$$\eta_0 = \eta_{cd}\eta_r \tag{1.7}$$

Another functional parameter that explains the performance of an antenna is the gain. Gain of an antenna (in a given direction) is defined as "the ratio of the intensity, in a given direction, to the radiation intensity that would be obtained if the power accepted by the antenna were radiated isotropically (which is equal to the power accepted (input) by the antenna divided by 4π)"[3]. The gain which is related to the directivity can be expressed as:

$$G = \eta_{cd} D \tag{1.8}$$

1.1.4 Radiation Pattern and Polarization

The radiation pattern of an antenna is the orientation of the fields in respect of spatial coordinates. A radiation pattern is taken at a particular distance, which should be greater than $\lambda_o/4$ to be considered as far-field. The radiation pattern can be visualized in E-plane and the H-plane.

The polarization is the wave transmitted or received by an antenna in the desired direction. Polarization of the EM field describes the orientation of its vectors at a given point and how it varies with time. In general, most antennas radiate either linear or circular polarization.

In general, if the plane contains an ellipse and the electric field traces an ellipse, the field is *elliptically polarized*. A linear polarized antenna radiates wholly in one plane containing the direction of propagation. In a circularly polarized antenna, the plane of polarization rotates in a circle making one complete revolution during one wave period. If the rotation is clockwise looking in the direction of propagation, the sense is called right-hand-circular (RHC). If the rotation is counter-clockwise, the sense is called left-hand-circular (LHC). Fig. 1.4 shows various wave polarizations.

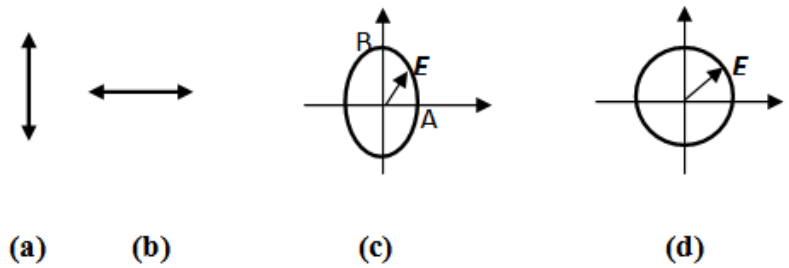

Fig. 1.4 Linear polarization (a) Vertical) (b) Horizontal (c) Elliptical polarization (d) Circular polarization

The ratio of amplitudes B to A, i.e., the ratio of the major axis to the minor axis, is called the axial ratio *(AR)*:

$$AR = \frac{B}{A}$$

For a circularly polarized wave, AR is one. For a linearly polarized wave, it is infinite or zero, thus $0 \leq AR \leq +\infty$.

The polarization has two components: co-polarization component and the cross-polarization component. *Co-polarization* represents the polarization where the antenna is intended to radiate (receive), while *cross-polarization* represents the polarization orthogonal to a specified polarization, which is usually the co-polarization.

1.2 Microstrip Antennas

Most conventional antennas like wire, dipole and aperture types are implemented using planar microwave technologies such as Microstrip, Slot lines, coplanar lines, etc. Microstrip patch antennas are one of the most basic and important types of planar antenna introduced by G. A. Deschamps in 1953. Still, it was not until the1970s that serious attention was paid to this element when low-profile antennas were required for an emerging generation of missiles [4].

Planar antennas, particularly miniaturized microstrip patches, are widely used in circularly polarized antenna research because of their unique and attractive properties such as low profile, lightweight, compact and conformable mounting structure, and easy fabrication and integrability into arrays and with MICs result in applications. However, the microstrip configurations also have limitations, including narrow bandwidth, spurious feed radiation, poor efficiency, polarization purity, limited power handling capacity, and tolerance problems [5].

The compact antenna configuration further degrades these parameters because of the existence of the fundamental relationship between size, bandwidth, and efficiency. As the antennas are made smaller, either the operating bandwidth or antenna efficiency must decrease. The small antennas usually provide lower gain than larger antennas [6]-[7]. Several works have been implemented to develop such antennas to overcome these limitations, such as bandwidth can be increased to more than 70% by using multilayer aperture coupled microstrip antennas. Low power handling problems can be overcome through an array configuration.

Patch antennas consist of a very thin ($t << \lambda_0$, where λ_0 is the free space wavelength) metallic strip (patch) placed a small fraction of a wavelength ($h << \lambda_0$, usually $0.003\lambda_0 \leq h \leq 0.05\lambda_0$) above a ground plane. The patch and the ground plane are separated by a dielectric sheet (the substrate) [3]. Fig. 1.5 shows a printed patch antenna. The shape and dimensions of the radiating patch usually determine the frequency of operation, and thus these antennas are classified as resonant antennas, as shown in fig. 1.6.

There are numerous substrates that may be used for the layout of microstrip antennas, and their dielectric constants are normally in the range of $2.2 \leq \varepsilon_r \leq 12$. The substrates with massive thickness whose dielectric constant is in the lower end of the range provide good antenna performance because they provide better efficiency, large bandwidth, loosely bound fields for radiation into space, however on the price of larger element length[8].

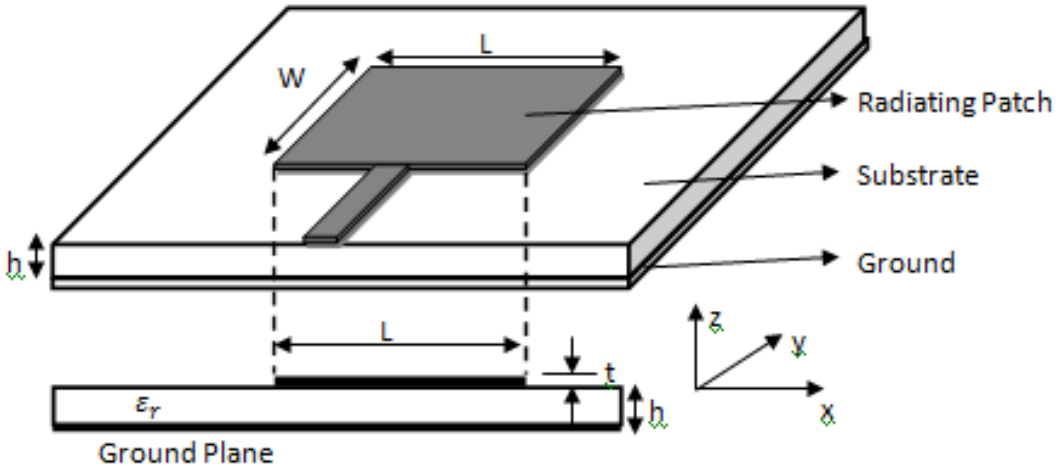

Fig. 1.5 Rectangular Microstrip Patch Antenna

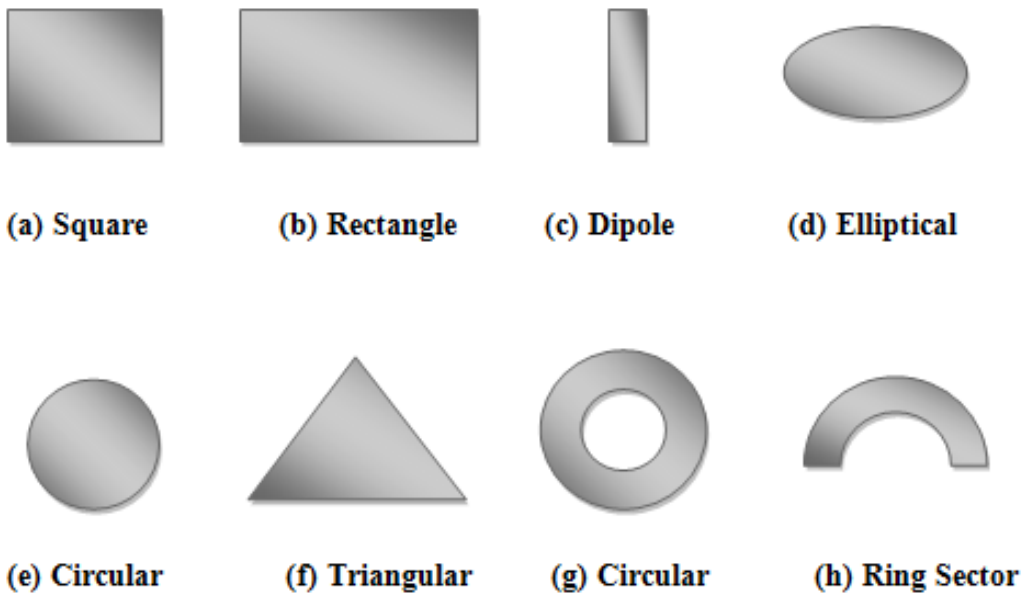

Fig. 1.6 various shapes of Microstrip Patch Elements

Thin substrates with better dielectric constants are appropriate for microwave circuitry due to the fact they require tightly bound fields to reduce undesired radiation and coupling and lead to smaller element sizes; but, due to their extra losses, however, they're very losses and have incredibly smaller bandwidths [8].

1.2.1 Patch Antenna Excitation Techniques

A number of factors govern the selection of feeding techniques for the patch antenna. It mainly depends on considering the efficient energy switch between the radiating and feed structures, i.e., impedance matching. Minimizing the spurious radiation and its impact on the radiation pattern is one of the essential factors for evaluating feed.

Several feeding techniques are used to radiate the microstrip patch antenna, and the antenna performance characteristics are optimized by offering many parameters to a designer. Few feeding techniques are microstrip line, aperture coupling, proximity coupling, and coaxial probe (direct contact feeding methods). Feeding method schemes are direct and non-contact. The RF power is fed directly to the radiating patch via a linking element. The principle used in the non-contact method is electromagnetic field coupling and is used to transfer RF power between the feed line and the radiating patch. The feeding techniques widely used are described below.

1.2.1.1 Microstrip Line feed

This feeding method consists of a conducting strip, in which its small width is compared to the patch and due to its simple modeling directly connected to the various positions of the patch edge as indicated in fig. 1.7. This feeding method is simple to match, easy modeling, and easy to fabricate. Its disadvantage is the increase in spurious feed radiation and surface waves. This occurred by increasing the substrate thickness to improve the bandwidth.

The physical dimension of the patch looks electrically smaller due to the fringing effects, as shown in fig.1.8. Electrically the dimension of the patch is extended on each end by a distance ΔL. For an efficient radiator, a practical width leads to good radiation efficiencies [9-10].

$$W = \frac{1}{2f_r\sqrt{\mu_o\varepsilon_o}}\sqrt{\frac{2}{\varepsilon_r+1}} = \frac{v_o}{2f_r}\sqrt{\frac{2}{\varepsilon_r+1}} \tag{1.9}$$

Where v_o is the free space velocity of light. The effective dielectric constant of the patch is found using the below equation.

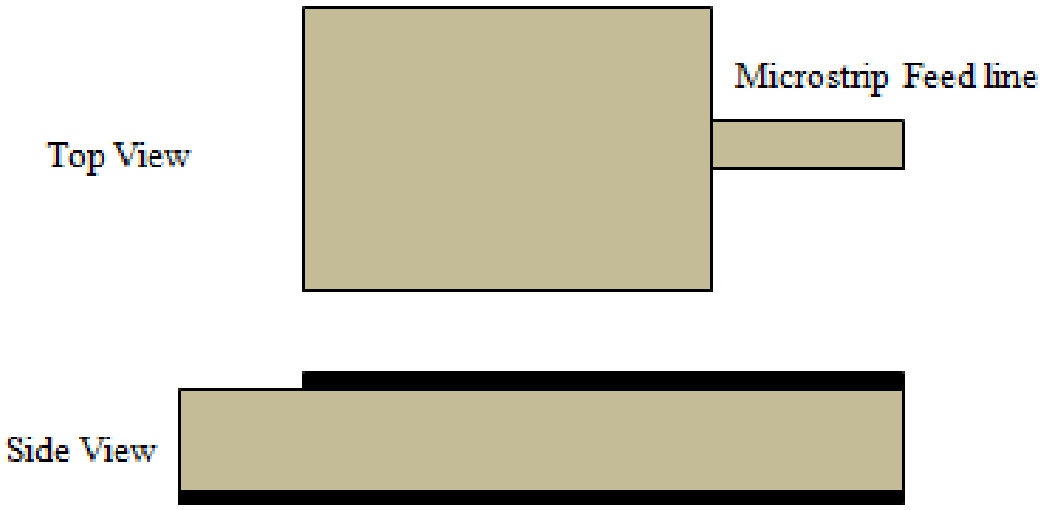

Fig. 1.7 Rectangular patch with microstrip line feed

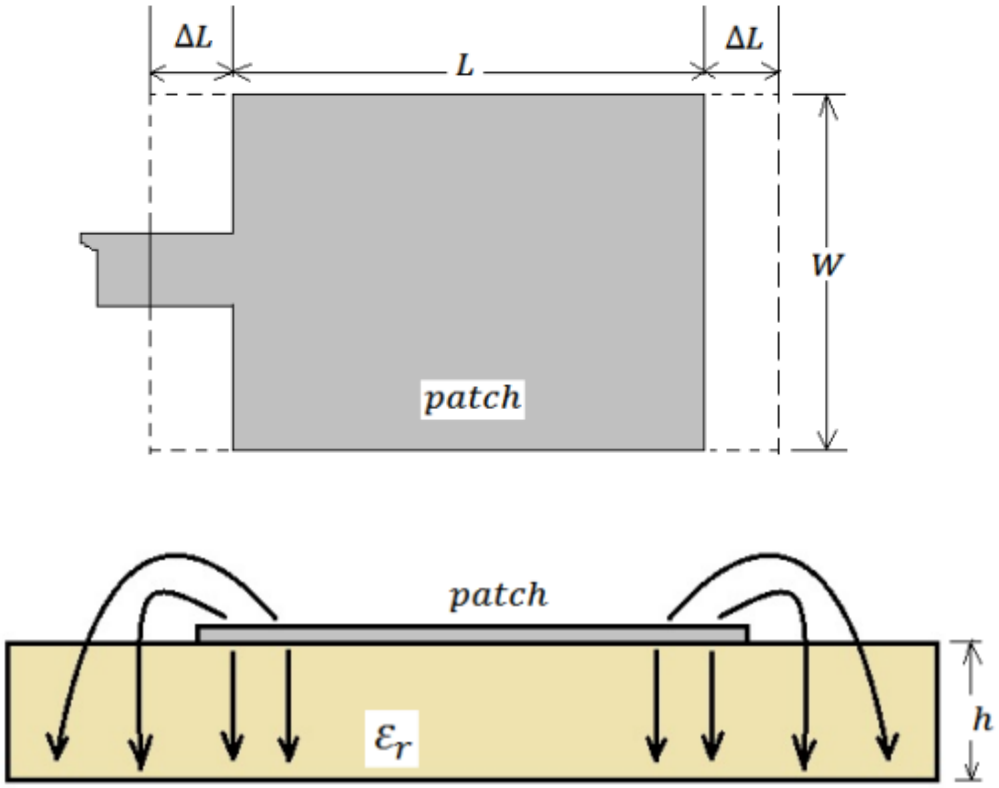

Fig.1.8 Fringing field effects on rectangular microstrip patch.

$$\varepsilon_{reff} = \frac{\varepsilon_r + 1}{2} + \frac{\varepsilon_r - 1}{2}\left[1 + 12\frac{\mathrm{h}}{w}\right]^{-1/2} \quad (1.10)$$

When width is found, then determine the extended length ΔL.

$$\frac{\Delta L}{\mathrm{h}} = 0.412\frac{(\varepsilon_{reff} + 0.3)}{(\varepsilon_{reff} - 0.3)}\frac{(\frac{W}{\mathrm{h}} + 0.264)}{(\frac{W}{\mathrm{h}} + 0.8)} \quad (1.11)$$

After finding ΔL, the actual length of the patch can be determined using the below equation.

$$L = \frac{1}{2f_r\sqrt{\varepsilon_{reff}\,\mu_o\varepsilon_o}} - 2\Delta L \quad (1.12)$$

1.2.1.2 Coaxial feed

Coupling of power through a probe is one of the basic mechanisms for the transfer of microwave power. The probe can be an inner conductor of a coaxial line, or it can be used to transfer power from a triplate line (stripline) to a microstrip antenna through a slot in the common ground plane. This technique is shown in fig. 1.9.

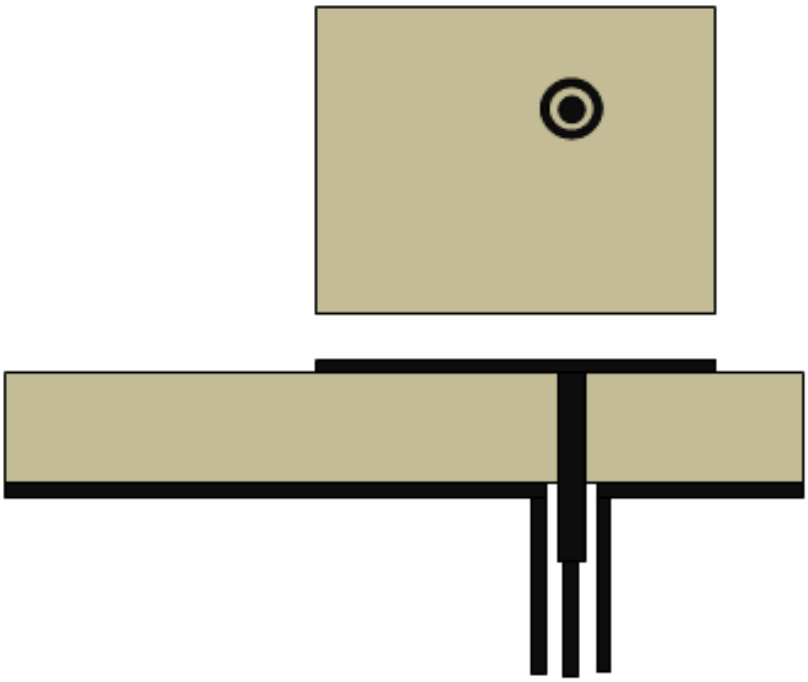

Fig. 1.9 Coaxial probe fed Microstrip patch antenna

1.2.1.3 Proximity Coupled feed

In this coupling, the feed is not in contact with the microstrip patch and is also said to be a coplanar microstrip feed, whose configuration is shown in fig.1.10. It consists of two substrates placed upon the other, i.e., the microstrip line is in the lower layer, and the upper layer patch antenna is present. Below the patch, the microstrip feed line is terminated openly at the terminals. It is also known as an "electromagnetically coupled" microstrip feed.

The nature of this technique is capacitive while coupling. Increasing the antenna's bandwidth and decreasing the unwanted radiation from the open end of the microstrip depends on the selected two-layer substrates. For these, the lower layer should be thin. To ensure larger bandwidth, the radiating patch is placed on the double layer.

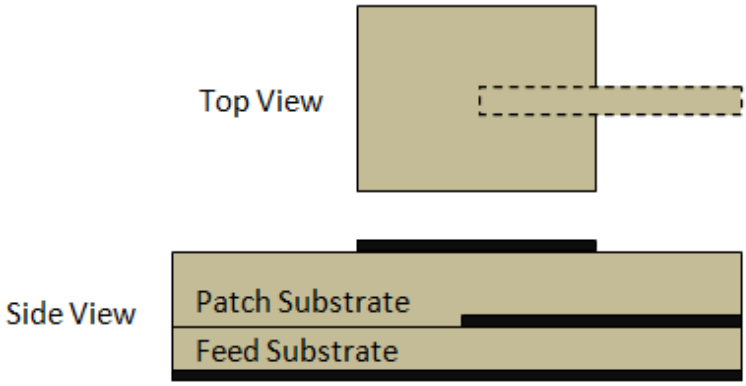

Fig. 1.10 Patch antenna with proximity coupled feed

1.2.1.1 Aperture Coupled feed

This configuration uses two substrates separated by a common ground plane. A microstrip feed line on the lower substrate is electromagnetically coupled to the patch through a slot aperture in the common ground. This slot can be of any size and shape, and they are adjusted to improve the bandwidth. The feed configuration is shown in fig. 1.11. The substrate of the feed can be thin and has a high dielectric constant, and the substrate of the patch can be thick and has a low dielectric constant. The polarization purity is improved by using this technique.

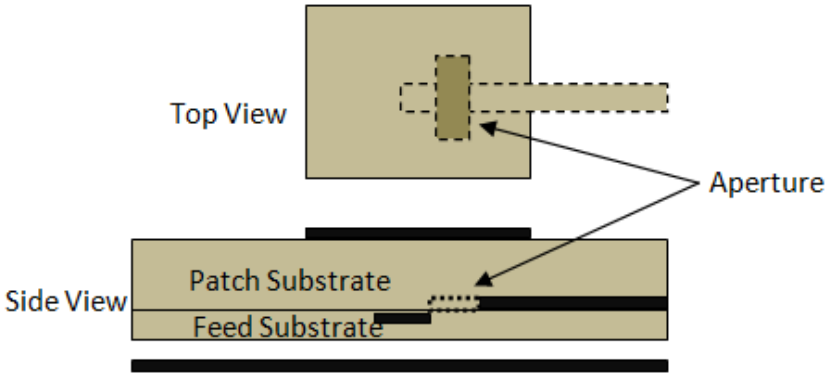

Fig. 1.11 Aperture coupled fed microstrip patch antenna

Circularly polarized antennas are excited by single feed or dual feed depending on its application and complexity of the feeds chosen. Here single feed technique is used in this research work. The single feed technique is chosen as it simplifies the feed network, and a perturbation in the patch results in circular polarization. Few shapes of CP patch designs like elliptical, circular, and rectangular are discussed. To design a CP antenna with an elliptical shape patch, the ratio between the major axis and minor axis is given below [10].

$$\frac{a}{b} = 1 + \frac{1.0887}{Q} \tag{1.13}$$

Here Q is the quality factor and can be measured experimentally or the result from full-wave electromagnetic analysis to approximate Q.

$$Q = \frac{f_o}{\nabla f}\frac{VSWR-1}{\sqrt{VSWR}} \tag{1.14}$$

Another form of single-feed CP patch antenna design configuration is shown in fig.1.12 (b); it is a square patch fed at a point along the diagonal line of the patch. The length and width of the patch are *L* and *W*, respectively. Circular polarization is obtained based on the condition given below.

$$L = W\left(1 + \frac{1}{Q}\right) \tag{1.15}$$

Antenna quality factor can be computed from eq. (1.14) and resonant frequencies associated for a rectangular patch with length L, width W denoted as f_1, f_2, are calculated below with the equations given below.

$$f_2 = f_o\sqrt{1 + \frac{1}{Q}} \tag{1.16}$$

Where f_o is the center frequency of the bandwidth.

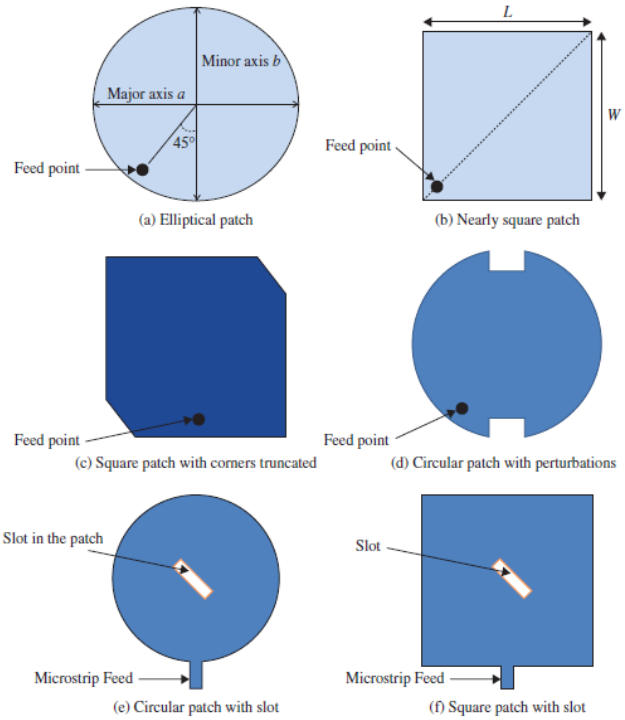

Fig.1.12 various forms of single feed CP antennas.

1.3 Benefits of Circularly Polarized Antennas

To generate circular polarization, two orthogonal components of the electric field are needed. These components need to be equal in amplitude but shifted in phase by 90°.

- Mitigation of multipath propagation**:** In a multipath propagation environment, the circularly polarized antenna can filter out the unwanted signals by counter polarizing the signals. The CP antenna may offer high data rate communication in indoor environments and decrease inference between direct signal to reflected signal with these capabilities.
- Misalignment of antennas causes polarization losses**:** To avoid polarization mismatch in linearly polarized communication systems, the receiving and transmitting antenna must be aligned. However, CP is not required; if the ideal CP signal is received by a linearly polarized antenna, the loss is 3 dB, regardless of the orientation of the receiving antenna.
- Interaction between light and magnetic fields results in the Faraday effect. It has an impact on linear, but not circular, polarized signals, and the effects are more severe at lower frequencies, such as C-Band, and not noticeable at higher ones, such as Ku-Band.

As signals pass through the atmosphere, they become de-polarized, causing undesirable reception of the opposing polarity.

- The antenna should be aligned in a proper position in satellite communication, i.e., point and transmit. For this requirement, circular feeds are set up faster, and there is less of a hazard of being misaligned.
- There is higher link reliability since there is a low risk of misalignment and encountering interference.

5G wireless communication systems provide high communication capacity, low latency, high reliability, low power consumption, wide-area coverage, support for many devices in a small area, and high communication rate[11].In 5G communications, the millimeter-wave band is very much attractive and useful for many applications, but due to losses like path loss, scattering, and non-line of sight and to overcome presently almost all countries using spectrum below 6GHz for IMT (international mobile telecommunication) and other 5G wireless communication systems. One of the potentials in the 5G spectrum is spectrum refarming [12]. For example, 3.3-3.4, 4.4-4.5, 4.8-5.0-GHz bands will be used as 5G candidate bands in China [13]-[14]. Fig.1.13 shows the bands in IEEE 802.11ac amendment for wireless communication applications [15-16].

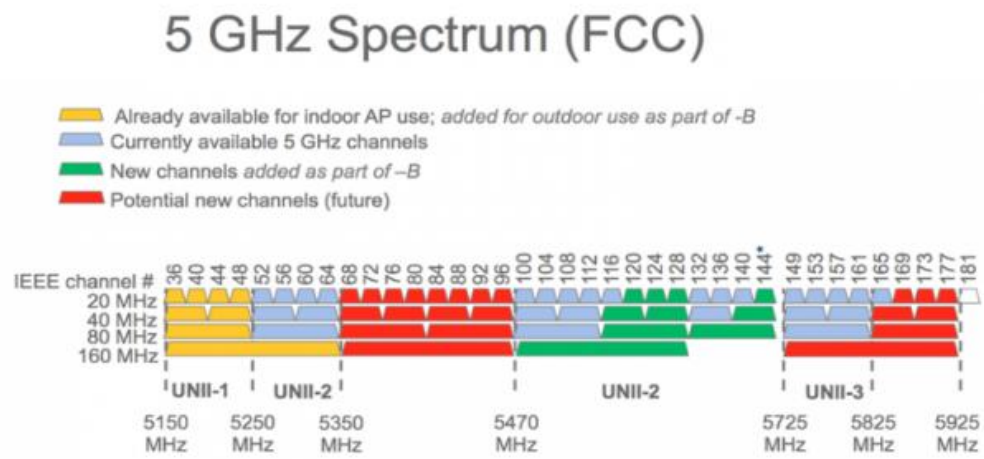

Fig.1.13 Spectrum of 802.11ac is the amendment by Federal Communications Commission (FCC) for WIFI and WLAN applications [15-16].

The most vibrant and fast-growing technology in the communication system is the wireless communication system. It uses radio waves for transmitting information from one point to other without any wire connection. Millions of people use this system in day-to-day applications [17]. The main component in wireless communication systems is an antenna. It

plays a main role in transmitting/receiving information in the form of radio waves in wireless communication systems.

In wireless communication, various applications are developed, such as WIMAX, WLAN, and C-Band, X-Band. Worldwide interoperability for microwave access (WiMAX) is based on the IEEE 802.16 set of standards that provides wireless broadband communication. A wireless local area network (WLAN) is a system that links two or more devices using wireless computer networks to form a local area network within a limited space. Users can access the various WLAN hotspots in many places with the help of portable devices.

C-Band is a band in the electromagnetic spectrum in the microwave range of frequencies ranging from 4 GHz to 8GHz and used for surveillance, weather radar, satellite communication, cordless telephones, and WIFI devices.

X-band is the band of frequencies in the microwave region ranging from 8GHz to 12 GHz and used for satellite communications, air traffic control, wireless personal area network (WPAN), remote sensing, vehicular applications, defense tracking, and modern radars.

Starting from 1G, the cellular concept was introduced, making possible large-scale evolution in mobile wireless communication. In 2G analog communication is replaced with digital communication and significantly improved signal quality. In 3G technology, the major focus is on both voice and data communication for a converged network. 4G has initiated various challenges like insufficient spectrum, bad connectivity, poor coverage, and poor quality of services. To overcome the shortcomings of 4G, a new generation is evolved as 5G and is expected to fulfill better reliability, more connectivity, lower latency, higher data rate, and better quality of service [18, 19].

Due to the rapid development of wireless communication technology from the above scenario, there is a demand for efficient antennas. Antennas are classified based on physical structure, the band of frequencies, functionality, and application. Three-dimensional antennas such as Yagi-Uda, monopole, helical, dipole biconical, and log-periodic antennas are not suitable for wireless communication systems because of their large size and need to be compact.

In the electromagnetic spectrum, each band of frequencies has its specific application allocated. Based on the frequency range, antennas are said to be narrowband and wideband. Based on the antenna size, the amount of power is radiated in a particular range of frequencies. The bandwidth of the antenna is measured in fractional bandwidth. If it is less than 20%, it is said to be a narrow band, otherwise wide band. Some of the narrowband antennas are GPS, WiMAX, WLAN, Bluetooth, etc. Wideband antennas are used in transmitting information at a high data rate for satellite and military applications. Therefore, two-dimensional compact antennas are used for portable devices. Among two dimensional, printed antennas like resonant type-microstrip patch antennas are used for many wireless applications. The position or orientation of the antenna is the main part of transmitting or receiving the information in wireless communication systems. In 5G wireless communication, because of the size constraint, the design of a compact antenna with excessive bandwidth and gain is a challenging task.

For indoor and outdoor, wireless communication applications require Omni-directional coverage. Narrowband antennas for WIMAX, WLAN, and GPS applications assure an Omni-directional pattern but have less gain, and for long-distance communication, high gain antennas are required.

1.3.1 Applications

5G communication enabled a new generation of applications in three major categories, depicted in fig.1.14.

- Massive machine to machine communications
- Ultra-reliable low latency communications
- Enhanced mobile broadband

Massive machine-to-machine communications are also called the Internet of things (IoT) which involves connecting billions of people without human intervention. Potential to revolutionize many industries processes and has applications in agriculture, manufacturing, and business communications [20-21]. In ultra-reliable low latency, communication includes the real-time control of devices, robots, vehicular to vehicular communication, and safety systems [22-23]. Enhanced mobile broadband provides faster data speeds, high communication capacity in keeping the world connected, as shown in fig.(1.14-1.15) [24].

Fig.1.14 5G wireless communications associated with various devices [24]

Fig.1.15 5G wireless communication applications [24]

1.4 Antenna Design Flowchart

Figure 1.16 shows the steps involved in designing an antenna, right from choosing the specifications to fabrication of the physical antenna and testing. The design procedure starts with determining antenna electrical and physical specifications.

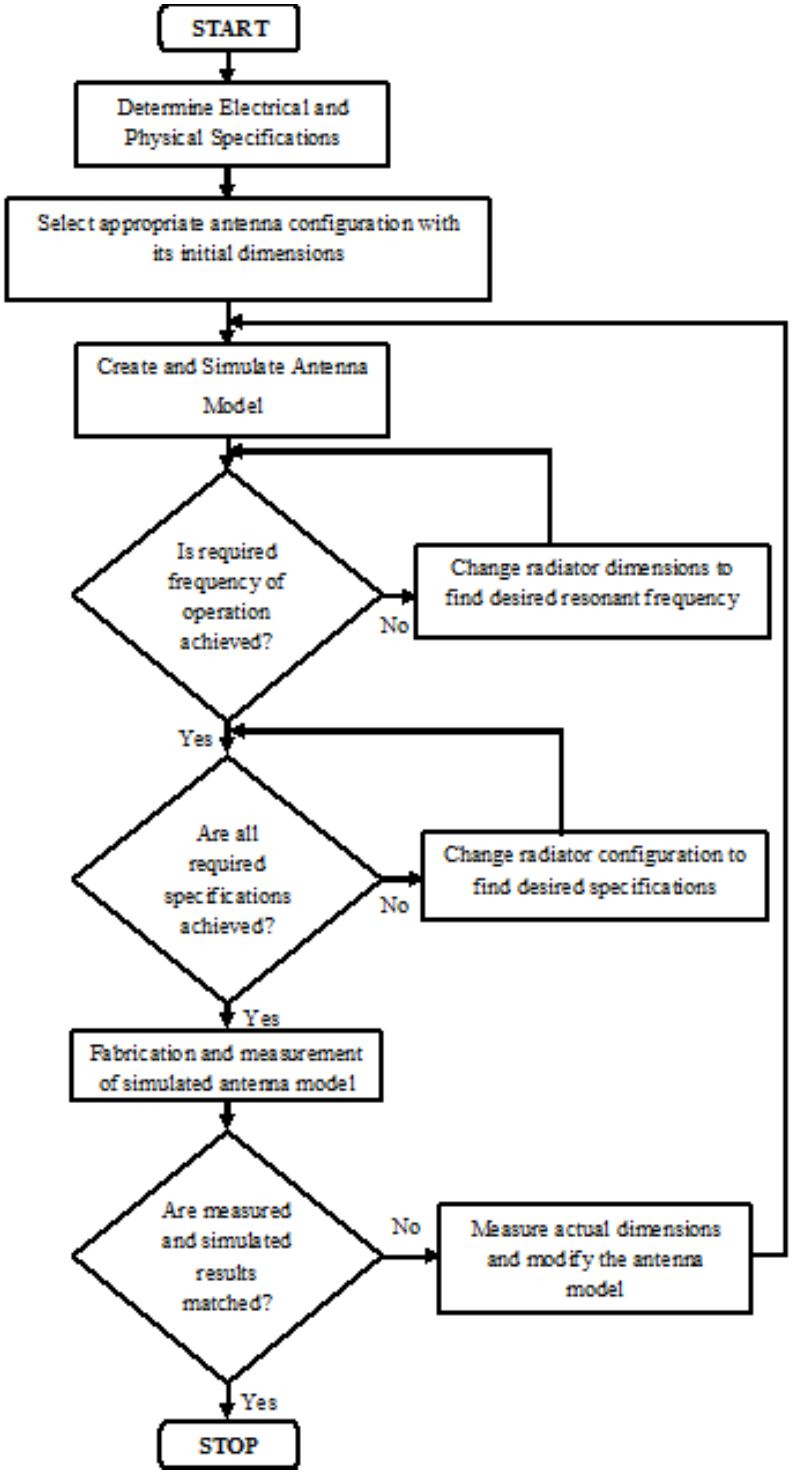

Fig. 1.16 Flow Chart of Antenna Design Approach

The proposed antenna configuration usually comprises an actual patch, otherwise called a radiator (the major part of the antenna), type of feed mechanism, and substrate material. In antenna configuration, these parameters are taken and are used as input data to calculate antenna dimensions from the modeling method.

From the above process, the obtained antenna dimensions are taken as input to computer simulation software. The received output from the software is the predicted performance characteristics of the antenna-like resonant frequency, input impedance, gain, return loss, bandwidth, and polarization. When the characteristics of the antenna model meet the required specifications, the antenna prototype is sent for fabrication, and then practical measurements are taken. Due to the practical implementation, there might be a fabrication tolerance for the designed structure, and this can be minimized by comparing measured results with simulated ones. Then new dimensions are taken and re-simulated in the antenna model for optimum performance.

1.4.1 Commercial Simulation Software Packages

The major step in designing an antenna with optimum performance is simulation software because it is an intermediate stage between the antenna model and the fabrication process. The antenna model, after fabrication process, ensures the performance characteristics to be accurate and possible through simulation tool and it helps to save money and time. The simulation software is selected in such a way that it gives accurate antenna performance with accurate accuracy. Hence simulation tool plays a key role in designing a microstrip antenna.

There are many electromagnetic (EM) simulation software packages available for designing an antenna, such as IE3D (Integral Equation 3-Dimension), HFSS (High-Frequency Structure Simulator), CST Studio (Computer Simulation Technology), ADS (Advanced Design System), FEKO, Antenna Magus, etc. Each simulation software characterizes in time or frequency domain based on numerical techniques they use. For the opted antenna geometry, the selection of simulation tools plays a key role in giving the best performance.

Accordingly, the best EM simulation is taken based on optimum performance with respect to the minimal simulation run time. Based on the antenna design chosen and its complexity, simulation run time, and accurate performance, the antenna prototype is constructed from these inputs, and also a maximum match of results of simulated and measured data is taken care of.[25-26] .

HFSS: HFSS is an interactive software package for calculating the electromagnetic behavior of a structure. The finite Element Method (FEM) is a numerical technique used in HFSS [46].In this technique, finite elements are present, subdivided into several minor

subsections called finite elements. HFSS uses these finite elements as tetrahedra, and the complete group of tetrahedra is called a mesh, as shown in fig. 1.17. Each tetrahedron is composed of four equilateral triangles and a collection of tetrahedra forms known as the finite element mesh. At each vertex of the tetrahedron, components of the field tangential to the three edges meeting at that vertex are stored. A vector field quantity such as the H-field or the E-field inside each tetrahedron is estimated using these stored values.

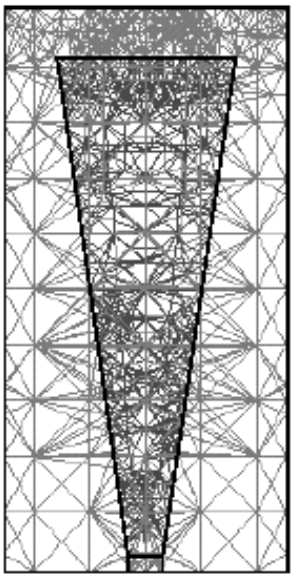

Fig. 1.17 Meshing for Finite Elements

Every HFSS simulation will involve six main steps to create and solve an appropriate EM model.

- **Create Model/Geometry**
- **Assign boundaries**
- **Excitation**
- **Set up the Solution**
- **Solve**
- **Post-processing**

IE3D: IE3D is an integrated full-wave electromagnetic simulation and optimization package for analyzing and designing 3D and planar microwave circuits. The electric field and magnetic field components are represented as weighted integrals of electric current on metallic structures and magnetic current derived from the electric field distribution on a metallic aperture [27].

1.4.2 Antenna Fabrication

Geometrical layout generation can be done in AutoCAD software for preparing the mask. The patch can be fabricated using conventional photolithography once the mask is printed on semi-translucent paper (transparent sheet). The steps involved in the fabrication process are shown in Fig. 1.18.

Afterward, the exposed parts are then washed away with a NaOH solution, allowing for some last adjustments to be done before the metal is etched away. Finally, the board is put inside the etching machine, which removes all uncovered metal areas and results in the final product.

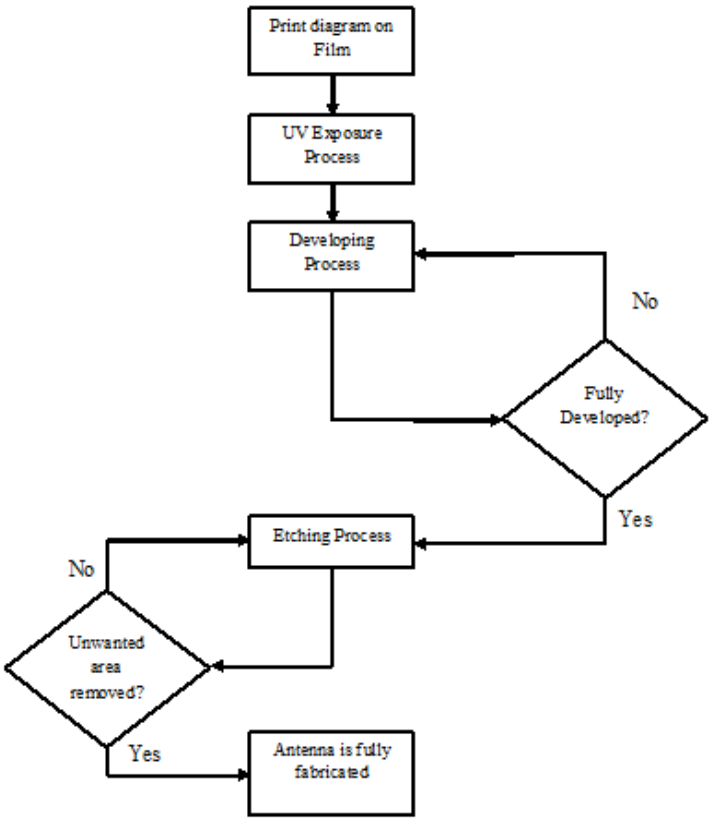

Fig. 1.18 Steps involved in the Antenna Fabrication process

1.4.3 Measurement

For the fabricated antenna, testing and measurement are the important steps in the complete process. Care has to be taken for the accurate measurement parameters and is also difficult to maintain because it depends on the facilities available in the measurement unit.

Anechoic Chamber: Generally, the E-plane and H-plane patterns can be measured in a far-field test setup (preferably in an anechoic chamber) with a standard gain antenna as a transmitting antenna and the Antenna Under Test (AUT) as a receiving antenna mounted on a pedestal that can turn the antenna around all axis.

The measurement facility used to verify the results in this thesis is an anechoic chamber at Radar Seeker Laboratory of RCI (Research Center Imarat)- one of the sister labs of DRDO (Defence Research and Development Organization), Hyderabad, India, which is a certified range of Ministry of Defence confirming to Aerospace and IS standards. The dimensions of this chamber are 22.5m in length, 12.5m wide, and 11.5m in height. It uses pyramidal microwave absorbers of size 12 inch-36 inch. It is a single reflector compact range with a quiet zone 3m×3m×3m with a FOM (Figure of Merit) of less than 0.5dB in amplitude and 5^0 in phase over the frequency range 1.5−110GHz. The sensitivity of the receiver is -120dBm. A model of the measurement facility is shown in fig. 1.19. The facility is field probed with a scanner to ensure quiet zone error limits, which are as follows:

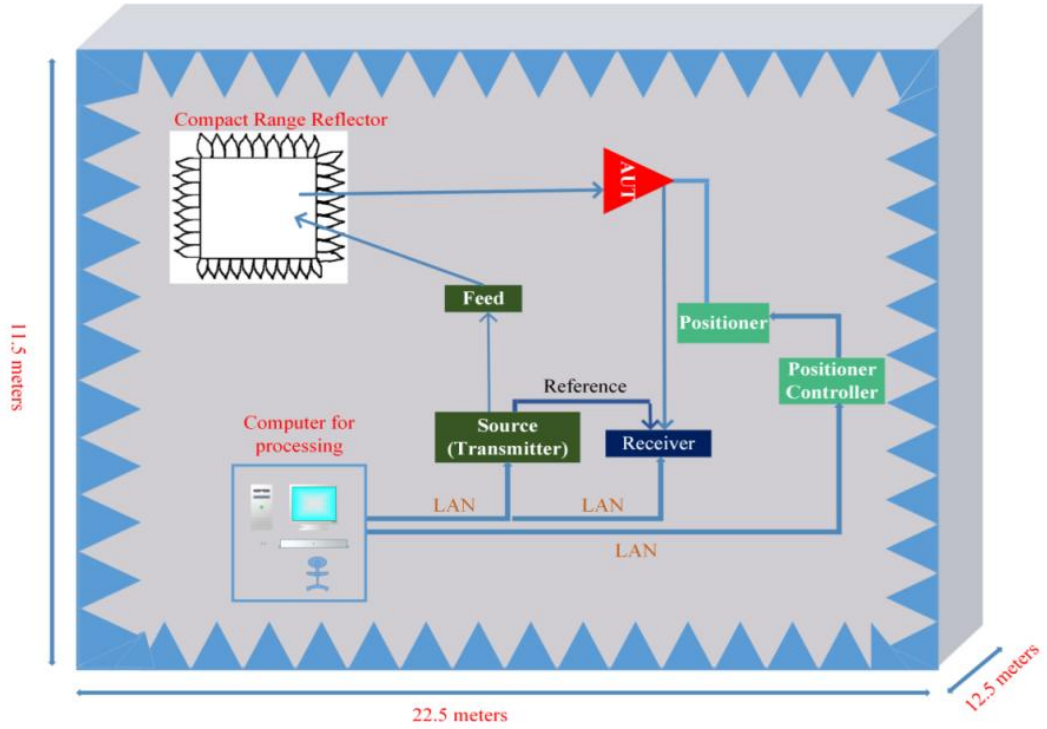

Fig. 1.19 Radiation patterns measurement setup

* The actual photos are not permitted by the defence authorities.

Table 1.1 Quiet zone (3m × 3m × 3m) error limits

Frequency range	Amplitude error		Phase error	
	Amplitude Taper (dB)	Amplitude Ripple (dB)	Phase Taper	Phase Ripple
2-4GHz	0.8	± 0.6	$< 5^0$	$\pm 5^0$
4-8GHz	0.8	± 0.4	$< 5^0$	$\pm 5^0$
8-20GHz	0.8	± 0.3	$< 5^0$	$\pm 5^0$
20-40GHz	0.8	± 0.3	$< 5^0$	$\pm 8^0$

1.5 Motivation

The demand for wireless communication has been increasing for 2 decades. Recently with the advent of 5G wireless communication applications, the usage of portable devices is more and becoming smaller. Some applications are smart homes, the internet of things and smart cities, data transferring and sharing, etc. The basic component is an antenna that operates at multi frequencies with good signal strength for these applications. For portable devices, microstrip, circularly polarized antennas are used to have less interference with good signal reception. A few techniques are applied to increase the performance characteristics of the circularly polarized antenna, such as slits, aperture coupling, superstrate, and frequency selective surfaces.

Aperture coupling is a feeding technique used to improve the antenna's bandwidth. Similarly, a shorting pin is a via placed in the dielectric layer to couple more power towards the copper patch. The metamaterial is an artificial material that does not exist in nature, but the electrical properties of the metallic elements will impact the properties of the antenna structure. Meta surface is a periodic arrangement of metallic elements, and Metamaterial superstrate is a technique used to enhance gain.

Due to the rapid usage of wireless communication, high communication capacity is required and possible through 5G wireless communication. Antenna design plays a major role and challenging task to attain high speed and data rate. Hence there is a need to study and design a compact circularly polarized antenna for 5G.

1.6 Problem Statement

To design, simulate and validate compact circularly polarized antennas for 5G wireless communication. Various techniques such as slits, shorting pin, aperture formation, superstrate, and metamaterials are used to enhance impedance bandwidth, axial ratio bandwidth, and gain of square microstrip circularly polarized antennas.

1.7 Research objectives and Scope

The objectives of the work are mentioned below:

- Design, fabricate and validate compact circularly polarized antennas for 5G wireless communication with simple and less complex structure.
- Design with compact dimensions with single feed and compare with the existing literature.
- Use the concepts of slits on the patch and partial ground for obtaining compact size and wide bandwidth.
- Improvement of gain of the antenna using dielectric superstrate concept.
- Improvement of impedance bandwidth and axial ratio fractional bandwidth of the circularly polarized antenna by using metamaterial concept (Frequency selective surface)
- To compare the simulation result with the experimental result of the above-designed antennas and also compare with the existing published work.

1.8 Contribution to the Knowledge

The key contributions of this work are summarized as follows:

a) A few simple microstrip circularly polarized slit antennas using a single coaxial feed technique are proposed for 5G wireless applications. Later various techniques are used on these basic structures to enhance the performance characteristics of the circularly polarized antennas for 5G wireless applications [2*, 3*].

b) A compact aperture coupled circularly polarized antenna is designed, and the performance is evaluated. By using the aperture coupling feeding technique for wideband and radiation characteristics for 5G radio application are obtained [4*].

c) A novel tri-band compact circularly polarized antenna with dielectric superstrate is designed for 5G WLAN and X- band applications [5*].
d) First-ever, compact Circularly polarized asymmetric U shape antenna with second-order bandpass frequency selective surface as superstrate for C-band and 5G WIFI application is designed and tested[6*]

1.9 Thesis Organization

The thesis presents the state of the art of circularly polarized microstrip antennas for 5G wireless applications. The design and analysis of circularly polarized antennas and improved performance characteristics of compact size, impedance bandwidth, axial ratio, fractional bandwidth, and gain are illustrated. The results are improved using slits, aperture coupling, dielectric superstrate, and metamaterials concept.

Chapter 1: Introduction

This chapter briefly introduces antennas and explains the importance of circularly polarized antennas in the present-day wireless environment. It also presents the importance of 5G wireless communications in day-to-day applications and their uses. Software simulation tools are also introduced to that forecast the performance of the antennas. The motivation behind this research work and thesis, objectives and contributions are also mentioned.

Chapter 2: Literature Survey

This chapter presents a detailed overview of the previous work in circularly polarized antennas for 5G wireless applications and presents their limitations. It also presents the techniques applied for the improvement of bandwidth and gain.

Chapter 3: Compact circularly polarized antennas with slits for 5G application

In this chapter, circularly polarized antennas with different slits on the patch are designed and fabricated for the 5G WLAN application. The circularly polarized antennas are designed with semi-circular and V-shaped slits on the circular patch. The circular polarization is obtained by creating asymmetry in the slits at the corners of the patch.

Chapter 4: Aperture coupled circularly polarized antenna for 5G application

In this chapter, a compact circularly polarized antenna with hook-shaped apertures was designed, fabricated, and validated experimentally for 5G application; the prototype is compared with the existing planar antennas. The compactness, wideband characteristics are obtained by incorporating various techniques like shorting pin, foam, copper plate, and bent shape feed, respectively.

Chapter 5: Compact circularly polarized antenna with dielectric superstrate for 5G WLAN and X-band application.

In this chapter, a compact circularly polarized antenna loaded with dielectric superstrate is designed, fabricated, and validated experimentally for 5G WLAN and X-band application; the prototype is compared with the existing planar antennas. The compactness, maximum gain characteristics are obtained by incorporating the dielectric superstrate and v-shaped slits on the patch. The proposed design is applicable for 5G WLAN and X- band applications.

Chapter 6: Circularly polarized asymmetric U shape antenna with second-order bandpass frequency selective surface.

This chapter presents the design and performance evaluation of asymmetric U shape antenna with second-order bandpass frequency selective surface as superstrate for C-band and 5G WIFI applications.

Chapter 7: Conclusions & Future Scope

A consolidation of the results is presented. Compact circularly polarized antennas with various techniques are designed for 5G wireless applications with wide bandwidth and better gain. Thus the results obtained indicate that the designed circularly polarized antennas are a good candidate for 5G wireless applications. This chapter concludes the thesis and the open issues for future scope are mentioned.

Chapter 2

Literature Review

This section briefly gives the published literature on circularly polarized antennas, 5G wireless applications, impedance bandwidth, and gain enhancement techniques enforced on planar antennas. The techniques existing in the published research are studied, and their drawbacks are highlighted.

CP antenna bandwidth is improved by loading the slots. A new flexible antenna designed for 5G mobile phones by Kamingmak [28]. The antenna is composed of a slotted hat shape patch, dielectric substrate, a double-sided printed-circuit-board (PCB), a metallic block. Here the design is complex, the impedance bandwidth of the antenna is over 10%, and the 3-dB axial ratio bandwidth is 3.05%.

Hang Wong et al. proposed a probe-fed antenna for 5G wideband wireless devices [29]. In this design, the meandering structure is embedded in the three substrates layers with the help of the probe technique. CP bandwidth is improved by embedding probe feed in a stacked layer of the various substrates for 5G wireless fidelity (Wi-Fi). By truncating the corners of the patch, the bandwidth of CP may also be improved [30-31].

Hang Wong et al. presented a circularly polarized planar antenna with embedded virtual short for wireless communication systems [32]. Here the size of the antenna is reduced by employing parasitic shorting strip elements but retained broadside radiation pattern. The antenna has a single band with an impedance bandwidth are 93MHz, an axial ratio of 21 MHz.

Nasimuddin et al. exhibited the four compact asymmetric-slit microstrip-designed antennas with circular polarization [33]. The antenna has four slits formed at the corners, out of which one slit area is more than the other, in turn, generates circular polarization. Although the proposed prototype is low profile, the measured 10-dB return loss and 3-dB axial-ratio bandwidths of the antenna prototype are low, around 2.5% and 0.5%, respectively.

In substrate integrated waveguide cavity, a slot antenna is placed at the backed position, this antenna can produce CP, but the size is bulky [34]. In the quasi magnetic-electric

region, a technique of shorting the patch is studied in [35]. On the patch, Slots are embedded and are positioned in a symmetrical manner [36]. Another form of arranging slots in a Crossed manner with unequal lengths on the circular patch results in CP [37]. An EBG antenna of a triangular shape is designed with effective directivity [38].

Circular polarization is classified on the number of feed points on the microstrip antenna. A single feed is more advantageous since it does not require an external polarizer. A simple and novel annular-ring slotted microstrip patch antenna loaded by a surface mount chip capacitor for circularly polarized (CP) radiation is designed by Jianxing Li et al. [39]. With the appropriate positioning of a capacitor on an annular slot in a microstrip patch, the fundamental resonant mode can be degenerated into two orthogonal modes with equal amplitude and quadrature phase.

Xiao Zhang designed a circularly polarized slotted patch antenna with vias at are center positioned at four quadrants [40]. The antenna has a 10-dB return loss bandwidth of 90.0 MHz (1.565–1.655 GHz) with a maximum gain of 4.65 dB at 1.58 GHz.

Wen-Shyang Chen et al. l designed a compact circularly polarized square microstrip antenna with four slits and truncated corners [41]. The designed prototype attained an axial ratio of bandwidth 0.84% at a resonant frequency of 2.2GHz and a maximum gain of 2.8dBic. The slit technique is loaded on textile for wireless applications [42]. Loading of shorting pin gives larger gain but very less in bandwidth and not compact [43].

He Huang et al. exhibited a dual-polarized patch antenna for 5G application. Here four triangular slots are etched on the patch to direct the current in the slant direction [44]. Then two coupled lines are crosswise placed on the top layer of the medium substrate to improve the structural symmetry and couple the energy to the patch. The fabricated design is useful for 5G radio applications.

Kirov et al. proposed a broadband circularly polarized antenna with an aperture coupling feeding technique is described [45]. Here cross slots are embedded in the ground plane for reducing the back radiation, and a stacking structure with a screen is discussed. The designed antenna operates in Ku-Band The maximum impedance bandwidth obtained from the various designs is 16%, and a gain of 6.8dBi is attained.

Lei Ge et al. designed a magneto-electric dipole antenna for a 5G WiFi application and resonates in the band of 5.07 GHz to 5.95 GHz for the china country. The obtained overlapped bandwidth of 16% and gain of 8.2dBi are attained [46].

Lau et al. proposed a wideband antenna with circular polarization, and a Wilkinson power divider is connected to the feed [47]. Here, the aperture is utilized, L-probe is used to feed the patch orthogonally, and the air is used as a dielectric substrate maintained a gap of $0.1\lambda_o$ between the patch and ground plane. The antenna resonates at 1.65GHz, respectively.

Liu et al. presented a single feed aperture coupled stack antenna with a square loop radiator. The square loop radiator with perturbation effects both the dual-mode and orthogonal mode simultaneously. The antenna presents an axial ratio of 2.5% is attained [48].

Nasimuddin et al. proposed an aperture coupled asymmetrical C-shaped slot antenna [49]. Circular polarization is achieved by loading asymmetrical C-shaped slots onto the patch using an aperture coupling. The obtained return loss bandwidth of 16% and axial ratio bandwidth of 3.3% were attained.

Aperture coupled circularly polarized square slot ring antenna fed through serial coupling is proposed by Chang et al. [50]. In this design, the aperture contains a square slot ring with four short branch slots protruding toward the center of the ring, but the axial ratio bandwidth of 8.7% is achieved with a large ground plane of 90mmx90mm, respectively.

Liao et al. adopted an aperture-coupling technique with a square patch antenna [51].In a square ring antenna, four square patches are added at the four angles to produce circular polarization for the wireless communication system. The impedance bandwidth of 7.44%, the axial ratio of 1.3%, and gain of 6dBi were achieved, respectively.

Lai et al. proposed a wideband antenna with circular polarization [52]. Here four Γ-shaped slots are embedded in the ground plane to generate four phases of sources to excite the antenna. The aperture-coupled antenna provides an impedance bandwidth of 16.5% and an axial ratio of 13.3%.

Haraz et al. designed a wideband aperture coupled antenna for a wireless communication system [53]. Here the antenna is modeled for a single transmitter and single

receiver with a robust channel modeling system. For indoor wireless channel, fractional bandwidth of 15% and gain of 7.25dBi were achieved.

Gupta et al. examined a dual-band rectangle dielectric resonator for wireless applications. With the help of a feeding structure, i.e., triangular ring-shaped aperture and an additional parasitic strip connector to the resonator generates circularly polarized waves in dual bands [54]. The dielectric resonator antenna's maximum impedance bandwidth of 14% and the axial ratio of 3% are attained.

Dash et al. proposed a superstrate loaded cylindrical dielectric resonator antenna is developed [55]. The antenna consists of a cross-shaped slot as the aperture for exciting the dielectric resonator, and on this, a superstrate is loaded for dual-band operation. The designed antenna obtained a maximum bandwidth of 600MHz and a maximum gain of 8dBi, respectively.

Wang et al. designed a dual circularly polarized microstrip array for satellite communication [56]. In this antenna, microstrip feed in the ground plane provides an orthogonal phase for circular polarization. Maximum impedance bandwidth of 6.75% and the axial ratio of 2.84%achieved.

A single-feed circularly polarised aperture-coupled square patch is presented by Buffi et al. [57]. In this research work, a square ring slot has been adopted to implement the coupling mechanism. Simple geometrical modification on the patch has been done, and an axial ratio fractional bandwidth of 9% is obtained.

Patel et al. introduced multiple split-ring resonator as superstrate or substrate on a microstrip patch antenna and numerically analyzed spacing between the rings for various designs and bandwidth of 980MHz and gain of 3dBi with antenna size 50mmx35mm respectively[58]. A dual-band is designed on a circularly polarized antenna with a metal ring superstrate presented by Chandrashekar. With the support of dielectric posts, a metal ring configuration is placed above the rectangular patch antenna. In this configuration maximum impedance bandwidth of 6% and gain of 10dBi is obtained at the resonant frequencies. [59].

Gupta designed an array of parasitic patches, which are loaded on the partial reflecting surface upon the high gain antenna. The configuration of parasitic patches and its effect on the

patch antenna is analyzed with various materials. With the help of this technique, the gain is enhanced, which is discussed in [60]. Sachin Kumar et al. adopted three configurations of circularly polarized antennas with stacking technique and loaded with a superstrate is analyzed[61-62].

The design of a pi-shaped patch antenna using superstrate configuration is proposed by Shah [63]. The antenna configuration consists of a defected ground plane, and a pi slotted radiating patch with omnidirectional radiation characteristics; the design size of the design is15mmx20mm. The antenna resonates at 3GHz, 3.6GHz, 3.7GHz, and 4.5 GHz, with an impedance bandwidth of 100-180MHz is obtained. J.S. Row investigated circularly polarized cross slot coupled antenna loaded with various thicknesses of superstrate. With the loading effect, the center frequency is shifted; bad impedance matching is adjusted by varying the thickness of the superstrate with improved impedance bandwidth [64].

Ta et al. proposed a new method to improve the gain and bandwidth of the dielectric superstrate antenna. With the effect of loading superstrate, gain enhancement, extra circular polarization radiation of the antenna and broadens the axial ratio bandwidth significantly. The overall size of the antenna is 40mmx40mmx17.45mm, respectively [65].

Mohamad et al. introduced anisotropic miniaturized element frequency selective surfaces for designing wideband circular polarization selective surfaces [66]. On this surface, metallic layers are designed as capacitive and inductive grid wires with asymmetric dimensions. Fractional bandwidth of 40% is obtained, and cross-polarization discrimination of 15dB is attained.

Chaimool et al. propose a metamaterials reflective surface as a superstrate for circularly polarized antenna [67]. The unit cells in the metasurface are corner truncated diagonally to each other and arranged in a 4x4 pattern. The bandwidth of 14% is reached with the metamaterials reflective surface.

Bouslama et al. designed a Frequency selective surface for the gain enhancement of microstrip antenna at the desired frequency for WLAN application [68]. Here the FSS acts as a

filter printed on the top of 0.381 mm thickness, ROTMM6 substrate, with the dielectric constant ε_r=6 and obtains gain up to 9.4dBi respectively.

Singh et al. designed a high reflective frequency selective surface (HRFSS) superstrate optimized for improved gain [69]. The design consists of a shorting pin at the bottom of the rectangular patch and a slot on the top surface that achieved a gain of 10.65dBi.

Gangwar et al. proposed a dielectric resonator antenna with superstrate is analyzed [70]. It behaves as a polarizer to achieve circular polarization, and frequency selective surface is incorporated as superstrate for the enhancement of bandwidth of 73.76%, but peak gain up to 5.6dBic is attained. Dey et al. present a circularly polarized antenna with FSS as a superstrate for WLAN application [71]. The patch is loaded with asymmetric complementary split-ring resonators to achieve circular polarization. Impedance bandwidth of 4.95% and gain of 3dBic is attained.

Mondal et al. investigated three shapes of different antennas with FSS based microstrip antenna for Wimax and WLAN application [72]. The design consists of E-shaped and T-shaped patches, and U-shaped slits with slots are loaded in the ground plane. Impedance bandwidth of 6.4Ghz and gain of 8 dBi are achieved, respectively.

Arnmanee et al. present a microstrip antenna integrated with modified FSS and High impedance surface elements to improve the performance characteristics of the design [73]. The design achieves a bandwidth of 200MHz and a gain of 10dBi. Zhou et al. presented a dual-band FSS based on circular aperture coupled patches [74]. The structure consists of circular patches and circular coupling apertures with different sizes of the same shapes. The bandwidth of 1 GHz is achieved in the frequency of interest band.

Manoochehri et al. designed a second-order bandpass frequency response using the Frequency selective surface technique [75].

Fakhte et al. focused on characteristics of the conventional patch antenna and combined the technique of FSS as superstrate and artificial magnetic conductor in the ground plane for X-band application [76]. The design presents a bandwidth of 20% and gain up to

16dbi.Nghianguyen-trong et al. presented a wideband circularly polarized Fabry-Perot resonator antenna for satellite applications [77].

Mutluer et al. presented a single layer multi-band reflective frequency selective surface (FSS) design [78]. The design is hybrid, three-armed geometry is placed in the center, and two armed geometries are placed in each quadrant of the unit cell; the design has a stable response up to 60 °of incident angles.

Chatterjee et al. proposed a second-order bandpass multi-layered frequency selective surface (FSS) as a superstrate with a non-resonant unit cell in each layer [79]. The composite structure attains a bandwidth of 65% and an average gain of up to 6-8dBi. Mudar Al-Joumayly et al. propose a method for designing low profile frequency selective surfaces (FSS) with second-order bandpass responses [80]. It consists of unit cells of sub-wavelength periodicities in the order of $0.5\lambda_0$.

Chapter 3

Compact circularly polarized antennas with slits for 5G application

This chapter introduces two circular polarization microstrip antennas for various wireless communication applications. At first, a semi-circular slit microstrip patch antenna for 5G WLAN applications and secondly, a compact circularly polarized antenna for 5G radio application. The performance of the proposed antennas is compared with the existing antennas.

3.1 Circularly polarized antenna with semi-circular shaped slits

3.1.1 Antenna design and configuration

The configuration of the CP with a semi-circular-shaped slit antenna is indicated in Fig.3.1 (a), and Fig.3.1 (b) shows the cross-sectional view. This antenna is intended at the desired frequency of 5.37 GHz with radius '*r*' on a square substrate of thickness '*t*.' Rogers RT Duroid 5880 is used as a substrate (t = 0.787mm, ε_r = 2.2, tanδ = 0.005) and the fabricated antenna is shown in Fig.3.2. For proper impedance matching, the antenna is fed through the coaxial feed.

For better radiation characteristics in a circular path antenna, semi-circular slits are formed at $\theta = 90°$ at all four quadrants and pitch the patch's electrical length. An asymmetry is created on the patch by making the dimensions of the radius of the slits equal in three quadrants of radius (r_1) and at other of the radius (r_2) at the fourth quadrant of the circular sector results in circular polarization.

A design technique is formulated based on the cavity model formulation. The process uses that the recognized information includes the resonant frequency (f_r), a dielectric constant of the substrate (ε_r), and the height of the substrate *h*. The radius *r* of the circular patch as a function of h and ε is given by [4].

$$r = \frac{F}{\sqrt{1+\frac{2h}{\pi\varepsilon r F}\left[\ln\left(\frac{\pi F}{2h}\right)+1.7726\right]}} \tag{3.1}$$

where *F* is given below:

$$F = \frac{8.791x10^9}{f_r\sqrt{\varepsilon_r}}$$

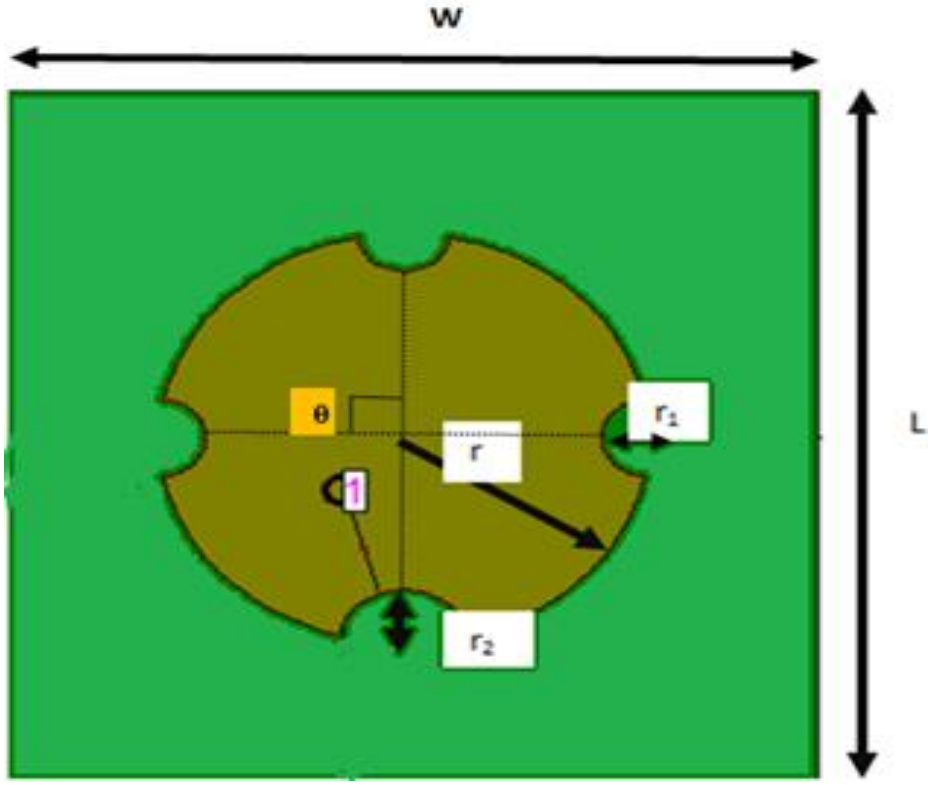

(a)

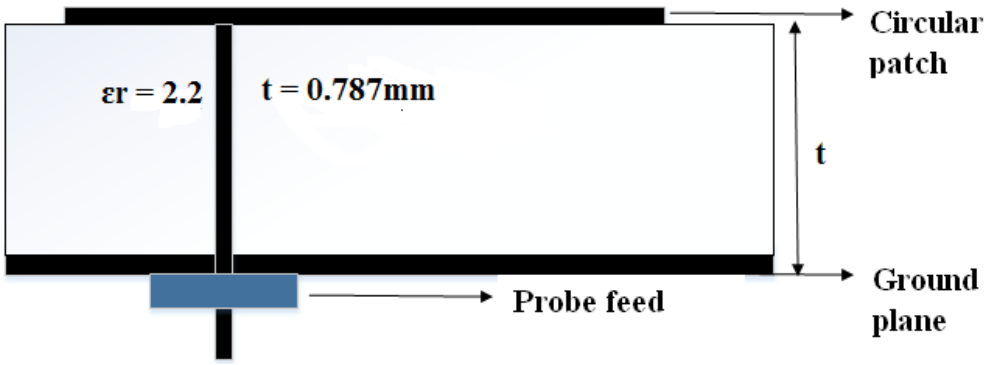

(b)

Fig.3.1The layout of the circularly polarized semi-circular slit antenna for 5G WLAN (a) top view (b) cross-sectional view.

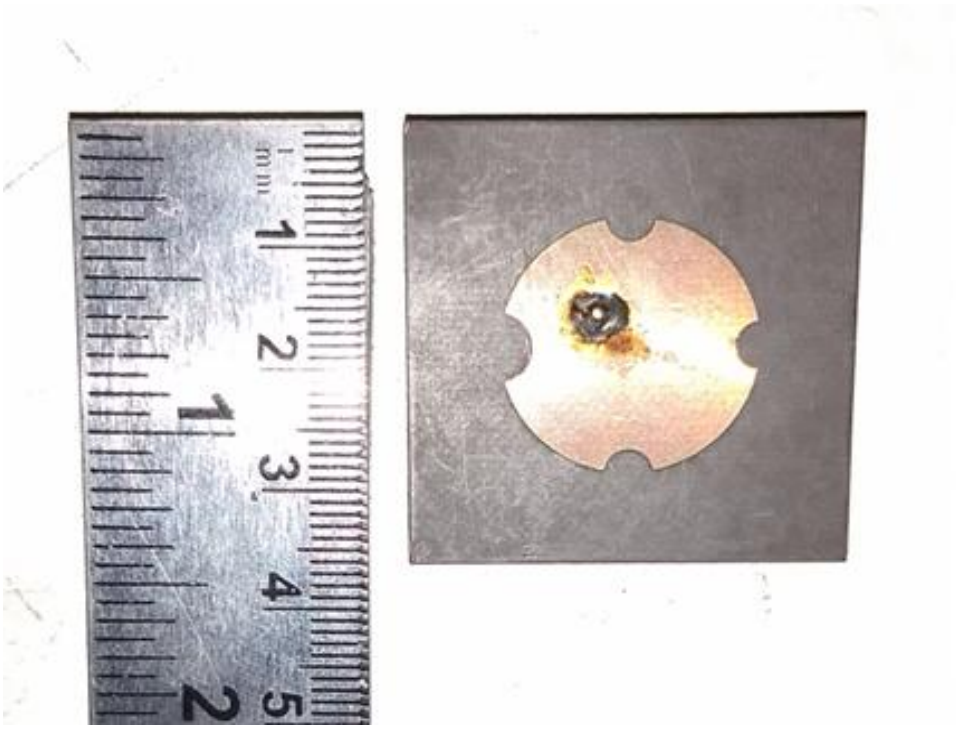

Fig.3.2 Fabricated antenna

3.1.2 Simulated results

To study the characteristic performance of the proposed antenna in terms of achieving the desired results to a software IE3D CAD tool, based on the moment method is used for essential numerical analysis and to obtain the appropriate geometrical parameters in fig. 3.1. Based on Green's function, only the primary formulation of the IE3D software is achieved through an integral equation, as explained in Chapter 2.

Fig.3.2 shows the fabricated antenna, and CP is obtained by generating asymmetry in semi-circular slits at four sides on the circular patch. The position of the feed is better analyzed at (−2.7, −2.7) with respect to the circular patch centre. For better performance, the value of r_2 is minimized. The parameters of the designed antenna are shown in Table 3.1.

Table.3.1 Parameters of designed antenna

Parameter	Value	Parameter	Value
L	36 mm	r_1	2 mm
w	36 mm	r_2	2.9 mm
r	10.6 mm	t	0.787 mm

Table.3.2 Effect of the radius of r_2 of a semi-circular slit on the performance characteristics of the semi-circular slit cp antenna.

r_2 value	Resonant frequency (GHz)	Impedance bandwidth(10 dB), %	Axial ratio bandwidth (3 dB)(%MHz)	Gain, dBi
3.1	5.51	4.71 (5.33 GHz – 5.59 GHz)	0.5 (5.34 GHz– 5.37 GHz)	6.681
2.9	5.37	3.9 (5.251 GHz– 5.45 GHz)	1.1 (5.33 GHz– 5.39 GHz)	6.638
2.8	5.50	4.53 (5.33 GH z–5.58 GHz)	0.7 (5.34 GHz– 5.37 GHz)	6.67

By varying radius, r_2 value on the semi-circular slit will effect parameters like reflection coefficient, gain, impedance bandwidth, etc., and are also evaluated. Table 3.2 shows the execution parameters of the anticipated antenna for various values of r_2, and the consequent performance characteristics are shown in Fig. (3.3-3.4). With numerous iterations, the value of r_2 is fixed at 2.9 mm for the WLAN application band. Modifying the radius r_2 results in the alter of resonant frequency and regularly bandwidth decreases.

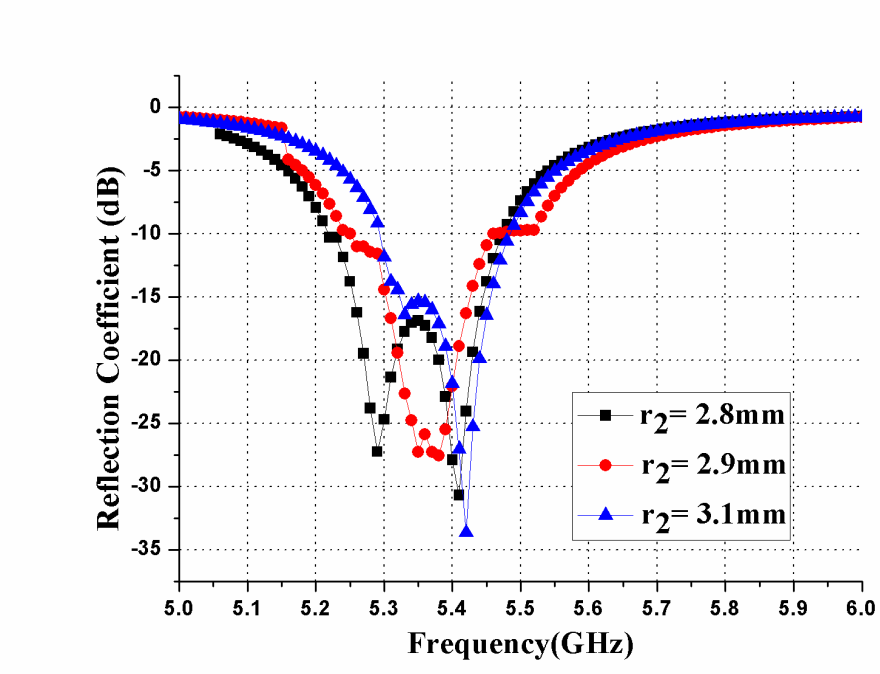

Fig.3.3 Return loss of the antenna for different values of radius r_2

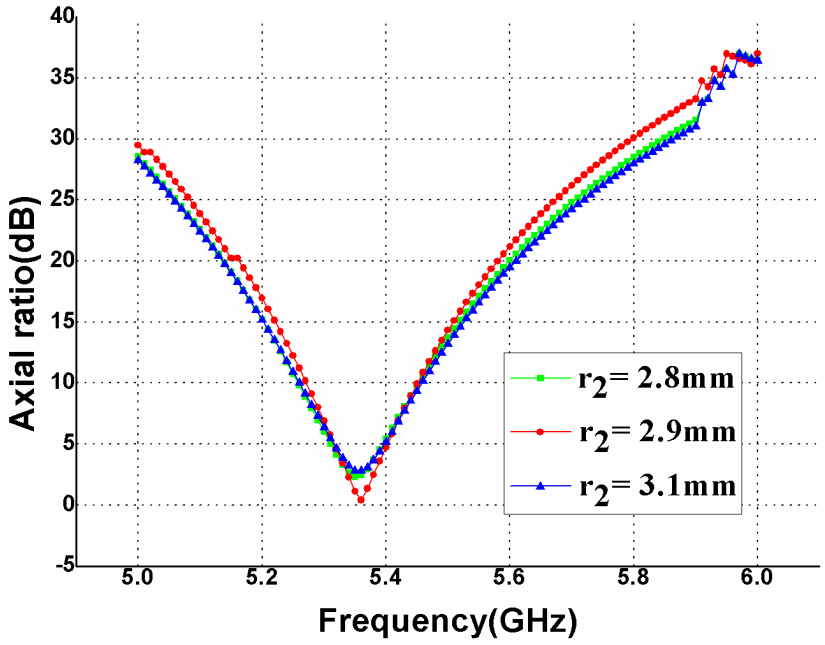

Fig.3.4 Axial ratio for various values of radius r_2

3.1.3. Measured results

After fabrication, the performance of the proposed prototype is analyzed by a parameter reflection coefficient or return loss; the return loss is shown in Fig. 3.5. The measured reflection coefficient is 28.45 dB at the desired frequency of 5.37 GHz with a bandwidth of 210 MHz in the range of 5.25–5.45 GHz. The above performance characteristics in return loss show that the proposed antenna is suitable for WLAN application.

The measured gain at the desired frequency of 5.37 GHz is 6.63 dBi and is illustrated in Fig. 3.6. One of the factors that majorly focused on whether CP is attained or not depends on the axial ratio presented in Fig.3.7.The measured axial ratio is 0.34 dB, and a 3dB bandwidth of 60 MHz in the frequency range of 5.33–5.39 GHz is attained.

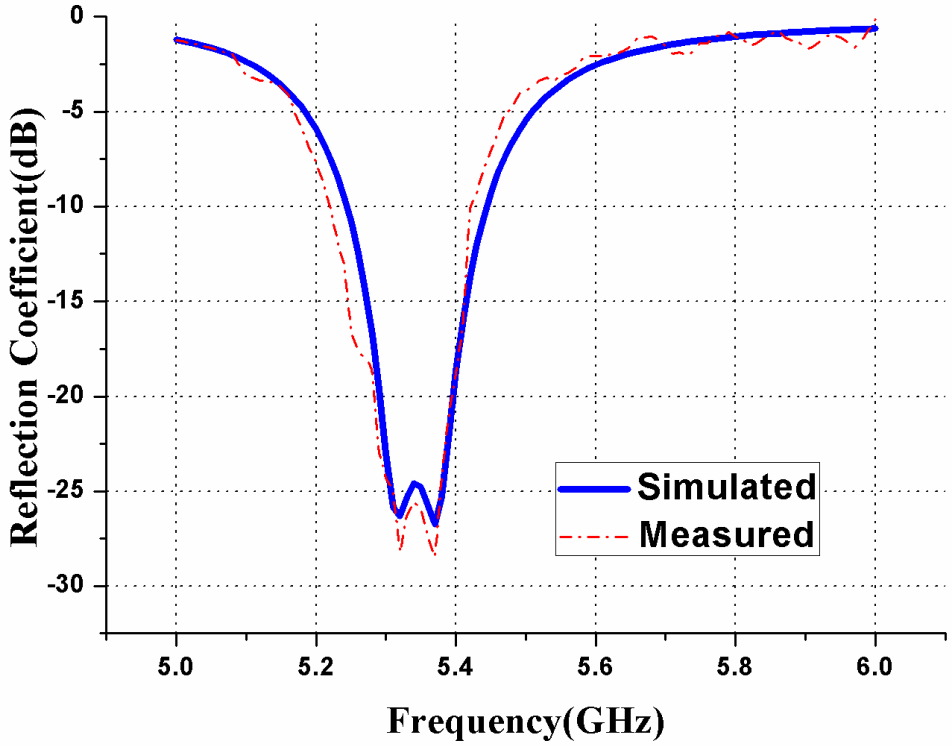

Fig.3.5 Reflection coefficient for the proposed design

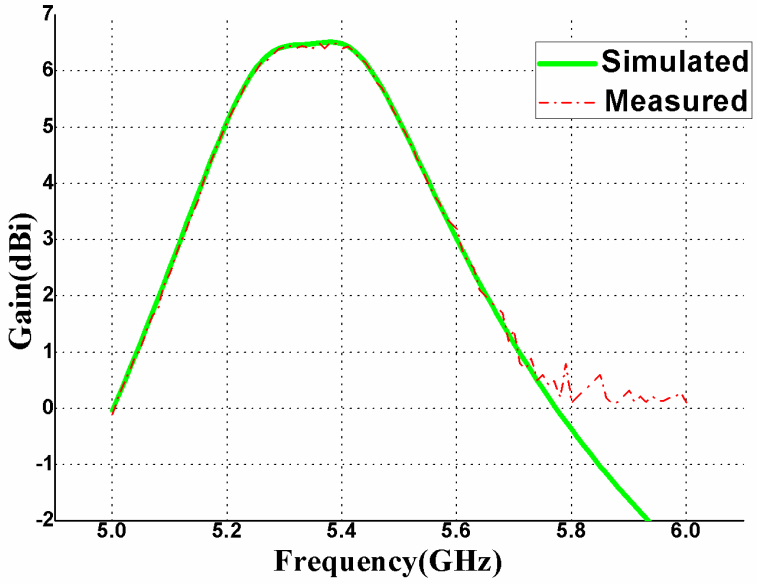

Fig.3.6 Gain of the antenna

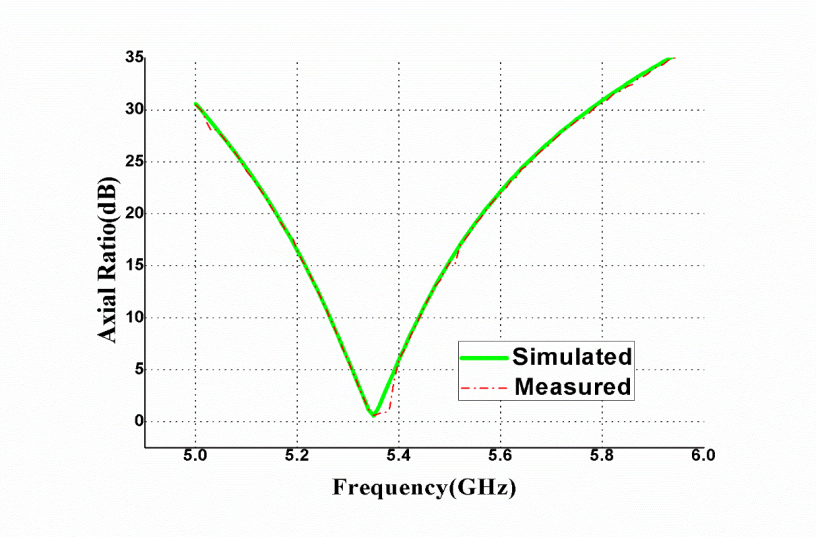

Fig.3.7 Axial ratio of the antenna

2D-Radiation Pattern

Figs.3.8-3.9 illustrate the azimuth and elevation planes in which both the simulated, measured results are compared at the desired frequency of 5.37 GHz. Fig. 3.10 presents VSWR (Voltage Standing Wave Ratio) for the antenna. The radiation efficiency of 74 % is attained for the prototype antenna (see Fig.3.11).

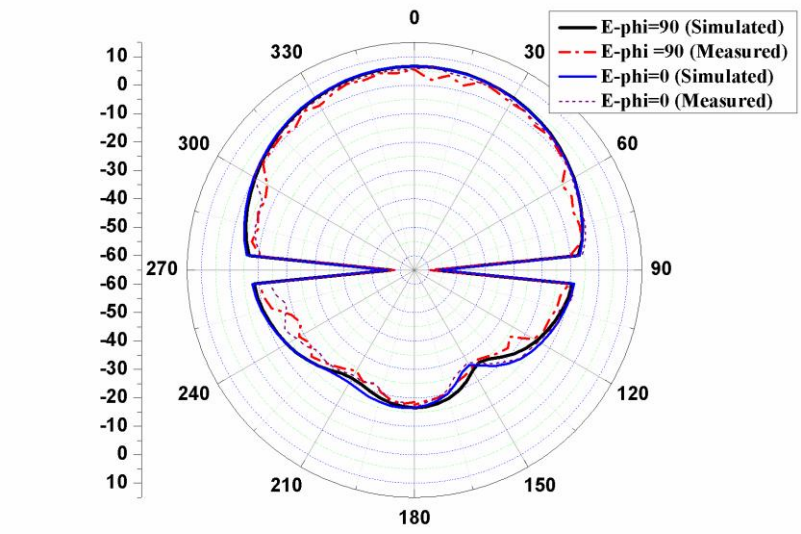

Fig.3.8 2-D Elevation pattern for the circularly polarized semi-circular slit antenna at the resonant frequency of 5.37GHz.

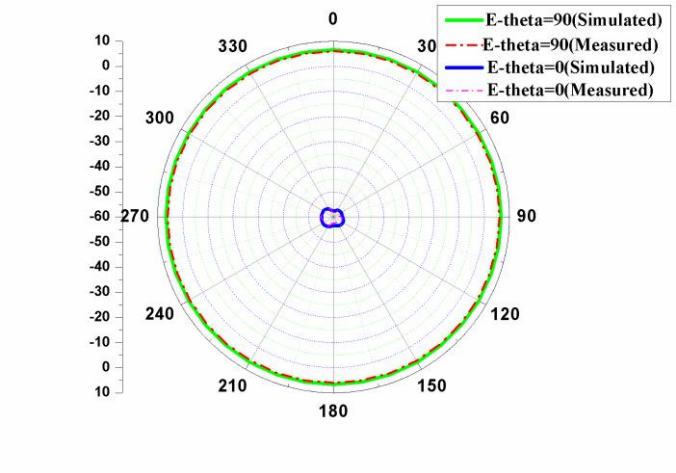

Fig.3.9 2-D Azimuth pattern for the circularly polarized semi-circular slit antenna at the resonant frequency of 5.37GHz.

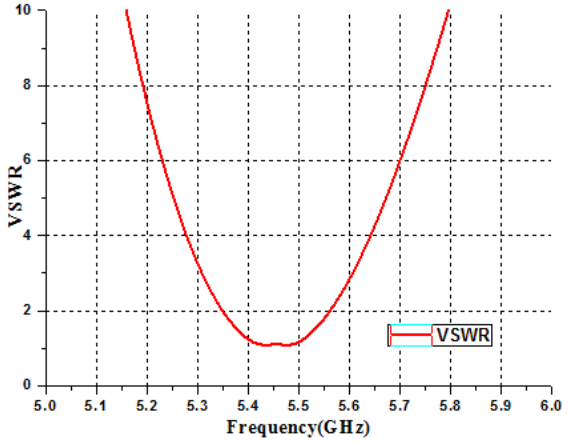

Fig.3.10 VSWR for the CP semi-circular slit antenna.

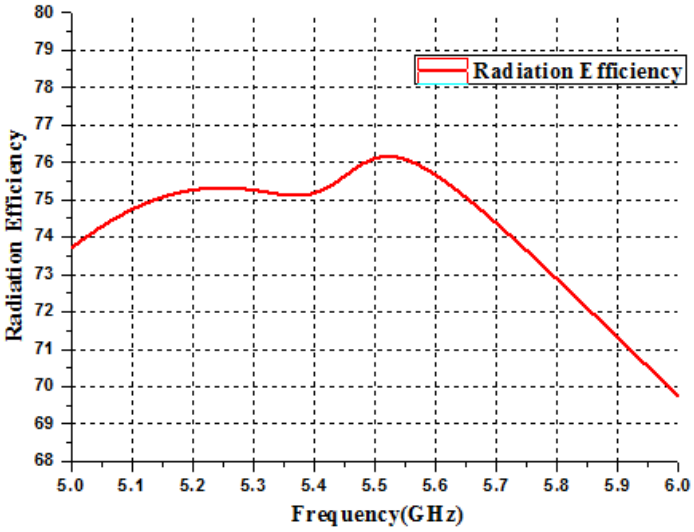

Fig.3.11 Radiation efficiency

3.1.4 Surface current distribution

Usually, in a conductor, current occurs due to the charge acceleration and deceleration. If it occurs in a dielectric material, it is a time-varying current due to the medium and will generate radiation in the antenna. Normally, the microstrip antenna is excited by a feed to couple electromagnetic energy in or out of the patch, and then charges get accumulated on which it will result in a current. Due to the formation of charge distribution, the potential difference exists, then the current starts flowing from the ground to the patch, in respect to it ,and charge distribution is present at the microstrip surface and ground plane.

Fig.3.12 illustrates that most of the high current density is at the edges and on the patch's top surface at the desired frequency. Therefore, the magnetic field component, which is oblique to the patch edge, is small. Reactive and resistive components are there at the input impedance of the microstrip antenna. The power radiated by the antenna is due to the resistive elements in antenna and power loss by radiation and dielectric mainly due to the occurrence of imaginary poles and even conduction losses. Current distribution on the microstrip patch surface with the addition of deep semi-circular slit changes current density in magnitude and the direction along with the various time intervals. It can be observed in Fig.3.12, which in turn creates CP at the desired frequency.

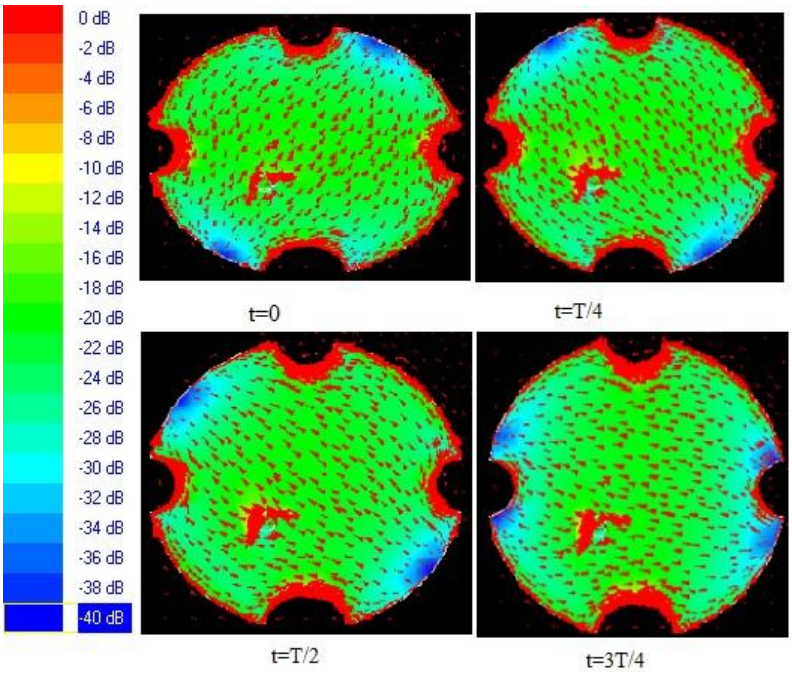

Fig.3.12 Surface current distribution for the antenna at a resonant frequency of 5.37GHz.

Now charge density is analyzed as a group of vectors in which each vector is a major current component in the microstrip radiating patch. The simulated normalized current distributions are indicated at various time intervals t = 0, T/4, T/2, and 3T/4. It is observed that the vector sum of the major components at t = 0 is orthogonal to that of t=T/4. Thus, a CP mode is obtained in a microstrip patch antenna; the performance parameters like radiation pattern, input impedance, bandwidth, and resonant frequency are guarded by the surface current produced on the microstrip patch.Table.3.3 shows the performance comparison of the proposed antenna with some of the existing designs.

Table.3.3 Performance comparison of the circularly polarized semi-circular slit antenna with some of the existing designs

References	Frequency, GHz	10 dB impedance bandwidth % (MHz)	3 dB axial ratio bandwidth % (MHz)	Gain, dBi	Size of the antenna
[32]	2.487–2.501	3.25	0.62	3.8	0.174 λ_0 × 0.174 λ_0 × 0.026 λ_0
[33]	2.404–2.416	2.10	0.5	4.35	0.288 λ_0 × 0.288 λ_0 × 0.0118 λ_0
[34]	14.38–14.94	4	0.83	7.1–7.4	1.03 λ_0 × 0.56 λ_0 × 0.0372 λ_0
[35]	5.84–6.00	2	0.33	8.5	0.5 λ_0 × 0.5 λ_0 × 0.03 λ_0
[36]	2.138–2.230	4.2	0.8	–	0.436 λ_0 × 0.436 λ_0 × 0.0116 λ_0
[43]	5.7–5.8	4.3	–	2.3–3.3	1.74 λ_0 × 0.313 λ_0 × 0.0386 λ_0
[37]	2.45–2.55	4	–	24 dB (directivity)	–
Proposed antenna	**5.35–5.56**	**3.9**	**1.1**	**6.67**	**0.65 λ_0 × 0.65 λ_0 × 0.01λ_0**

3.1.5 Measurement Set up

When an antenna is fabricated with a finalized design its performance parameters like return loss, axial ratio, gain, radiation efficiency, and radiation characteristics are measured using the Network Analyser. and Antenna measurement setup, to evaluate the performance, and

the antenna parameters using a vector network analyzer are calibrated once the ports are matched, Fig. 3.13. After the matching is done, the antenna is connected to port 1 and matched load to port 2, as shown in Fig.3.14 and Fig.3.15 illustrate the measured return loss for the proposed antenna.

Fig.3.13 Ports are connected via a coaxial cable for matching

Fig.3.14 An antenna connected to one port and matched load with other port.

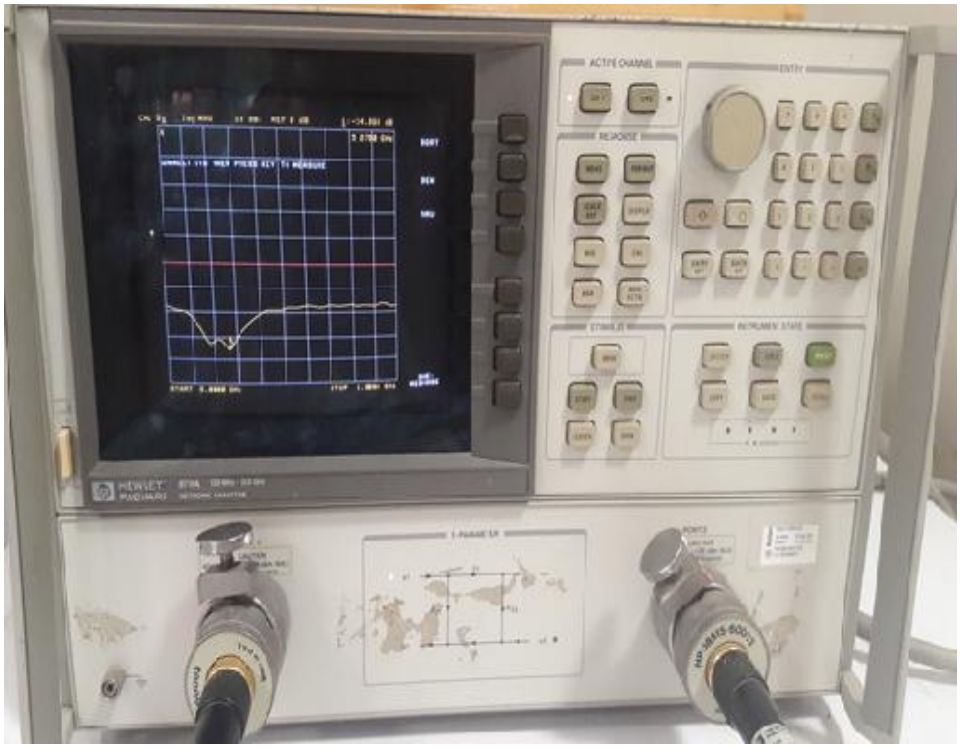

Fig.3.15 Measured return loss for the circularly polarized semi-circular slit antenna for 5G WLAN application

The proposed circularly polarized antenna is compared with similar antennas updated in the literature with respect to various design parameters, as shown in Table 3.3. The measured results of the proposed antenna are in agreement with the simulated ones.

3.2 Circularly polarized antenna with V-shaped slits

3.2.1 Antenna structure

The designed circularly polarized patch Antenna (CPPA) of circular shape with radius r= "10.4mm" is fabricated using FR4 substrate of thickness h= "2mm" and ε_r=4.4. The dimensions of the patch antenna with the ground plane on the other side are shown in Fig.3.16. Triangular-shaped narrow slits are cut on the four quadrants of the circular patch. One of the corner slits is cut deeper to create asymmetry in the structure, resulting in circular polarization.

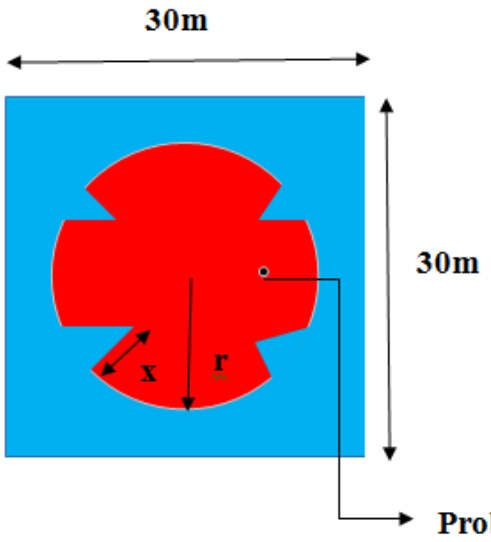

(a)

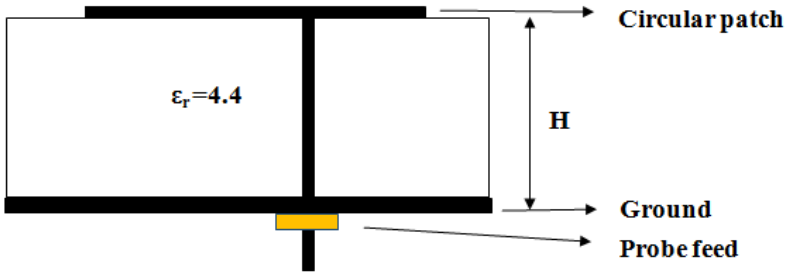

(b)

Fig.3.16 Layout of the proposed antenna (a) Top view (b) Cross-sectional view.

Here 'x' is the distance between the corner edge ends to the slit edge. A parametric analysis is carried out for feed point and distance 'x' as shown in Figs.3.17-3.18. Surface charge distribution on the patch for various intervals is shown in Fig.3.19, and Fig.3.20 shows the smith chart of the fabricated antenna. After parametric analysis with optimum parameters, the antenna design is fabricated shown in as Fig.3.21.

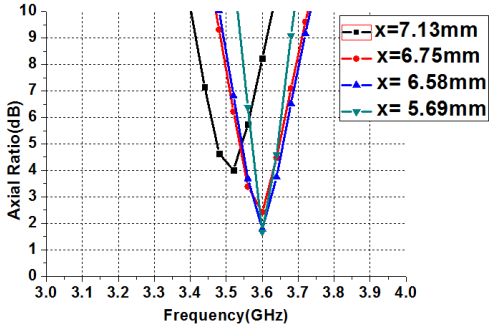

Fig.3.17 Simulated axial ratio for the proposed antenna with different x values.

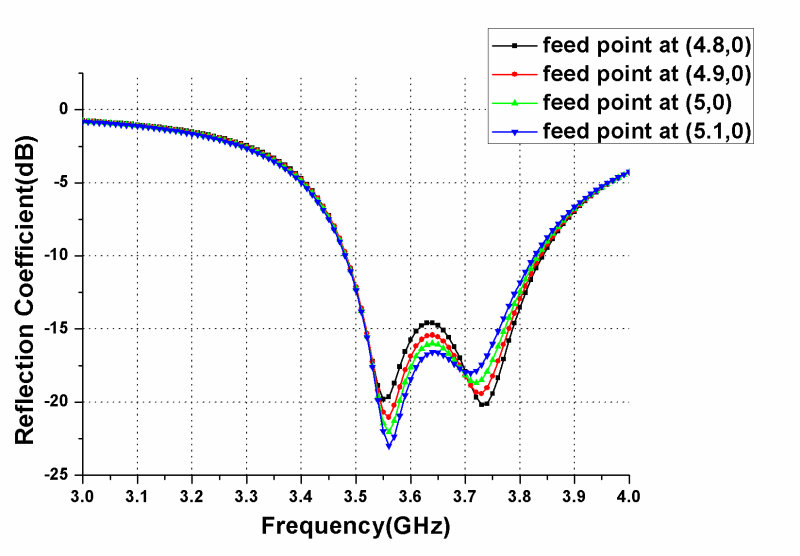

Fig.3.18 Simulated Reflection coefficient for the proposed antenna with different feed point locations.

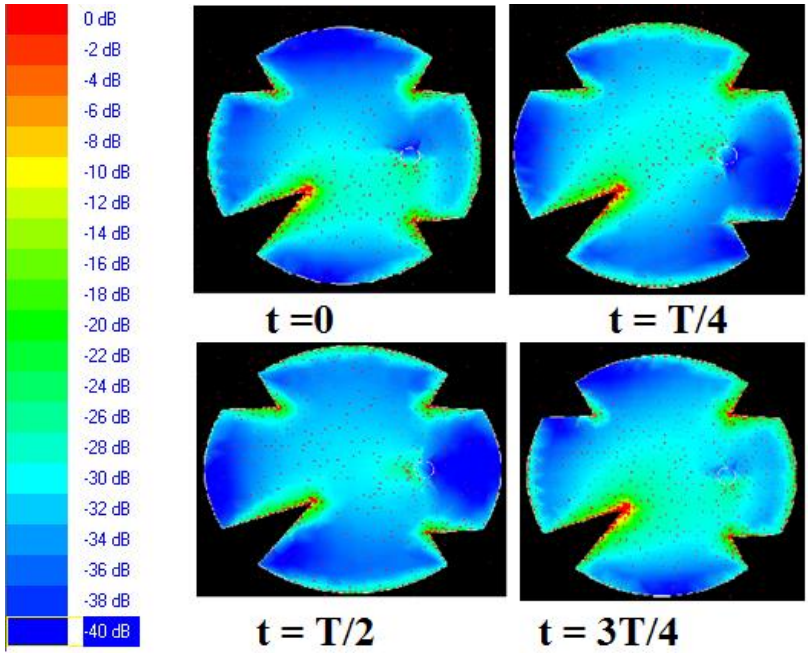

Fig.3.19 Simulated current distributions of the proposed antenna at resonant frequency 3.56GHz.

3.2.2 Simulated and measured results

To check the performance of the proposed design, the return loss is shown in fig.3.22. For the fabricated antenna, the measured reflection coefficient is 26.5dB at resonant frequency 3.56 GHz with 10dB impedance bandwidth of 360MHz falls in the range 3.44GHz-3.8GHz.It clearly shows that the designed antenna is suitable for the WiMAX application.

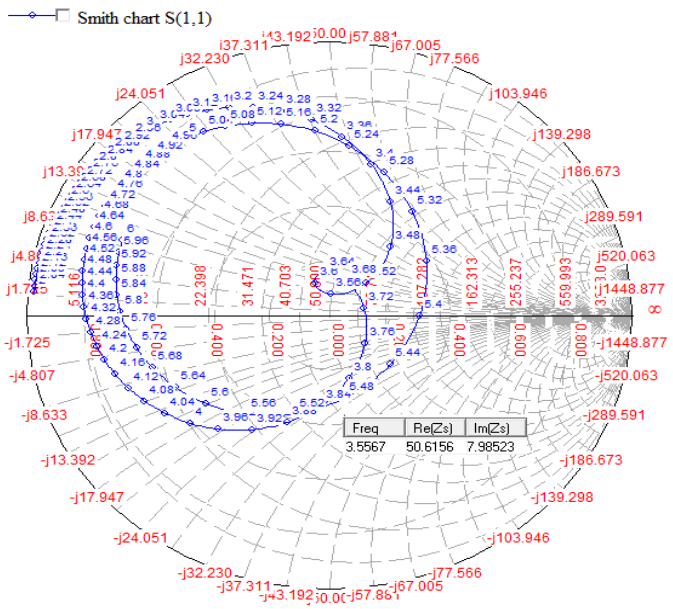

Fig.3.20 Smith Chart of the antenna.

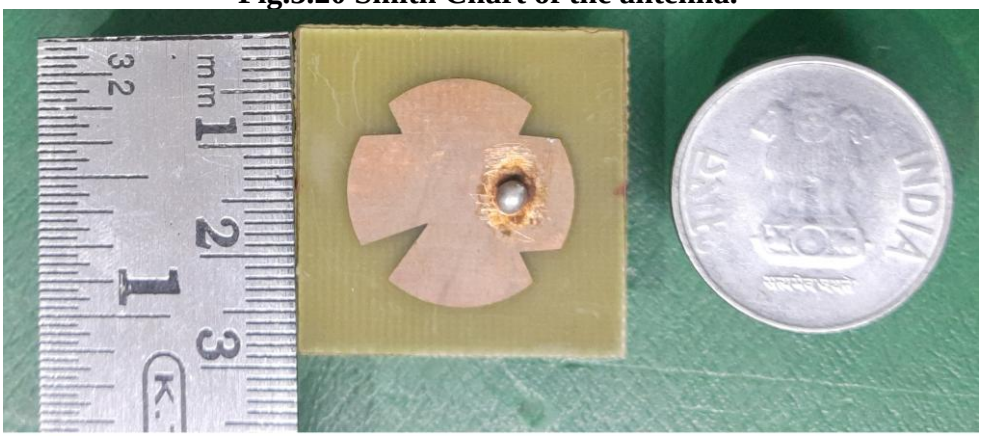

Fig.3.21 Fabricated antenna designed at 3.56GHz.

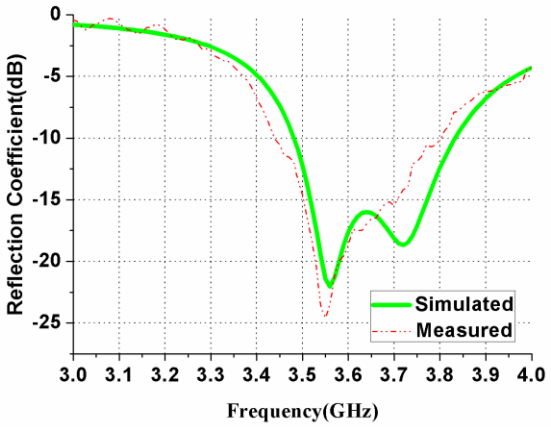

Fig.3.22 Reflection coefficient (simulated vs. measured) of the antenna

For the proposed antenna, the gain graph is shown in Fig.3.23; the axial ratio of 1.7dB and bandwidth of 70MHz in frequency range 3.56GHz-3.63GHz are obtained are shown in fig.3.24. The performance parameters are summarized in Table.3.4. Radiation patterns in azimuth and elevation planes, VSWR(voltage standing wave ratio) are shown in Figs. 3.23-3.26.

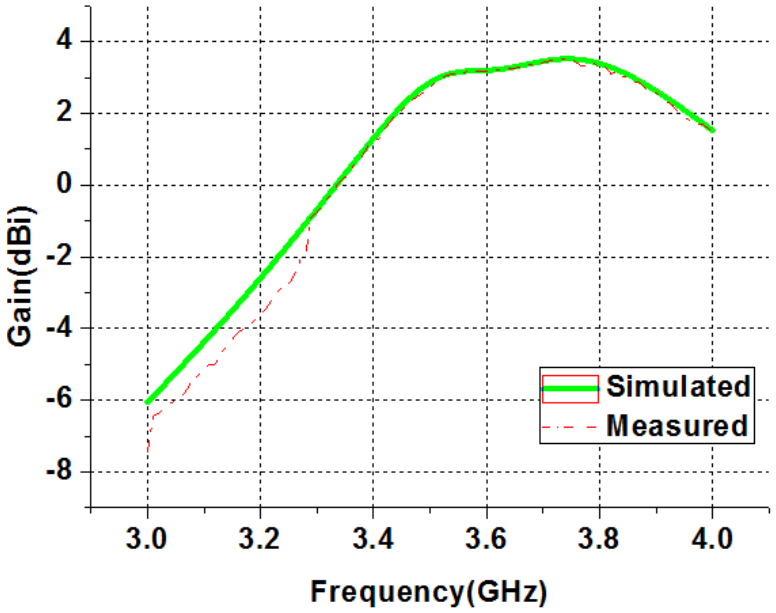

Fig.3.23 Simulated and measured results for Gain at the resonant frequency.

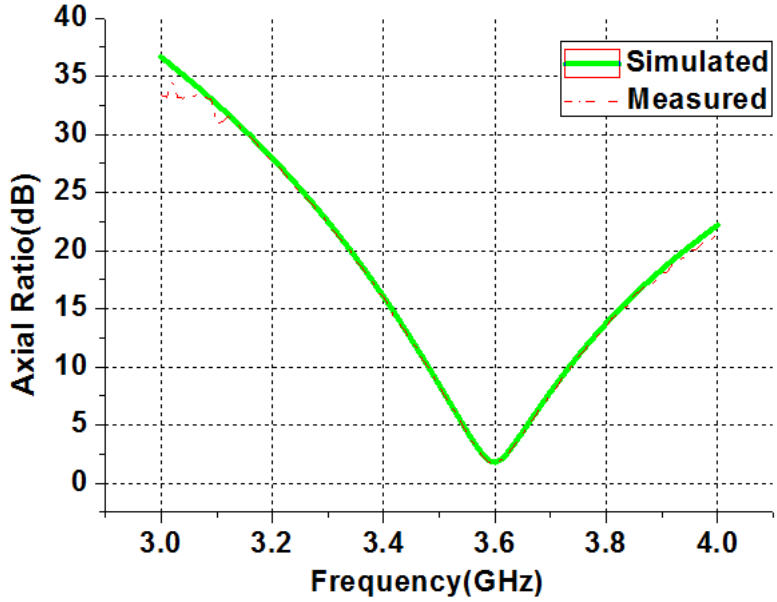

Fig.3.24 Simulated and measured results for axial ratio at the resonant frequency.

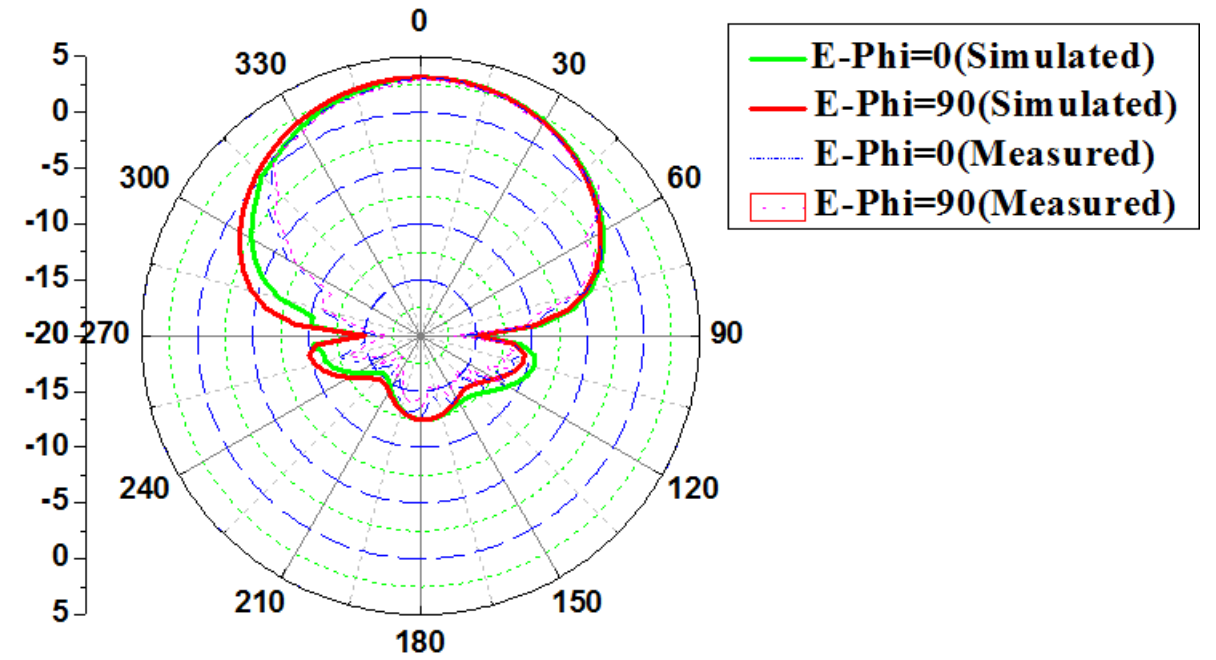

(a)

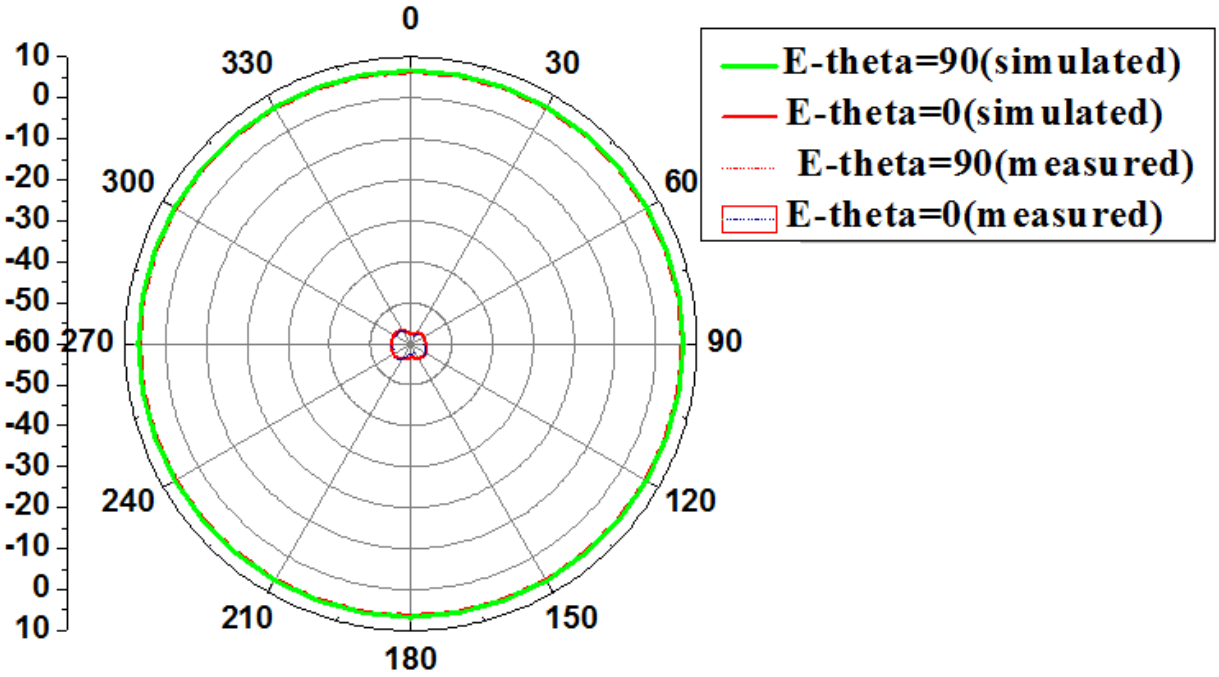

(b)

Fig.3.25 2D radiation patterns (a) Azimuth pattern at 3.56GHz (b)Elevation pattern at 3.56GHz

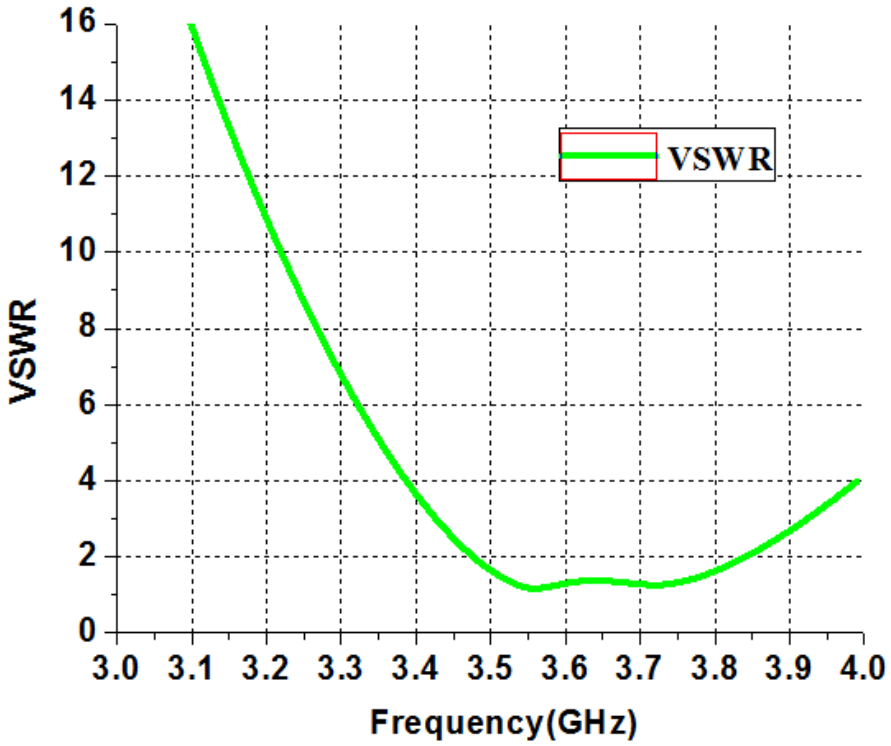

Fig.3.26 VSWR for the proposed antenna.

Table.3.4 Parameters of the antenna

Resonant frequency (GHz)	Return loss bandwidth (MHz,%)	Gain (dBi)	Axial ratio bandwidth(MHz,%)	Axial ratio(dB)
3.56	360,10.11	3.2	70.1,9%	1.7

3.2.3 Discussion on results

The performance of the proposed antenna is better than the earlier designs. The inductive and capacitive loading technique to generate circular polarization yielded low return loss and was not compact. Loading of shorting pins creates short from the ground to the patch produced low impedance bandwidth. The formation of slits and slots on the patch varies the results a lot, which depends on the shape, size, and position of the patch. A comparison of these techniques in terms of return loss, axial ratio, and gain with the proposed design is made and listed in Table.3.5. The proposed antennas' measured and simulated results show good agreement.

Table.3.5 Comparison between the existing techniques.

References	Return loss impedance bandwidth(MHz)	Axial ratio bandwidth(MHz)	Gain(dBi)
[39]	62	18	5
[40]	150	30	10.6
[43]	250	-	4.43
[32]	80	21	3.8
[33]	50	12	4.3
Proposed design	360	70	3.16

3.3 Summary

In the research, a compact semicircular microstrip patch CP antenna for 5G WLAN application has been reported. The size of the compact microstrip patch antenna is 36 mm × 36 mm × 0.787 mm. By changing the radius r_2 at one corner of the semicircular slit, the desired resonant frequency band with circular polarization is achieved. A detailed description of how CP is obtained with slit formation at the corners illustrates surface current distribution at various time intervals.

The specified fabricated design has been illustrated and compared with multiple existing models of different performance parameters. A detailed description of techniques has been discussed and compared with the novelty of the design. The measurement setup has been described, and an antenna has been connected after matching the ports. A detailed picture of the fabricated microstrip patch antenna with a semi-circular slit connected to the network analyzer has been shown. The proposed structure gives better return loss, axial ratio, gain, and omnidirectional pattern. The resonant peak at 5.37GHz falls in 5G WLAN (5.1GHz – 5.725GHz) and is suitable for 5G WLAN applications.

A circularly polarized patch antenna is fabricated at 3.56GHz for the WiMAX application. The dimensions of the proposed antenna are $0.35\lambda_0 X 0.35\lambda_0 X 0.023\lambda_0$ and return loss bandwidth of 360MHz, Axial ratio bandwidth of 70MHz and Gain of 3.16dBi are obtained. Parametric analysis is done for various feed point locations to obtain better return loss characteristics and

different values of depth of one of the slits to obtain a better axial ratio. Measured and simulated results show good agreement. The proposed antenna is low cost, compact, and better than existing designs. In terms of the bandwidth the proposed antenna's performance is superior compared to the designs given in [32] , [33], [39], [40], and [43] .Also gain obtained in this work is comparable to that of the designs reported [32], [33], [39], [40], and [43]. But when we compare gain bandwidth product the proposed antenna's performance is higher.

- Swetha Ravikanti and L. Anjaneyulu, "Compact Circularly Polarized Patch Antenna for WiMAX Applicationswith Improved Impedance Bandwidth and Axial Ratio" published in Engineering, Technology & Applied Science Research Vol. 10, No. 1,p. 5104-5107, 2020 (ESCI),https://doi.org /10.48084 /etasr.3207.
- Swetha Ravikanti and L. Anjaneyulu "A Novel And Compact Circularly Polarized Antenna for 5G Wireless Local Area Network Application ", published in Electrical, Control, and Communication Engineering Journal, Vol.16, no.1,p.44-50, November 2020. (ESCI), https://doi.org/10.2478/ecce-2020-0007.

Chapter 4
Aperture coupled circularly polarized antenna for 5G application

This chapter introduces the concept of aperture coupling and proposes a hook-shaped aperture coupled circularly polarized antenna for a 5G application that is designed, fabricated and compared between simulated and measured results. The performance of the proposed antennas is compared with the existing antennas.

A basic monopole antenna belongs to the radio antennas, which are made by a conducting rod and placed perpendicularly on the conductive surface, called ground plane. The feed line of the connector is connected to the conducting rod, and the lower end of the connector is connected to the ground plane. The basic monopole antenna and feeding techniques are shown in Fig. 4.1. But, a basic monopole is a resonant antenna that can provide a very narrow band. So, it is not suitable for wide band application.

Therefore, 3D monopole or Planar Monopole Antenna (PMA) was introduced first by Dubost and Zisler in 1976 [81]. The 3D monopole provide wide impedance bandwidth. Planar monopole is constructed by the metal plate with different shapes, where the metal plate is placed perpendicularly on the ground plane and fed by a coaxial probe, as shown in Fig.4.2. The radiation pattern is relatively omnidirectional with low manufacturing cost.

Fig.4.1 Basic monopole antenna

The longest electrical path that the generated currents can travel on the surface of the monopole defines the lower frequency limit of the impedance bandwidth. The upper limit depends on other factors, such as the shape of the monopole and the separation from the ground plane. THerefore, the PMA can be useful for wideband applications. However, PMA has a large ground plane, which has limited application for compact devices.

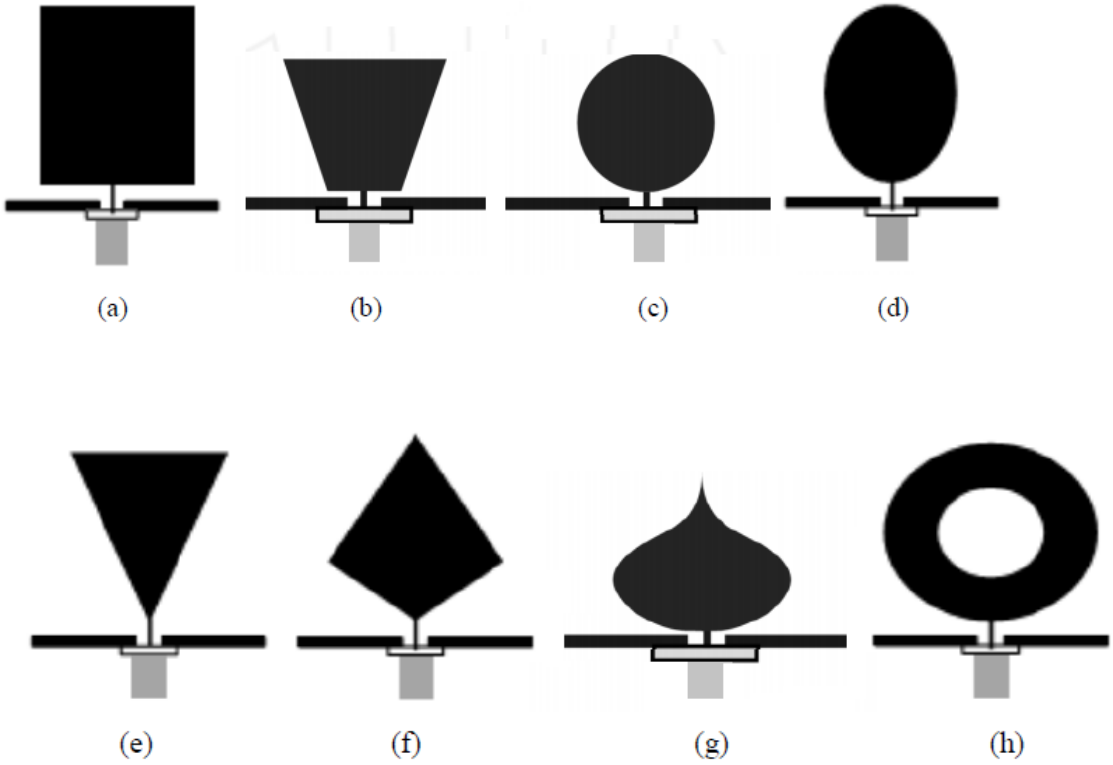

Fig.4.2 Geometries of planar monopole antennas (a) rectangular (b) trapezoidal (c) circular (d) elliptical (e) triangular (f) polygon (g) planar inverted cone antenna (PICA) (h) circular slot

Now, the latter limitation can be overcome by a printed monopole antenna [4]. It consists of a metal patch on one side of a dielectric substrate, and the ground plane is located on the opposite side of the printed circuit board.

Besides, the antenna characteristics can be met by optimizing the substrate parameters of the radiating patch without having to increase the antenna size significantly in an aperture coupled feeding mechanism. This feeding mechanism is useful since the optimization of the feed position and the radiating patch design are carried out independently. In this report, a novel three-layered hook-shaped aperture coupled antenna structure is discussed for 5G applications, with improved bandwidth, gain, and axial ratio. Section 4.1 discusses the details of the composite geometry, a parametric study for investigating the effect of the thickness of

the substrate; the shorting strip is first carried out on the performance of the proposed design in section 4.2 and Section 4.3 discusses results and discussion.

4.1 Structure of the aperture coupled circularly polarized antenna.

The designed structure uses a minimized ground, apertures on one side of the substrate, foam in between the substrate and a copper patch and shorting pin at the edge of the feed line. The antenna is designed on an FR4 substrate (εr =4.4) with thickness h =2mm, as shown in Fig.4.3. Four hook-shaped apertures are placed at 90˚ to each other in the ground plane, out of which one is smaller in size to generate asymmetry, which results in circular polarization. Excitation of the antenna is designed on the ground plane and is bent to increase the electrical length. A foam of thickness 2mm is placed on top of the substrate with hook-shaped apertures. A rectangular copper radiating patch of thickness 0.5mm is placed on top of the foam. The foam layer helps in the enhancement of bandwidth.

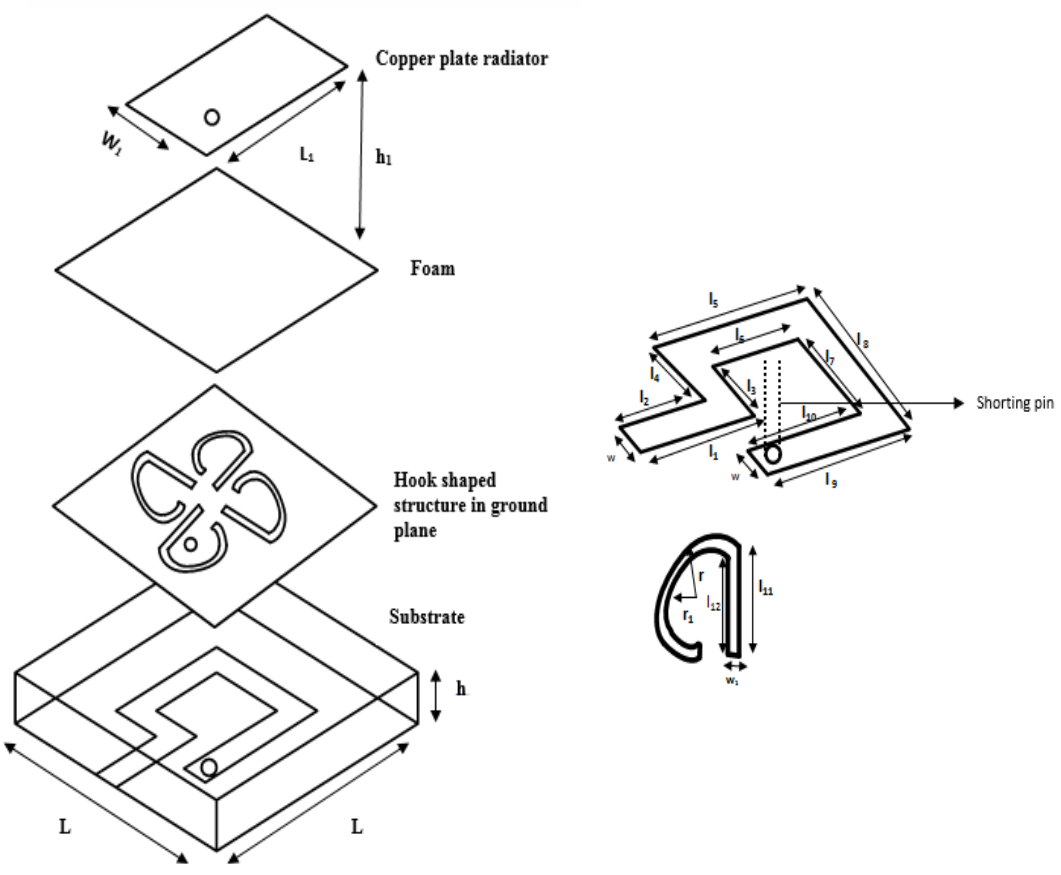

(a) **(b)**

Fig.4.3 3-Dimensional (a) top view, feed line, and (b) aperture of the novel hook-shaped aperture coupled circularly polarized antenna.

Further, a shorting pin of a radius of 1.2mm is used to connect the feed line and the radiating patch through a hole in the ground plane. This arrangement couples more power to the radiating patch in addition to the power coupled through hook-shaped apertures.

The shorting pin also ensures to reduce spurious radiation. Table.4.1 shows various dimensions, and Fig.4.4 shows the overview of the antenna. When a shorting pin is connected to the patch, an inductance is introduced in parallel, which results in frequency tuning and can be used to control the dual-frequency separation.

Table.4.1. Description of parameters

S.No	Parameter	value(mm)		S.No	Parameter	value(mm)
1	l_1	11.5		13	L	36
2	l_2	8.5		14	h	2
3	l_3	8.5		15	w_1	0.5
4	l_4	11.5		16	L_1	28
5	l_5	15		17	W_1	24
6	l_6	9		18	w	2
7	l_7	11		19	h_1	2
8	l_8	14		20	r	5.42
9	l_9	15		21	r_1	5.92
10	l_{10}	12		22	r(smaller hook)	5.23
11	l_{11}	6		23	$r_{1(}$(smaller hook)	5.73
12	l_{12}	5.5		24	ε_r	4.4

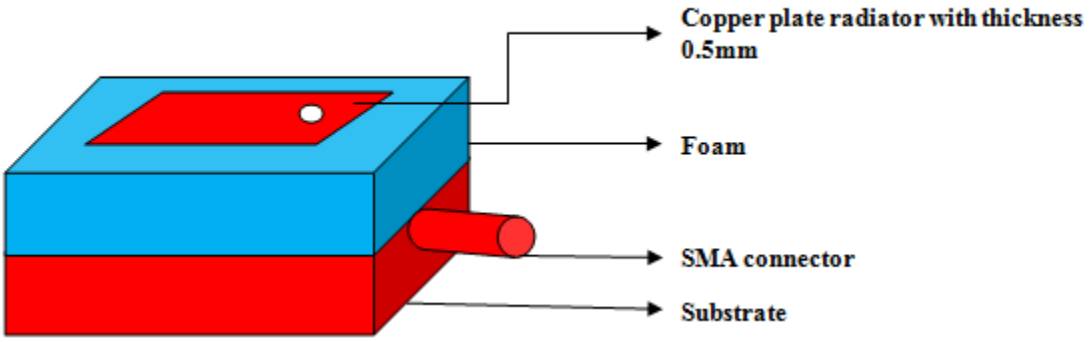

Fig. 4.4 Overview of the proposed antenna.

A shorting pin is introduced near the edge of the feed line to strengthen the surface current density, and reduce the higher-order modes near the vicinity of the pin. It helps in the reduction of the size of the patch, proper impedance matching, and low cross-polarization [82-85]. Generally, the patch resonates at half-wavelength, and its length is large. Reducing the

resonant length to half by placing a short at fundamental mode where the electric field is zero results in the quarter-wave patch, which has an area about one-fourth of the regular patch.

The use of one or more shorting pins reduces the size of the patch to about one-ninth of the area of the original regular patch. From the entire design, the line feed acts as if a probe feed with the help of an aperture structure and shorting pin. When the power is fed through the feeding mechanism, four hook-shaped slots are coupled and result in sequential phased sources to excite the patch antenna.

4.1.1 Aperture geometry details

Fig.4.5 shows the aperture design. Consider $(x_1, y_1), (x_2, y_2), (x_3, y_3)$ are the three points on the arc (h, k) is the center of the arc, and r is the radius of the arc.

Equation of a circle is $(x-h)^2 + (y-k)^2 = r^2$ (4.1)

Substituting $(x_1, y_1), (x_2, y_2), (x_3, y_3)$ in equation 1, we get 3 equations, and the unknowns (h, k) and radius r are calculated.

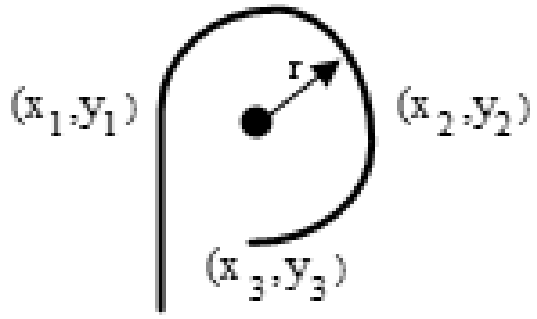

Fig.4.5 Circular arc-shaped aperture for the proposed design.

4.2 Parametric analysis

4.2.1 Variation of reflection coefficient with respect to thickness

The proposed antenna is designed on an FR4 substrate with ϵr=4.4, and parametric analysis is done for thicknesses of 1.6mm, 2mm and by varying the radiating patch size as 28x24mm' 26x24mm as listed in Table.4.2. According to Table.4.2, return loss bandwidth is higher for thickness 2mm with patch size 28x24mm.

Table.4.2 Comparison of reflection coefficient **for various thicknesses of substrate**

S. No	Thickness of the substrate (mm)	Radiating patch size (mm)	Resonant Frequencies (GHz)	Return loss bandwidth (%)	Range(GHz)
1	2	28X24	3.47	29.10	2.8 – 3.81
			4.53	3.53	4.45 - 4.61
2	2	26X24	2.64	3	2.6 – 2.68
			3.49	21.7	3.08 – 3.84
			4.37	6.4	4.21 – 4.49
3	1.6	28X24	2.77	3.6	2.71 – 2.81
			3.63	18	3.22 – 3.88

For the thickness of the substrate 2mm with radiating patch size 26x24mm, the antenna resonates at three bands, but the bandwidth is low compared to others, and gain is low compared to others. So the thickness of the substrate is 2mm with a patch size of 28x24mm is opted as illustrated in Fig. (4.6 - 4.7).

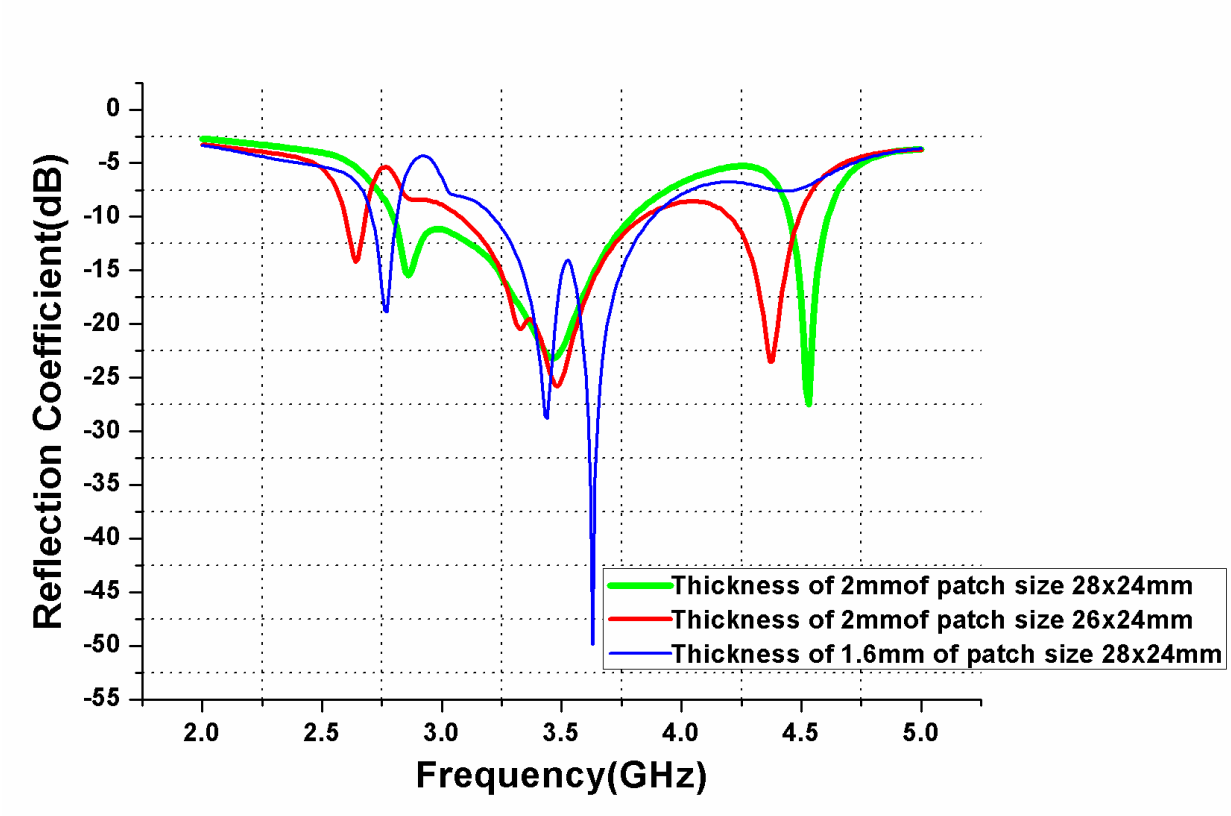

Fig.4.6 Reflection coefficient for various thicknesses of the antenna.

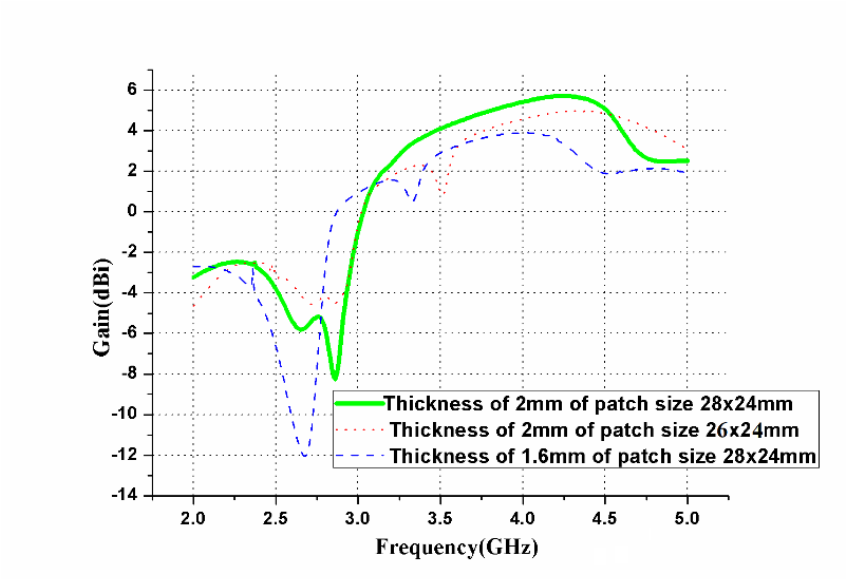

Fig.4.7 Gain for various thicknesses of the antenna.

4.2.2 Variation of reflection coefficient and gain with and without shorting pin

A shorting pin at the edge of the feed line to the top of the radiating patch for the proposed design results in wide impedance bandwidth. At the resonant frequency of 3.47GHz, the bandwidth and gains are 1.01GHz and 4.08dBi, respectively. Without shorting the pin, impedance bandwidth is more, but gain is reduced at the resonant frequency. The return loss and gain, without and with shorting pin, are shown in Fig. (4.8-4.9) and Table.4.3.

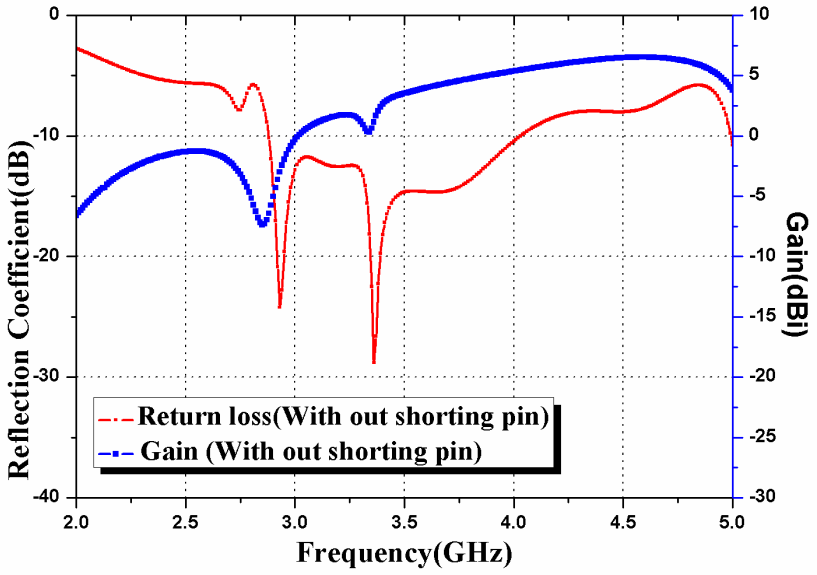

Fig.4.8 Reflection coefficient and gain performance without a shorting pin of the antenna.

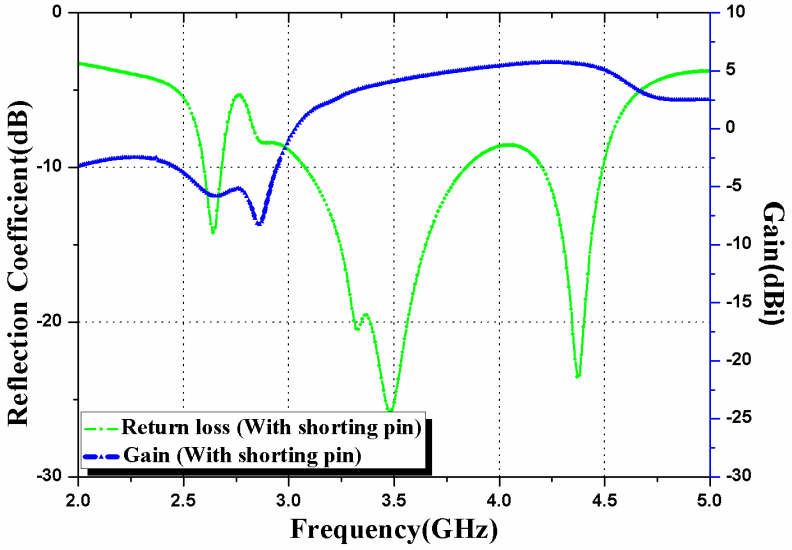

Fig.4.9 Reflection coefficient and gain performance with a shorting pin of the antenna.

Table.4.3 Effect of shorting pin on the performance characteristics of the hook-shaped aperture coupled circularly polarized antenna

S.No	Shorting pin effect	Return loss bandwidth(GHz) at the resonant frequency	Gain(dBi) at resonant frequency
1	Without Shorting pin	1.15GHzat 3.36GHz	1.146
2	With Shorting pin(height=4mm)	1.01GHzat 3.47GHz	4.08

4.2.3 Variation of reflection coefficient and gain with the height of the shorting pin and width of the feed line

Two parameters are varied with respect to design, i.e., the height of the shorting pin and feed line strip width. By varying the height of the shorting pin, strip width (w), the impedance bandwidth, and gain are studied at the resonant frequencies and shown in Table 4.4 and Fig 4.10.

Firstly, to achieve a wide band performance, a study on various thicknesses of the substrate is carried out to enhance the bandwidth of the proposed design, as shown in Fig.4.6. A shorting pin is used in the ground plane to strengthen the design's surface current density and compactness. The performance of the proposed design is improved, as seen in Figs. 4.7– 4.10.

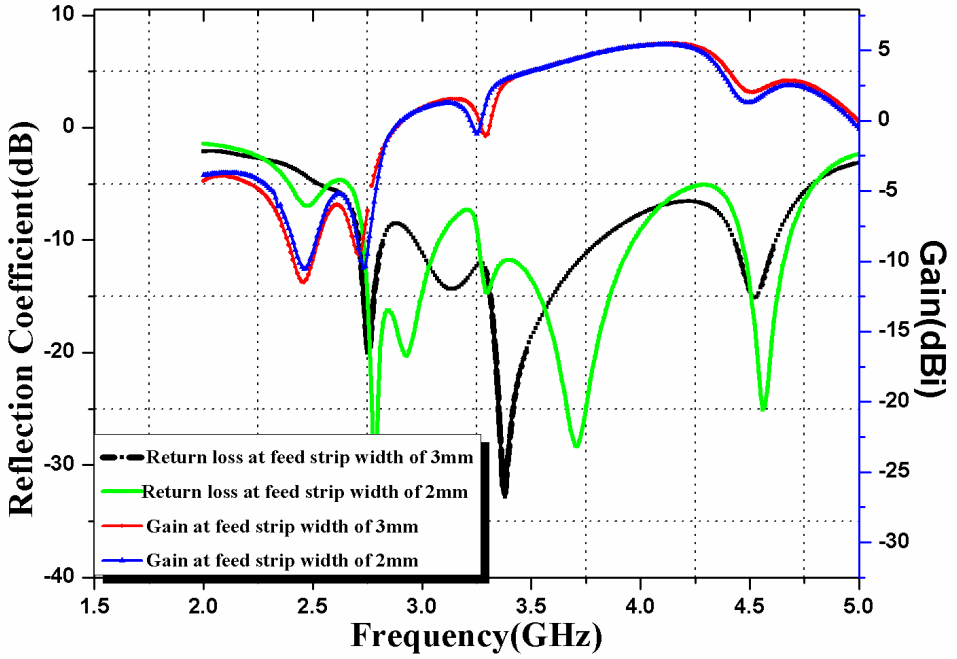

Fig. 4.10 Reflection coefficient and gain performance with respect to the height of the shorting pin for the antenna.

Table.4.4 Effect of the height of a shorting pin and width of stripline on the antenna.

S.No	Height of the shorting pin and feed line width	Return loss bandwidth (MHz)	Gain (dBi)
1	2mm height, strip width of 3mm	830	2.62
2	2mm height , stripwidth of 2mm	650	4.52
3	4mm height , stripwidth of 2mm(optimum)	1100	4.08

4.3 Measured Results

A novel hook-shaped aperture coupled circularly polarized antenna is fabricated using FR4 substrate, foam, and a copper plate of thickness 0,5mm is shown in Fig.4.11.

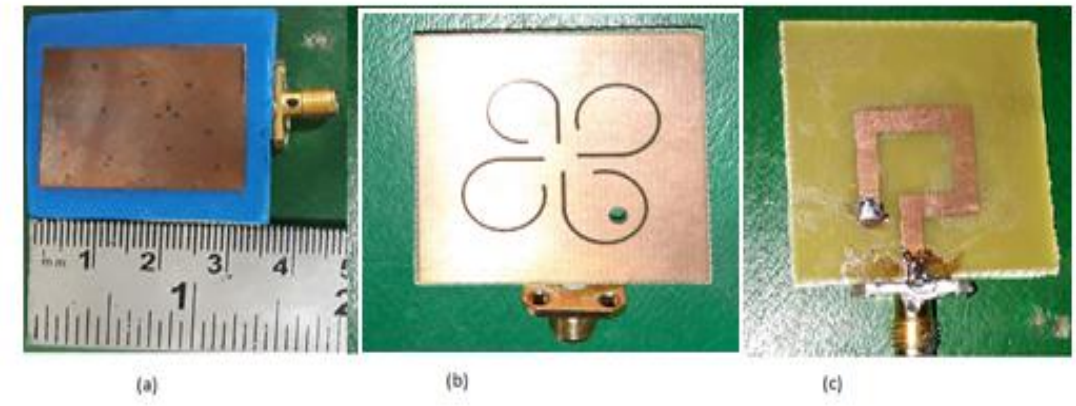

Fig. 4.11 Fabricated hook-shaped aperture coupled CP antenna (a) Top view (b) Aperture (c) feedline structure.

Reflection coefficient

The performance of the fabricated design is obtained by a major parameter called **Reflection coefficient**. The **Reflection coefficient** at the resonant frequency of 3.47GHz is 23dB and the obtained impedance bandwidth (<=-10dB) is 29.10% (2.8-3.81GHz). The resonant frequency of the proposed design falls in the 5G band, which is shown in Fig.4.12.

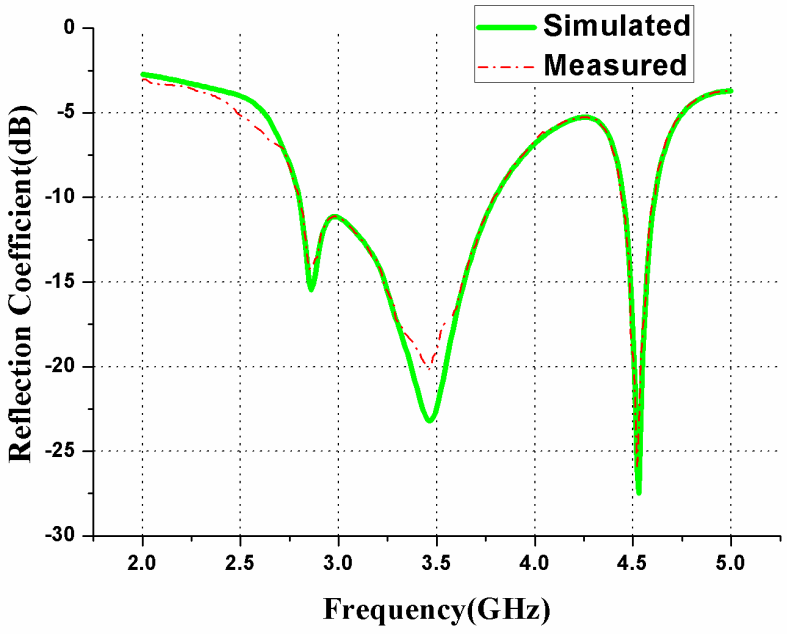

Fig.4.12 Reflection coefficient for the antenna.

Axial Ratio

It is the ratio of orthogonal electric fields in circular polarization. The axial ratio for the fabricated antenna is 13.47% (3.61-4.11GHz), as shown in Fig.4.13. It helps the proposed design to maintain the optimum circular polarization from the positioning of the transmitting or

receiving antenna. Cross polarization discrimination (CPD) is calculated using the axial ratio as shown below [28] and obtained 48.54dB.

$$CPD = 20 * log \frac{(ar+1)}{(ar-1)} \quad (4.2)$$

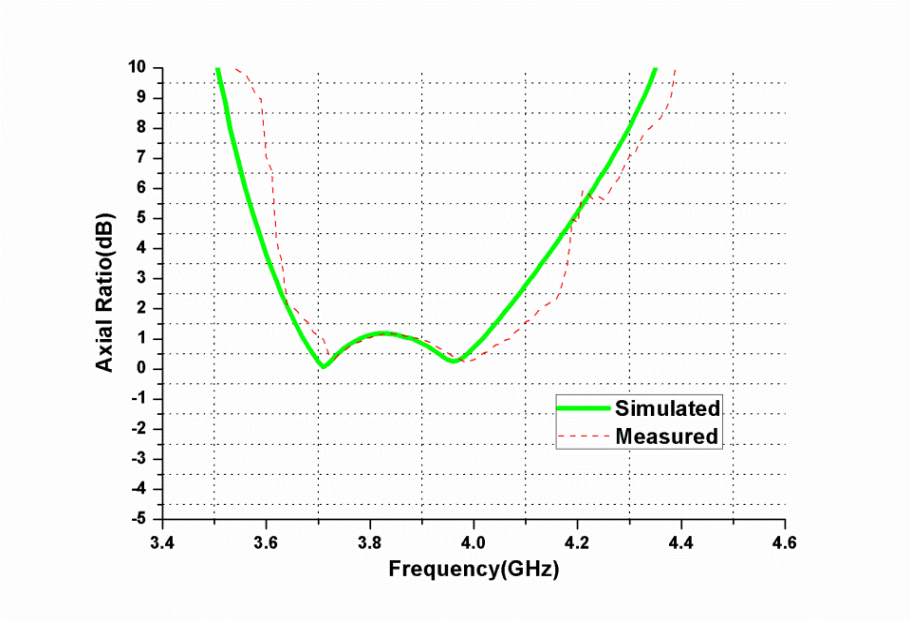

Fig. 4.13 Axial Ratio for the antenna.

Gain

The Gain at the resonant frequency of the fabricated antenna is 4.08dBi, shown in Fig.4.14. Azimuth and elevation radiation patterns are shown in fig.4.15.VSWR (Voltage standing wave ratio) is less than 2 for the fabricated antenna and is shown in Fig.4.16. Figs. 4.17- 4.18 indicates that the Co-polarization and cross-polarization for E and H-planes, isolation of greater than 20dB is observed.

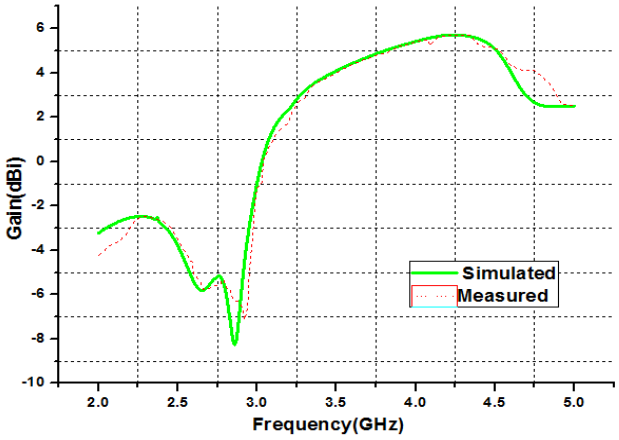

Fig. 4.14. The gain of the antenna

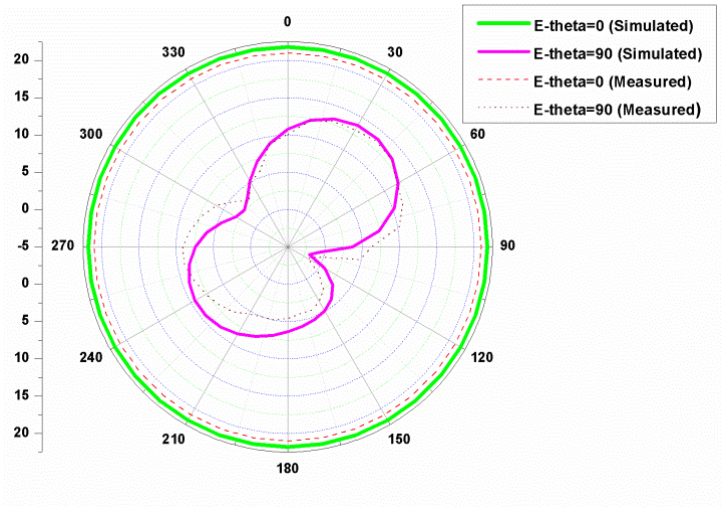

(a)

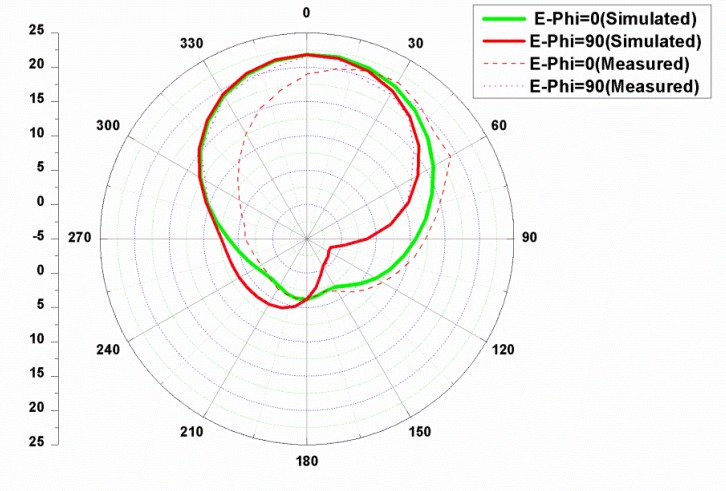

(b)

Fig.4.15 Azimuth Pattern and Elevation pattern of the hook-shaped aperture coupled circularly polarized antenna at a resonant frequency of 3.47GHz.

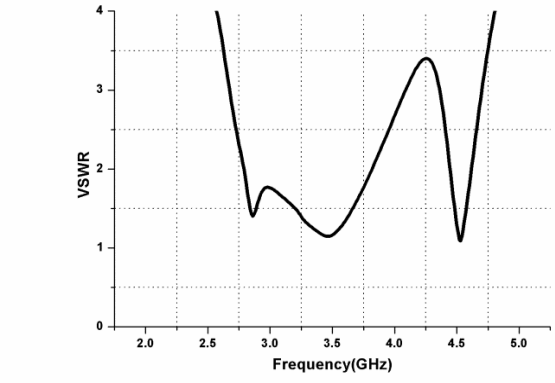

Fig.4.16 VSWR of the antenna.

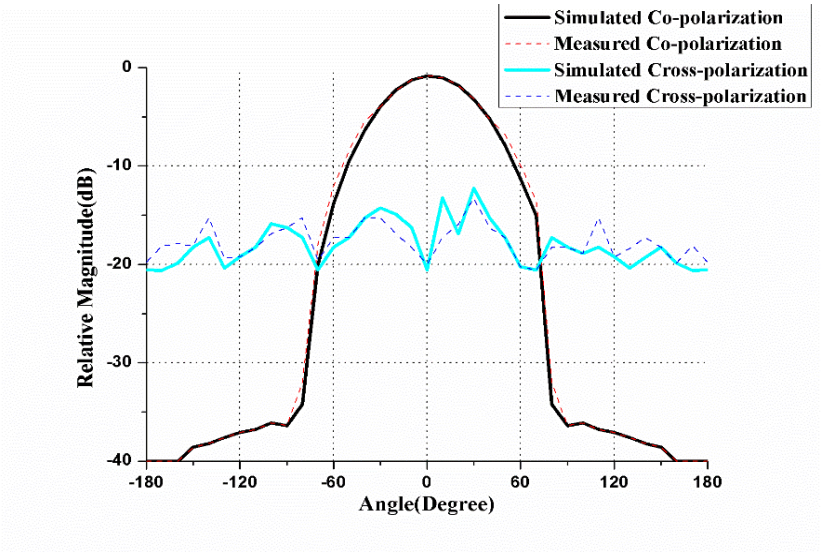

Fig.4.17 Co-polarization and cross-polarization at resonant frequency 3.47GHz for E-plane for the antenna.

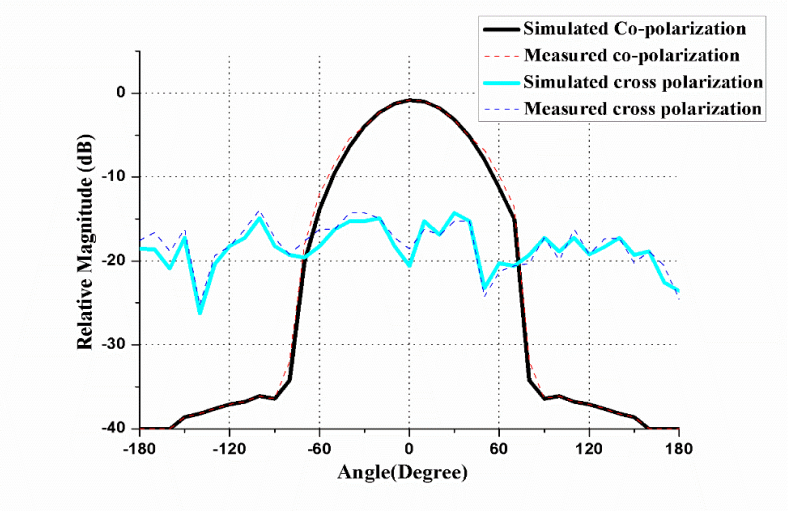

Fig.4.18. Co-polarization and cross-polarization at resonant frequency 3.47GHz for H-plane for the antenna.

4.3.1 Surface current distribution

Fig.4.19 shows the current distribution on the radiating patch of the proposed design at the resonant frequency 3.47GHz. In the current distribution for analyzing the current density in HFSS software, frames chosen are 16 and subdivided into 4 divisions as t=0, T/4, T/2, 3T/4 frames. At t= 0, T/2 current density is heavy and uniform at all the corners. For t= T/4, 3T/4 current is floating at the centre more than the edges. Fig.4.20 shows the aperture current distribution at the resonant frequency. Here the field and the current density are changing from one hook to the other at all four cycles. When a feed line radiates the electromagnetic energy,

the power is sequentially coupled from one hook to the other, as seen in the current distribution.

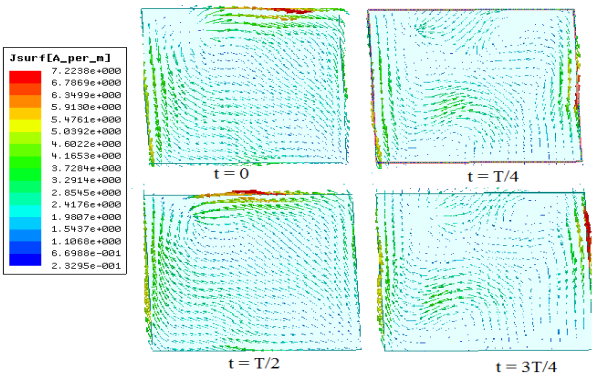

Fig.4.19 Surface current distribution at the resonant frequency 3.47GHz for the antenna.

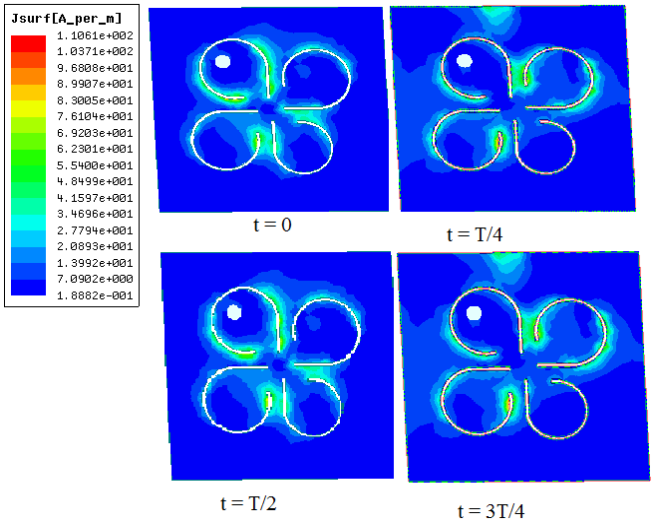

Fig.4.20 Aperture Surface current distribution at the resonant frequency 3.47GHz for the antenna.

4.3.2 Measurement Set up

To evaluate the performance, the antenna parameters using a vector network analyzer are calibrated once the ports are matched, as shown in Fig. 3.13. After zero reflections, the antenna is connected to port 1 and matched load to port 2; Fig. 4.21 illustrates the measured return loss for the proposed antenna. The axial ratio of the fabricated antenna is measured using the swept-frequency method [25]. A comparison between existing designs to the proposed is listed in Table.4.5.

The procedure for the measurement of a fabricated antenna is described as follows.

1. Switch on the network analyser 8719A (130MHz-13.5GHz), set up the start frequency and end frequency. In this analyzer, the starting frequency chosen 2GHz and end frequency 5GHz are set using start and end frequency buttons in the network analyser.

Fig.4.21. Measurement of return loss for the antenna.

2. To check matched condition, i.e., No reflections, Connect two ports. In the menu, click on the CAL button, select Calibration menu, go to response, select thru, and click done.

3. If there are reflections, connect port1 to matched load, select the CAL button in the menu, go to calibrate kit, and select N50Ω.

4. Connect antenna via two-sided female pin to port 1 as shown in Fig.3.13.Return loss in decibels as demonstrated in Fig.4.21 is displayed in network analyser with the help of above steps.

Table.4.5 Comparison of various techniques with the antenna.

S. No	References	Resonant Frequency (GHz)	Impedance Bandwidth (MHz)	Gain (dBi)	Axial ratio Bandwidth(MHz)	Size of the antenna (mm^3)
1	[21]	3.5,5.8	105,864	6.2,6.5	69,179.8	50x50
2	[22]	3.63,5.1	228,232	6.11,0.14	-	2x76x3.14
3	[23]	3.5	500	8	200	21x21x36.124
4	[24]	3.5	200	8.1	-	70x70x5.5
5	Proposed	3.47	1100	4.01	500	36x36x4

4.3.3 Discussion on simulated and measured results

Basic monopole antenna consists of a large ground plane and has limited applications for compact devices, and is overcome by printed monopole antenna. With these main criteria, a printed monopole microstrip antenna with circular polarization is used to enhance the performance characteristics of the proposed design.

The proposed design consists of a bent feed line whose length is equal to $\lambda_o/4$ at the center frequency. With the help of the bent structure in the design and hook-shaped aperture on the ground, the plane enhances the bandwidth of the antenna. In addition to that, at the end of the bent feed line, a shorting pin is used for proper impedance matching, and low cross-polarization of 20dB is maintained, as shown in fig.16. Parametric analysis is carried out for the effect of shorting pin on the performance of the proposed aperture coupled circularly polarized antenna, and its height plays a key role in it, as observed from Table.4.5.The proposed design has a monopole antenna with wideband antenna characteristics observed.

4.4 Summary

The proposed hook-shaped aperture coupled circularly polarized antenna is fabricated on the FR4 substrate of thickness 2mm and is designed with aperture coupling feeding. Circular polarization is achieved by making a hook-shaped aperture radius that is small when compared to the other three hook-shaped aperture and is located on top of the substrate. Parametric analysis was carried out, and surface current distribution was shown for the proposed antenna. For the novel, hook-shaped aperture coupled circularly polarized antenna, satisfied impedance

bandwidth, axial ratio are obtained with the usage of foam in between the substrate and patch, and connectivity of shorting pin from the edge of the feed line to the patch.

The performance parameters of the designed antenna are impedance bandwidth of 29.10%, axial ratio bandwidth is 13.47%, and gain is 4.08dBic at the resonant frequency 3.47GHz and falls in the 5G radio band. This hook-shaped aperture coupled circularly polarized antenna performance characteristics shows better enhancement in impedance bandwidth and axial ratio. The simulated results are in good agreement with the measured results.

- Ravikanti Swetha and Lokam Anjaneyulu “Novel design and characterization of Wide Band Hook Shaped Aperture Coupled Circularly Polarized Antenna for 5G Application", Published in Progress In Electromagnetics Research C, Vol. 113, p.161-175, 2021, doi:10.2528/PIERC21040202.

Chapter 5

Compact circularly polarized antenna with dielectric superstrate for 5G WLAN and X-band application.

This chapter introduces the concept of superstrate and proposes a V-shaped slit circularly polarized antenna with superstrate that is designed, compared theoretically, and evaluated. The performance of the proposed antennas is compared with the existing antennas.

Circularly polarized microstrip antennas need to be protected from environmental hazards such as ice layers during flights and uncertain weather conditions. The dielectric superstrate protects the metallic structured antenna from ecological risk due to uncertain weather conditions. Trentini demonstrated the superstrate technique first in a resonant cavity for high gain and simple microstrip configuration in 1956 [86].

High gain antennas have advantages of increase of performance, efficiency, transmission range, and reduction of transmission power. When a superstrate is imposed on a patch, it may effect the radiation characteristics, gain, and efficiency of the antenna. Such protective covers may shift the antenna's resonant frequency due to a change in effective permittivity of the circularly polarized microstrip antenna.

5.1 Analysis and configuration of circularly polarized V-shaped slit patch antenna with superstrate

The proposed V-shaped slit circular patch antenna geometry is shown in fig.5.1, and its 3D model simulated and drawn using Ansoft HFSS is shown in fig.5.2. Slitting is a technique to exploit multiband or wideband and radiation efficiency characteristics of the antenna. It removes a particular metallic part on the patch of different shapes by cutting narrow slits on the patch's radiating boundaries, resulting in lowered fundamental resonant frequency.

A dielectric superstrate or cover is superimposed on the patch to protect from environmental hazards. Such a dielectric cover or superstrate placed over the patch causes the

change in fringing fields between the ground plane and the patch, which accounts to calculate effective relative permittivity of the substrate.

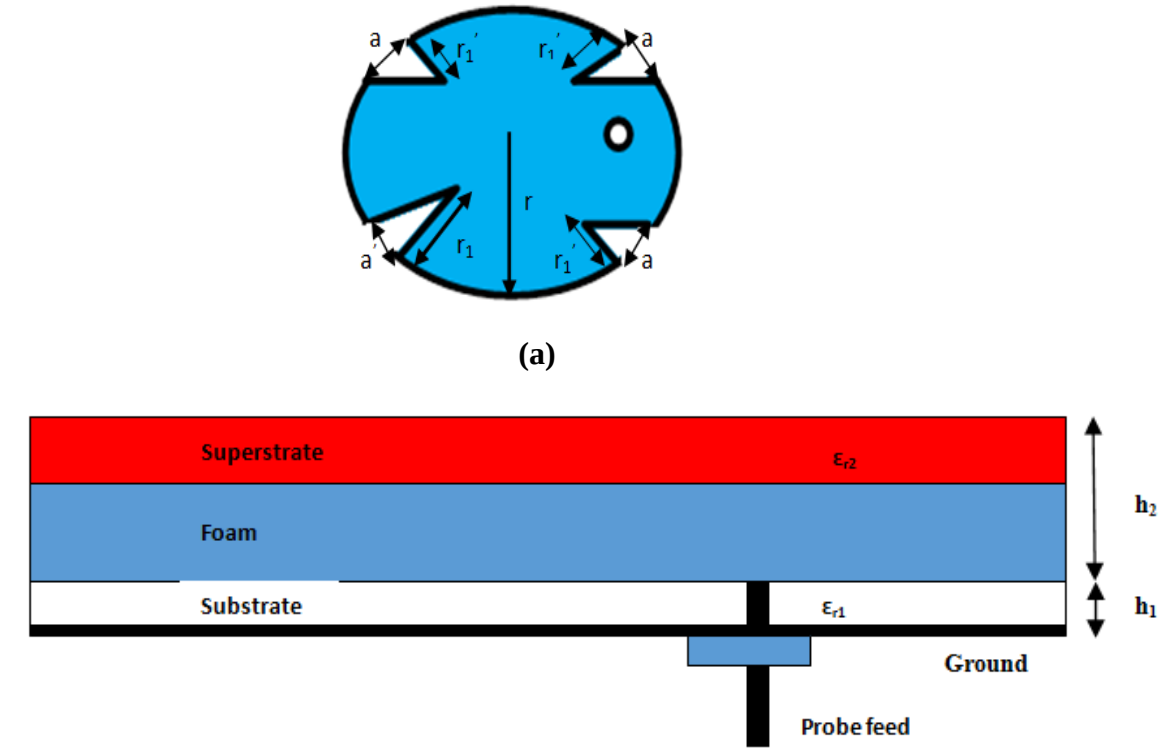

Fig.5.1 The layout of the proposed antenna (a) V-shaped slit patch (b) Side view of the circularly polarized patch antenna with superstrate.

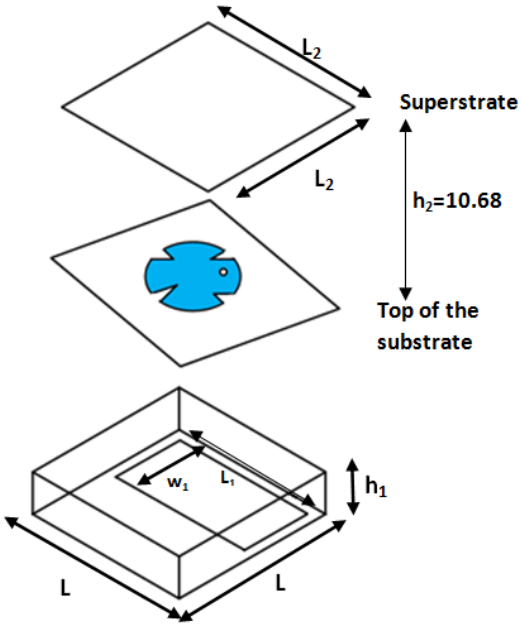

Fig.5.2 3-Dimensional proposed design of the triple-band circularly polarized antenna at resonant frequencies 5.3GHz, 7.9GHz, and 11.1GHz.

The proposed design consists of a minimized ground and circular patch etched onto the substrate RT Duroid 5880(ε_r=2.2) with thickness h_1=1.5748mm. A foam of thickness t_1=7.5mm is placed between the substrate and superstrate FR4 (ε_r=4.4) of thickness h_2=3.18mm. A circular patch of radius r=10.4mm is taken, and V-shaped slits are cut on the four quadrants of the metallic circular patch, as shown in Fig.5.2 (a). The slit is cropped deeper at one corner to create asymmetry in the structure to obtain circular polarization. Here, the distance r_1 is different from the other three similar distances (r_1^1).

Due to this, there is a change in the resonant frequency of the -shaped slit circularly polarized antenna. In the proposed design, r is the radius of the circular patch, and the substrate material used is RT Duroid 5880 with dielectric constant ε_{r1} and for superstrate ε_{r2}. The proposed circularly polarized v-shaped patch antenna is fed by a coaxial probe feed.

The position of the probe feed (0, 5) is also optimized to generate circular polarization. The structure is designed in HFSS (High-frequency structure simulator) software and resonates at 5.3GHz, 7.9GHz, and 11.1 GHz. The optimum design parameters of the antenna are tabulated in Table 5.1.

Table. 5.1. Antenna specifications

Parameter	Value
Substrate	Rogers RT Duroid 5880
Relative dielectric constant of substrate(ϵ_{r1})	2.2
Superstrate	FR-4
Relative dielectric constant of substrate(ϵ_{r2})	4.4
Radius of the circular patch(r)	10.4mm
Substrate Thickness (h_1)	1.5748mm
Superstrate and foam Thickness (h_2)	10.68mm
Dimension of V-shape slit (r_1)	7mm
Dimension of V-shape slit(r_1^1)	3.89mm
Size of the substrate	36mmx36mm
Length of the bottom partial Ground plane(L_1)	35mm
Length of the bottom partial Ground plane(L_2)	28mm
Width of the bottom partial Ground plane(w_1)	16mm
Probe position	0,5mm

When a dielectric superstrate is placed above the patch causes the change in fringing fields between the patch and ground plane results in a change of effective relative permittivity of a substrate. This is considered to evaluate the change in characteristic performance of the proposed antenna due to superstrate. The effect of an effective dielectric constant on the circular patch's radius and performance with circular polarization is analyzed.

In fig.5.2, h_1 represents the height of the dielectric substrate, and that of the superstrate is h_2. Guha and Siddiqui calculated the effective dielectric constant of the substrate is as follows [87]:

$$\varepsilon_{reff} = \varepsilon_{r1}p_1 + \varepsilon_{r1}(1-p_1)^2 x[\varepsilon^2{}_{r2}p_2p_3 + \varepsilon_{r2}\{p_2p_4 + (p_3+p_4)^2]\varepsilon^2{}_{r2}p_2p_3p_4 + \varepsilon_{r1}(\varepsilon_{r2}p_3 + p_1)x(1-p_1-p_4)^2 + \varepsilon_{r2}p_4\{p_2p_4 + (p_3+p_4)^2]^{-1} \quad (5.1)$$

Where

$$p_1 = 1 - \frac{h_1}{2w_e}\ln\left(\frac{\pi w_e}{h_1} - 1\right) - p_4 \quad (5.2)$$

$$p_2 = 1 - p_1 - p_3 - 2p_4 \quad (5.3)$$

$$p_3 = \frac{h_1 - g}{2w_e}\ln\left[\frac{\pi w_e}{h_1}\frac{\cos(\frac{\pi g}{2h_1})}{\pi(0.5 + \frac{h_2}{h_1}) + \frac{g\pi}{2h_1}} + \sin(\frac{g\pi}{2h_1})\right] \quad (5.4)$$

$$p_4 = \frac{h_1}{2w_e}\ln(\frac{\pi}{2} - \frac{h_1}{2w_e}) \quad (5.5)$$

$$g = \frac{2h_1}{\pi}\arctan\left[\frac{\frac{\pi h_2}{h_1}}{(\frac{\pi}{2})(\frac{w_e}{h_1}) - 2}\right] \quad (5.6)$$

$$w_e = \sqrt{\frac{\varepsilon_r'}{\varepsilon_{reff}}}\left[\left\{w + 0.882h_1 + 0.164h_1\frac{\varepsilon_r' - 1}{\varepsilon_r'^2}\right\} + h_1\frac{\varepsilon_r' - 1}{\pi\varepsilon_r'}\left\{\ln(0.94 + \frac{w}{2h_1}) + 1.451\right\}\right] \quad (5.7)$$

$$\varepsilon'_r = \frac{2\varepsilon_{reff} - 1 + (1 + \frac{10h_1}{w_e})^{-0.5}}{1 + (1 + \frac{10h_1}{w_e})} \tag{5.8}$$

$$w = r(\pi - 2) \tag{5.9}$$

By iteration method w_e and ε'_r parameters are calculated with initial value $\varepsilon'_r = \varepsilon_{r1}$ and $\varepsilon_{reff} = \varepsilon'_r$. Placing a superstrate with appropriate thickness on the patch reduces the surface waves to a certain extent. To accommodate this, a new dielectric constant and effective radius of the circular patch is defined as:

$$a_{eff} = r\sqrt{(1+q)} \tag{5.10}$$

$$\varepsilon_{re} = \frac{\varepsilon_{r1}}{\varepsilon_{reff}} \tag{5.11}$$

Guha and Siddiqui [87] calculated the parameter q and also a_{eff} from Eq.(10) , with the help of eqs. (4)-(9), ε_{reff} is calculated in Eq.(11) and the input impedance of circular patch is calculated as in Bahl and Bhartia [4].

$$Z_{in} = \frac{1}{\left\{(\frac{1}{R_0}) + (\mathrm{j}wC) + (\frac{1}{\mathrm{j}wL})\right\}} \tag{5.12}$$

Where the resonance resistance is stated below

$$R_0 = \frac{h^2 E_0^2 J_n^2(kp_0)}{2P_T} \tag{5.13}$$

Here P_T is the total power loss which includes the power attenuated and radiated in the resonator. $J_n$is the first kind of the Bessel function of order n,k is wave number at the operating frequency.

$$L = \frac{R}{2\pi f_r Q_T} \; C = \frac{Q_T}{2\pi f_r R} \tag{5.14}$$

Where Q_T is the total quality factor, which is necessary for calculating the input impedance.

The simulated Reflection coefficient (dB) and gain (dBi) plots of the triple-band compact circularly polarized microstrip antenna without superstrate are shown in Fig.5.3and Fig.5.4.

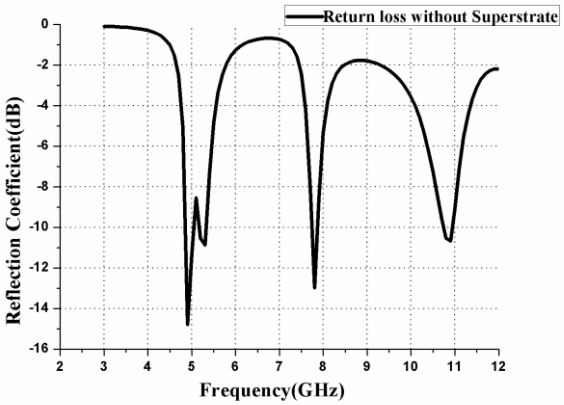

Fig.5.3 The Reflection coefficient of the antenna without superstrate.

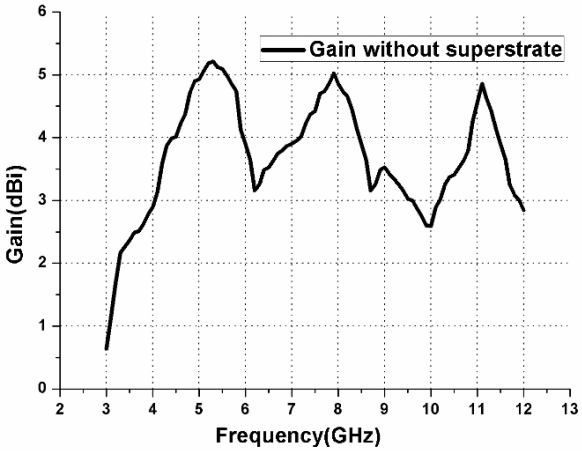

Fig.5.4 The gain of the antenna without superstrate.

5.1.1 Surface Current Distribution

Huygen's principle states that if we replace the radiating structure with its equivalent currents on its radiation environment, the fields radiated would be the same as the radiating structure. Similarly, these surface currents also act as a secondary source, and if they connect all the sources in a closed surface, a wavefront acts as a secondary source.

The full wave can be constructed from these secondary sources without the primary source of the wave. Slitting is the technique applied on the metallic part of the patch that leads to a lengthened current path for a fixed dimension also reduces, as stated by Wong [88]. Due to the bending of the patch surface current path, the resonant frequency is lowered along with the

antenna excitation. In this work, three band characteristics are obtained by cropping orthogonal V-shaped slits at the boundary of the circular patch antenna, as shown in Fig.5. Due to the lengthening of the current path in the presence of slits on the circular patch, two additional resonances are obtained. Additional resonance bands can be approximated as in Krishna et al. [89] and stated as below

$$f_{ri} = \frac{1.841 \text{x} c}{P_e \sqrt{\varepsilon_{reff}}} \tag{5.15}$$

$$P_e = P_i \sqrt{\left\{1 + \frac{2h}{\pi R \varepsilon_{re}} (\ln \frac{\pi R}{2h} + 1.7726)\right\}} \tag{5.16}$$

Where i=1,2,3

$$P_1 = 2\pi r + 4r_1' \tag{5.17}$$

$$P_2 = 2\pi r + 2r_1' + 2r_1 \tag{5.18}$$

$$P_3 = 2\pi r - 3a - a' \tag{5.19}$$

P_1 is due to the slits in the y-axis, P_2 is due slits in the x-axis, and P_3 is due to the remaining part of the sectors of the circular patch after slits removal where r_1', r_1, a are shown in Table.5.1.

Here antenna resonates at three frequencies, i.e., 5.3GHz, 7.9GHz, and 11.1GHz, and its current distribution is visualized in Fig.5.5. It shows the surface distribution is split from one resonant frequency to the other due to the V-shaped slit perturbation in the circular patch.

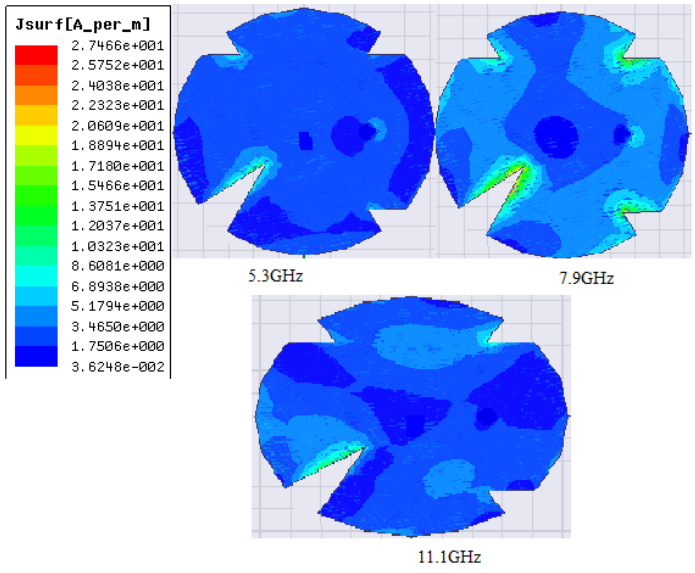

Fig.5.5 Surface current distribution at three resonant frequencies of the antenna with superstrate.

5.1.2 Selection of superstrate material

Parametric analysis is carried out for available materials like FR4, RT Duroid 5880and RF-10. The performance parameters like return loss and gain are observed for all the above materials, as shown in Figs.5.6-5.7. Few combinations of materials have been tried as substrates and superstrate. Reflection coefficient and gain values at resonant frequencies are shown in Table.5.2. The combination of RT Duroid 5880 Substrate and FR-4 superstrate material yielded the best results and are shown in table.5.2 and hence fixed. The proposed design is analyzed by placing a partially reflecting surface (i.e., superstrate) at the height of 7.5mm from the ground surface.

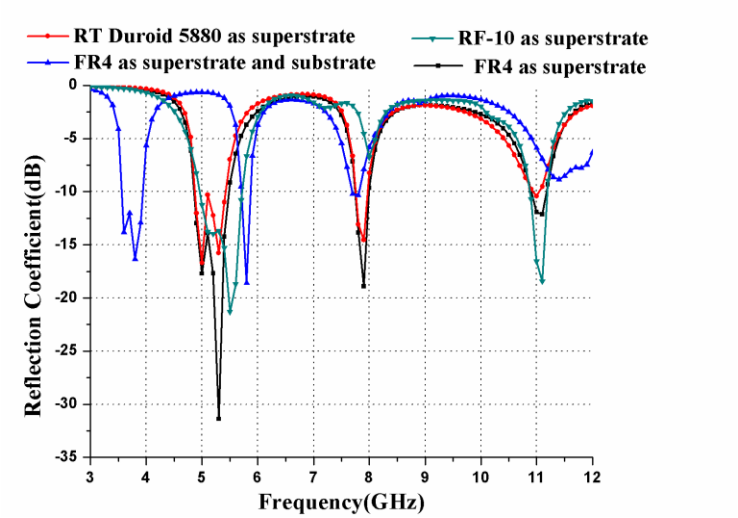

Fig.5.6 The Reflection coefficient of the proposed antenna with different materials as the superstrate.

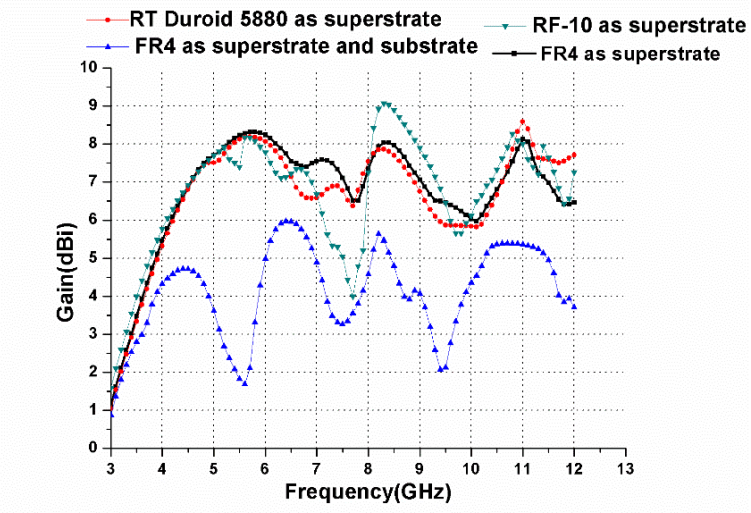

Fig. 5.7 The gain of the proposed antenna with different materials as the superstrate.

Table.5.2 Comparison of various materials as superstrate and substrate

Design	Material combination	Resonant Frequency(GHz)	Return loss bandwidth(MHz)	Gain(dBi)
1	**FR-4 superstrate RT Duroid 5880 Substrate**	**5.3 7.9 11.1**	**700 (4.9-5.6GHz) 260 (7.74-8GHz) 300 (10.9-11.2GHz)**	**8.04 6.89 8.06**
2	RT Duroid 5880 superstrate and substrate	5.0 7.9 11	560 (4.87-5.43GHz) 220 (7.75-7.97GHz) 200 (10.9-11.1GHz)	7.5 7.22 8
3	Fr-4 superstrate and substrate	3.8 5.8 7.75	370 (3.56-3.93GHz) 100(5.7-5.8GHz) 140(7.68-7.82 GHz)	3.29 3.31 3.55
4	RF-10	5.5 11.1	700(5-5.7GHz) 250(11.15-10.9GHz)	7.4 7.6

Fig.5.8 shows the return loss and gain of the proposed antenna with and without superstrate. It is observed that the reflection coefficient of the antenna with superstrate is improved from 15dB to 32dB. The gain (dBi) of the proposed triple-band circularly polarized antenna with superstrate is improved by 3dBi when compared to without superstrate. Fig.5.9 shows that comparing the reflection coefficient with all results without superstrate, it is found that there is lowering of resonance frequencies for all the bands and lowering of frequency is due to dielectric superstrate which is inversely proportional to the dielectric constant.

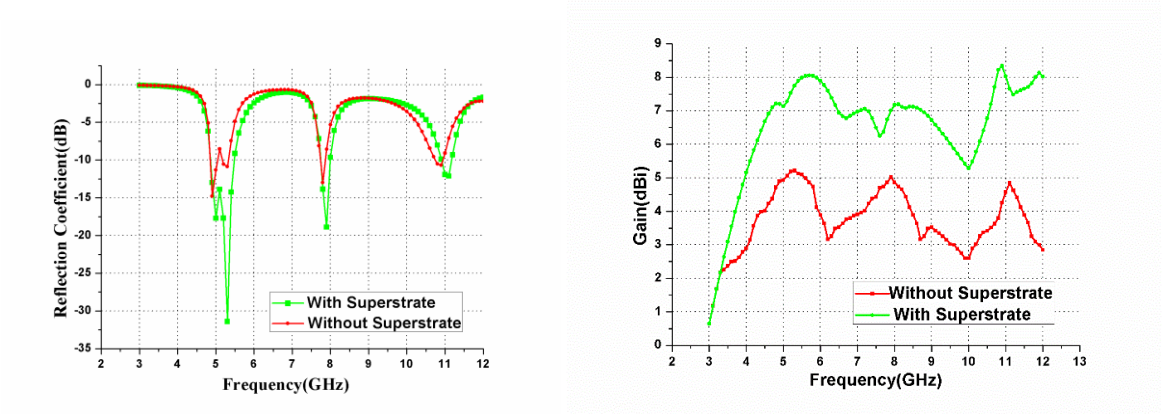

(a) (b)

Fig.5.8 (a) Reflection coefficient and (b) gain of the proposed triple-band compact antenna with and without superstrate.

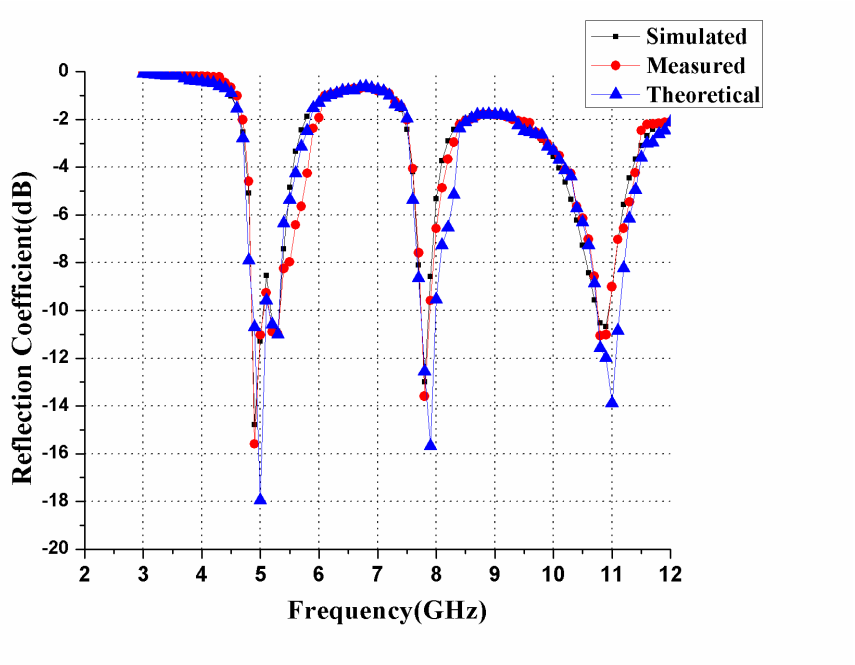

Fig.5.9 Reflection coefficient performance of the antenna in terms of measured, theoretical, and simulated results loss without superstrate for the circularly polarized antenna.

The proposed design generates a triple band, the first, second resonance is due to the slit formation on the patch. The third resonance is due to the defected structure at the bottom of the substrate. The performance characteristics are enhanced by placing a superstrate at the top of the proposed design, as shown in fig.5.10. From Fig.5.10 (c), there is a shift in the resonant frequencies by placing a superstrate and hence proved as discussed in section 5.1.1 about the effect of effective dielectric constant.

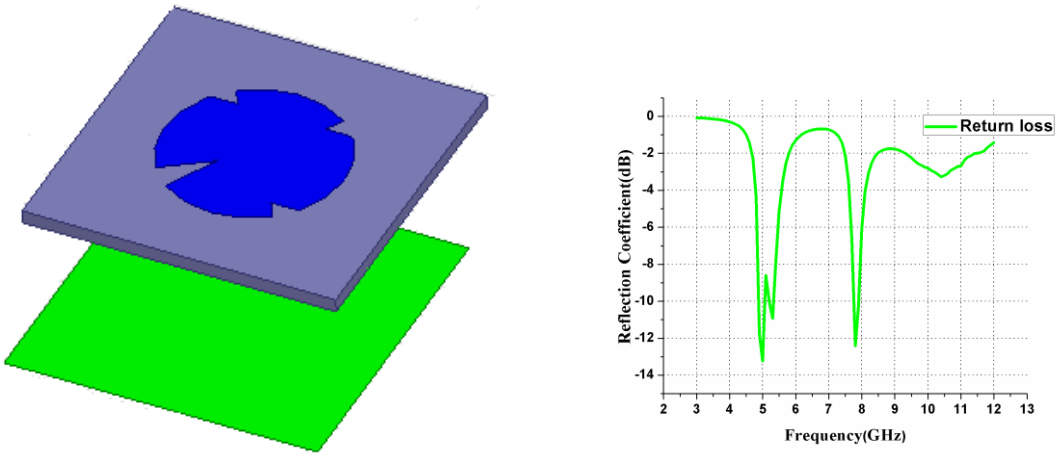

(a)

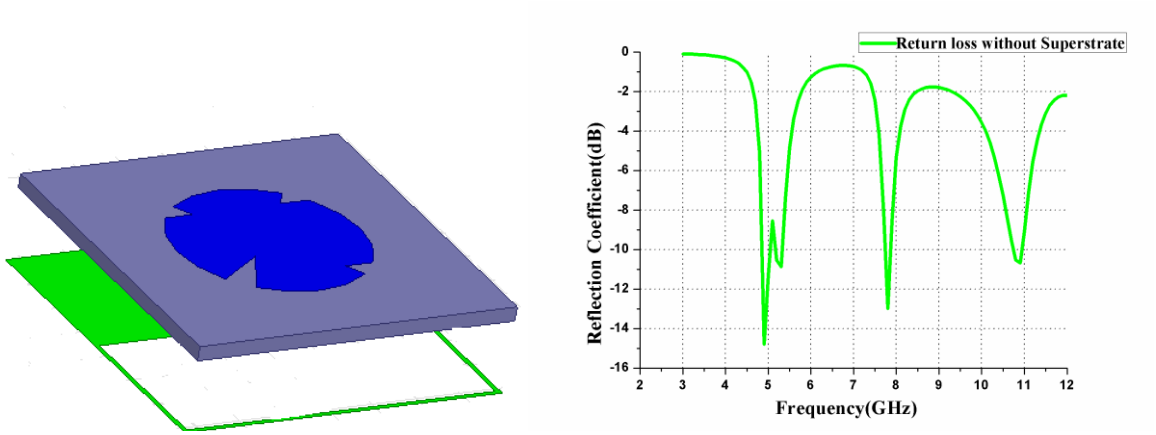

(b)

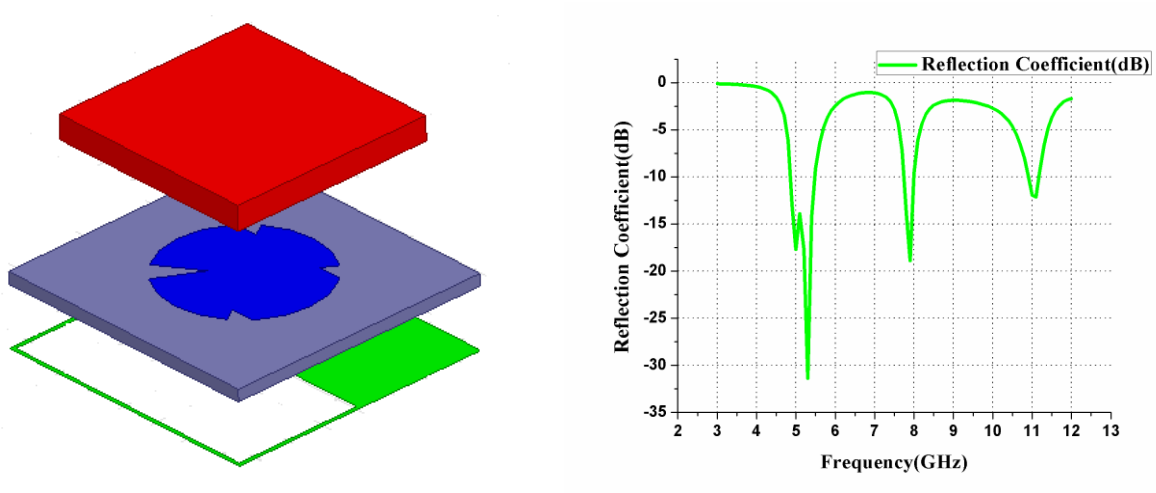

(c)

Fig.5.10 3-D structure of the step-by-step design and its reflection coefficient characteristics.

5.1.3 Measurement set up

To verify the triple-band characteristics of a v-shaped slit circularly polarized antenna, feasibility, a compact microstrip antenna with superstrate prototype has been fabricated and tested. The photograph of the fabricated antenna is displayed in Fig.5.11.

The gain is measured using the absolute gain measurement technique for the proposed design and is based on the Friss transmission formula given below [90-91].

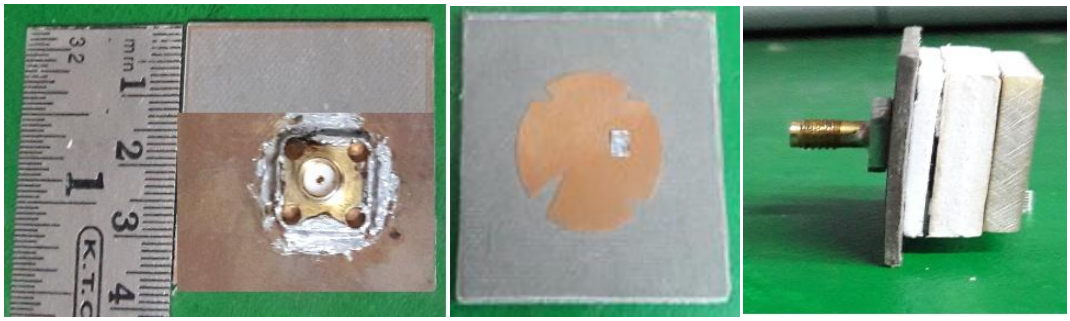

(a) **(b)** **(c)**

Fig.5.11 Fabricated proposed triple-band compact circularly polarized microstrip antenna (a) bottom View (b) patch (c) side view with superstrate.

$$\frac{P_r}{P_t} = G_t G_r \left(\frac{\lambda}{4\pi R}\right)^2 \tag{5.20}$$

G_t = Transmit antenna gain
G_r = Received antenna gain
P_t = Input power of the transmitting antenna
P_r = Power at the receive antenna terminal.
AUT = Antenna under test

The above formula gives the relationship between the powers received to the transmitted between two antennas and separated by a distance R in the far-field. Both the antennas are impedance matched to their transmission lines.

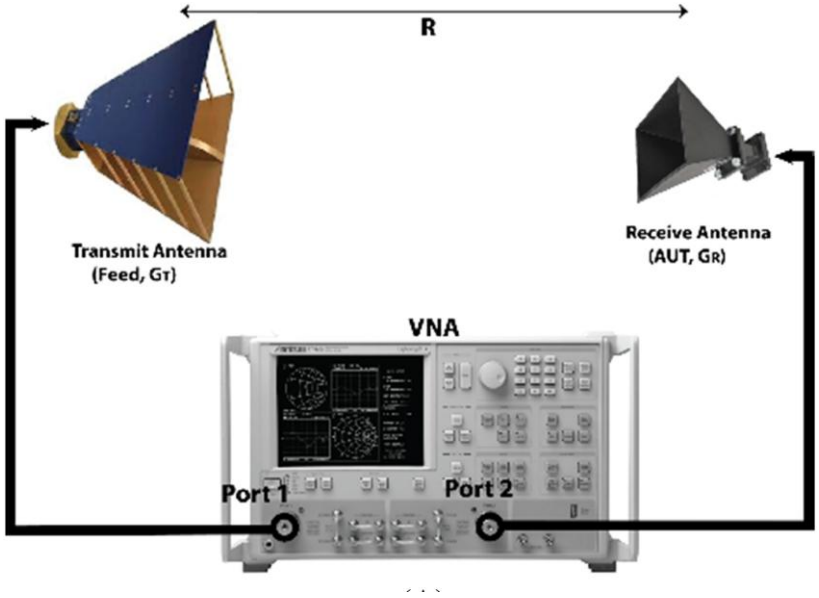

Fig.5.12 Measurement set-up for absolute gain

The anechoic chamber used for gain measurement has a capability of far-field measurement from 800 MHz to 18 GHz is shown in fig.5.12. Proper calibration of transmit and received power is done once the impedance is matched in the vector network analyzer (VNA). The transmit antenna and antenna under test (AUT) with RF cables are connected along with VNA, then using SOLT (Short, Open, Load, and through) method locations are calibrated. Once the antennas are aligned for boresight measurement in an anechoic chamber, transmission coefficient |S21| for transmit-receive antenna combination from the VNA is measured. The measured transmission coefficient is squared to get P_r/ P_t. The reference antenna (pyramidal horn) with manufacturer provided gain data, and the unknown gain is estimated [92].

The axial ratio of the fabricated antenna is measured using the Swept-frequency method. The procedure for the swept-frequency method is as follows and shown in Fig.5.13 [93].

1. The system consists of a feed system under test, a linearly polarized antenna, network analyser, and sweeper. Initially, a reference angle is fixed for a feed system under test; power ratio is obtained from a scalar network analyser with the help of frequency sweep. The first measured trace is stored in memory and taken as a reference.
2. The feed system is rotated from 0° to 180° minimum in increments of 10° to 15° from the reference, and a swept measurement is made, then subtracted from reference trace and plotted, forming an axial ratio envelope. This method eliminates system gain, path loss, and removes tilt angle.

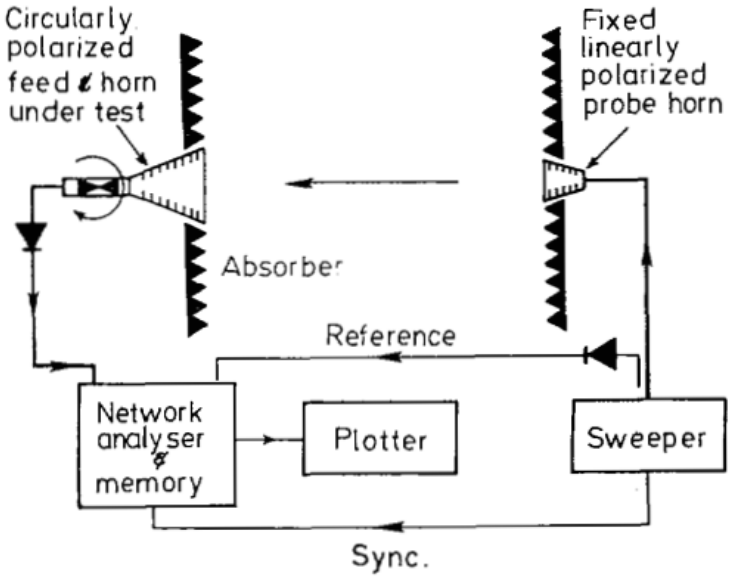

Fig.5.13.Measurement set up of axial ratio for the circularly polarized antenna.

5.2 Measured and Simulated results

Reflection coefficient

The simulated and measured return loss of the proposed design is shown in fig.5.14. The antenna resonates at three frequencies, i.e., are 5.3GHz, 7.9GHz, and 11.1GHz. It shows that the measured reflection coefficient is 32.2dB, 18.9dB, 12.1dB at resonant frequencies 5.3 GHz, 7.9GHz, and11.1GHz. The measured 10dB impedance bandwidths for the resonant frequencies are 700MHz, 260MHz, and 300MHz.It clearly shows that the designed antenna is suitable for the 5G WLAN application and X-band application.

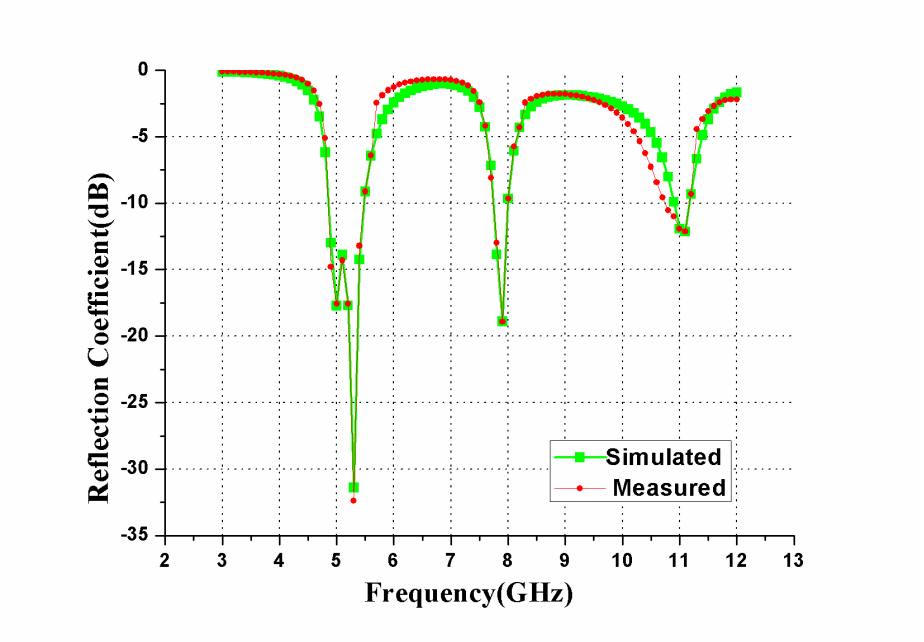

Fig.5.14 The reflection coefficient results of the proposed antenna simulated vs. measured.

Gain

Gain is the measure of the power of antenna radiation in desired direction with reference to a reference antenna. The measured gains at resonant frequencies 5.3GHz, 7.9GHz, and 11.1GHz are 8dBi, 6.89dBi, and 8dBi, respectively, as shown in Fig.5.15.

Axial Ratio

Axial ratio is a factor that indicates the Circular polarization of an antenna and is shown in Fig.5.16. For the proposed antenna, the measured axial ratio is shown below in Table.5.3 is 0.47dB, 0.925dB, 1.55dB, and bandwidth of 700MHz in frequency range 5.1GHz-5.8GHz is obtained.

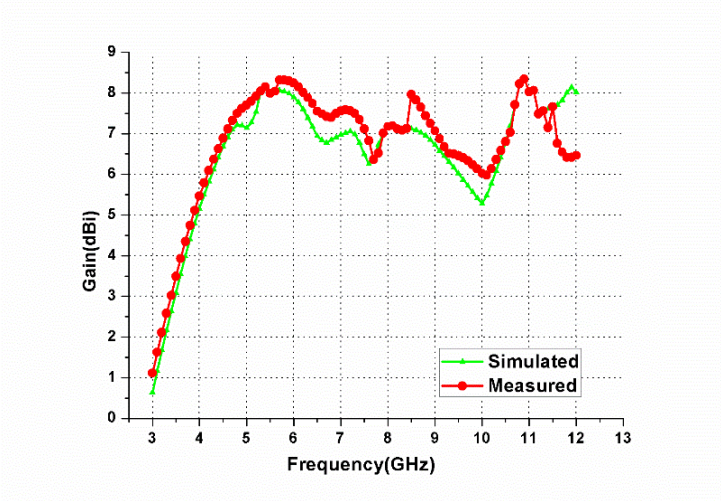

Fig.5.15.The gain results of the proposed antenna simulated vs. measured.

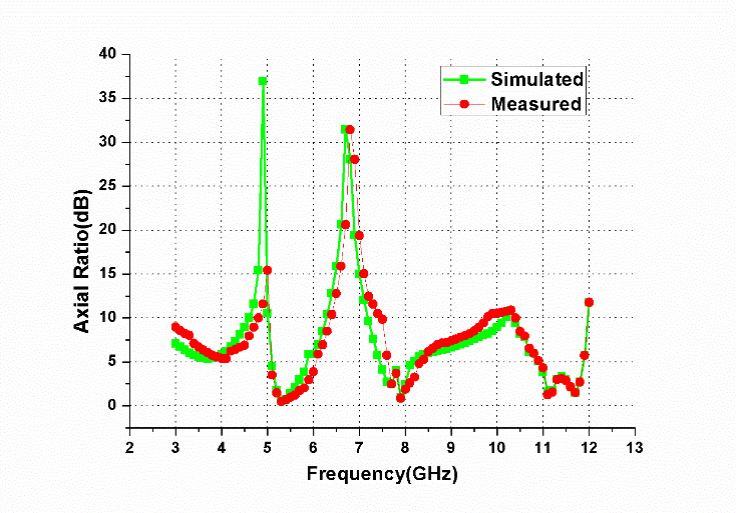

Fig.5.16. The axial ratio of the proposed antenna simulated vs. measured results.

Table.5.3 Performance of the proposed design

S.No	Resonant Frequency(GHz)	Axial Ratio(dB),Bandwidth(MHz)	Frequency Band(GHz)
1	5.3	0.47,700	5.1-5.8
2	7.9	0.925,250	7.8-8.05
3	11.1	1.55,300	11-11.3

5.2.1 Radiation Pattern

Elevation and azimuth patterns in two dimensions are shown for various resonant frequencies, i.e., 5.3GHz, 7.9GHz, and 11.1GHz. Fig.5.17 indicates that the patterns are

directional in Elevation Plane. Fig.5.18 describes they are omnidirectional in the Azimuth plane. The voltage standing wave ratio (VSWR) is less than two, as shown in Fig.5.19. Radiation efficiency is above 97%, as illustrated in Fig.5.20.

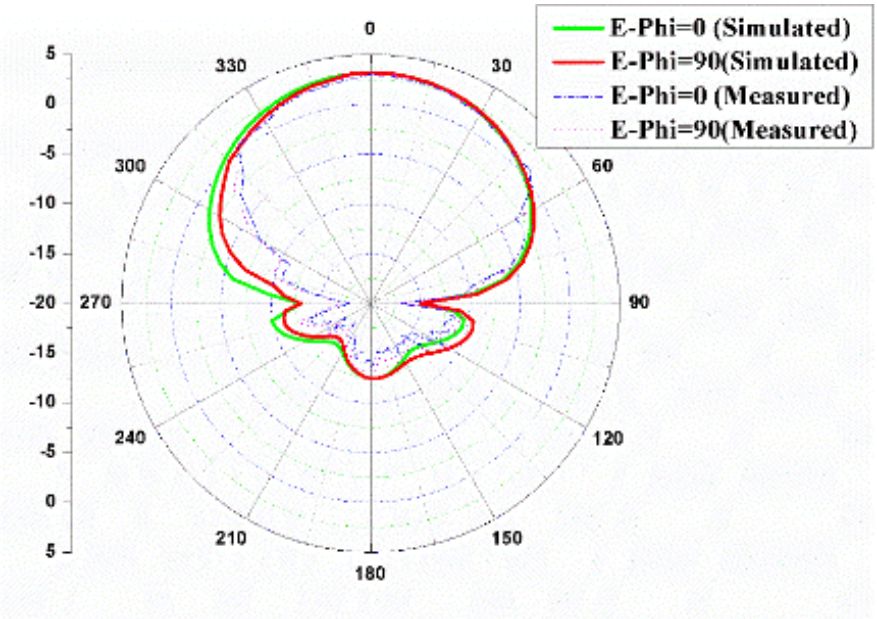

(a)

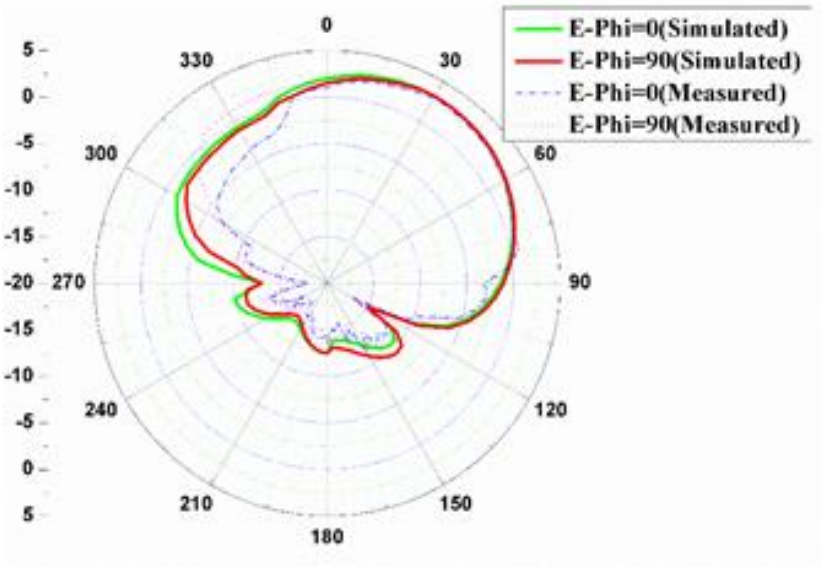

(b)

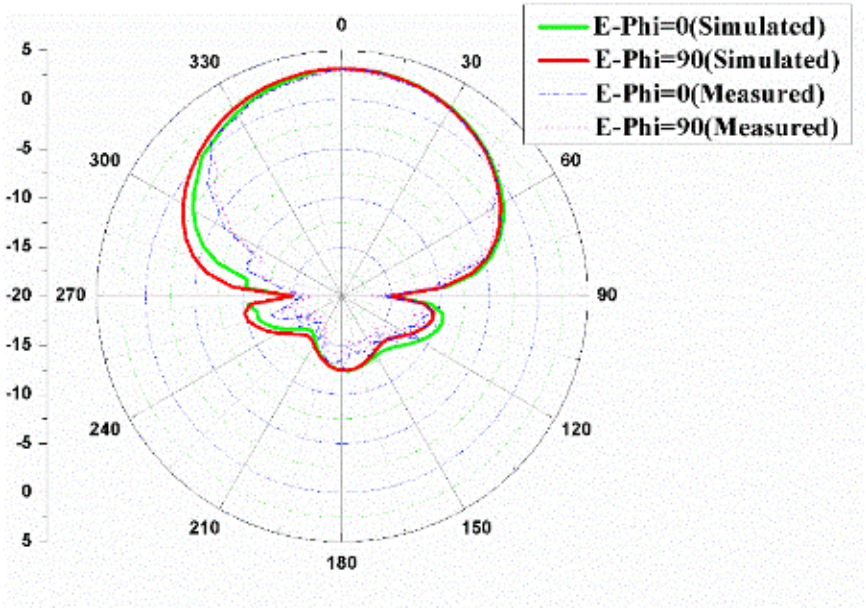

(c)

Fig.5.17. 2-D elevation pattern of proposed triple-band compact circularly polarized microstrip antenna simulated vs. measured results at resonant frequencies at (a) 5.3 GHz (b) 7.9GHz and (c) 11.1Ghz.

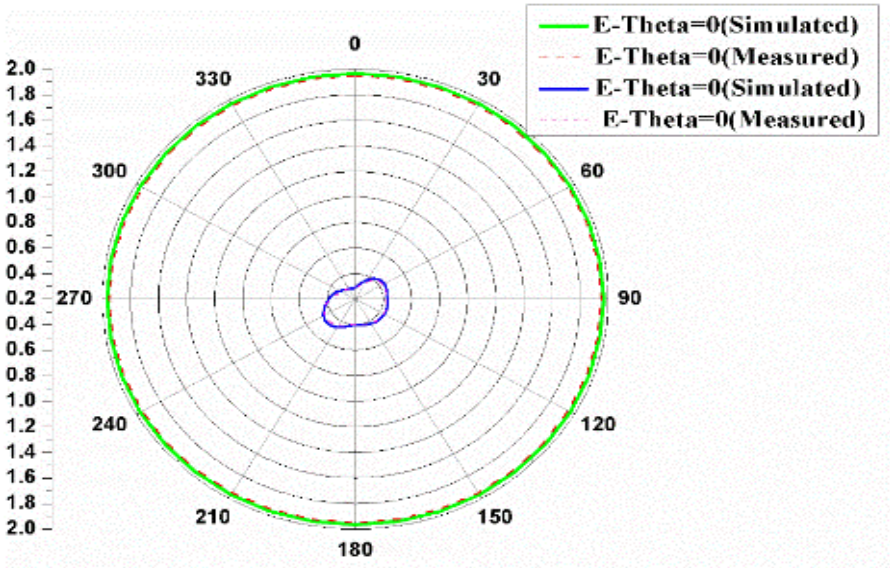

(a)

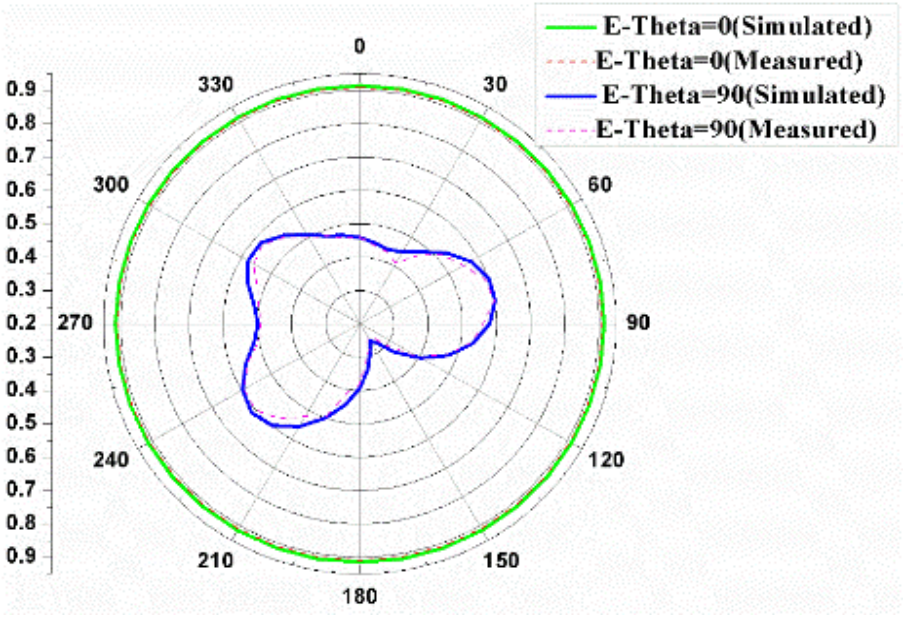

(b)

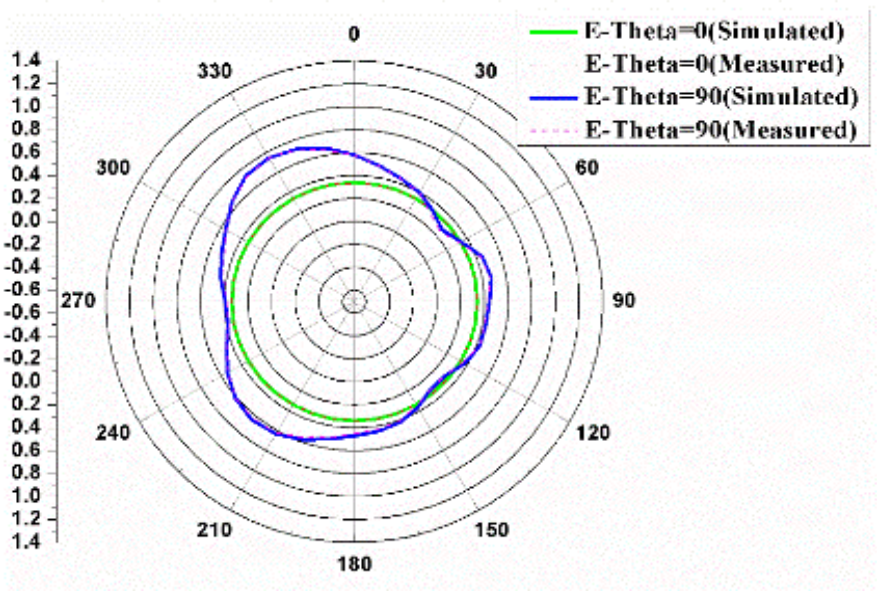

(c)

Fig.5.18 2-D Azimuth pattern of proposed triple-band compact circularly polarized microstrip antenna simulated vs. measured results at (a) 5.3 GHz, (b) 7.9GHz, and (c) 11.1 GHz.

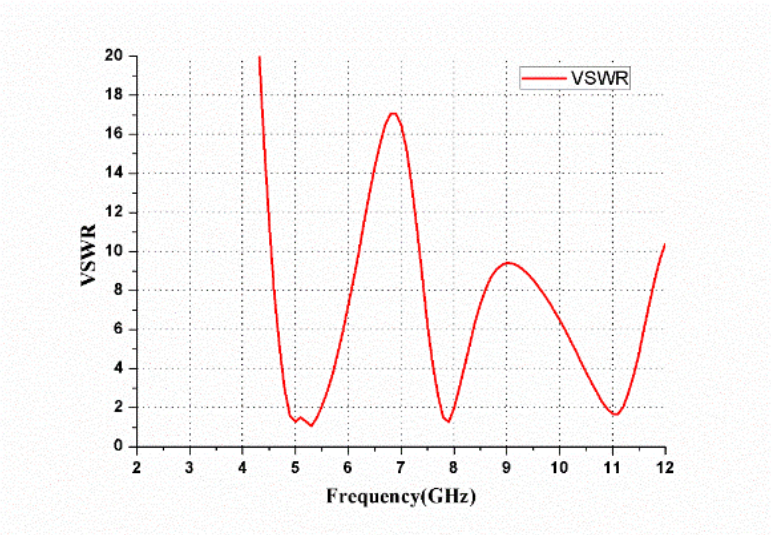

Fig.5.19. Simulated voltage standing wave ratio of the proposed antenna with superstrate.

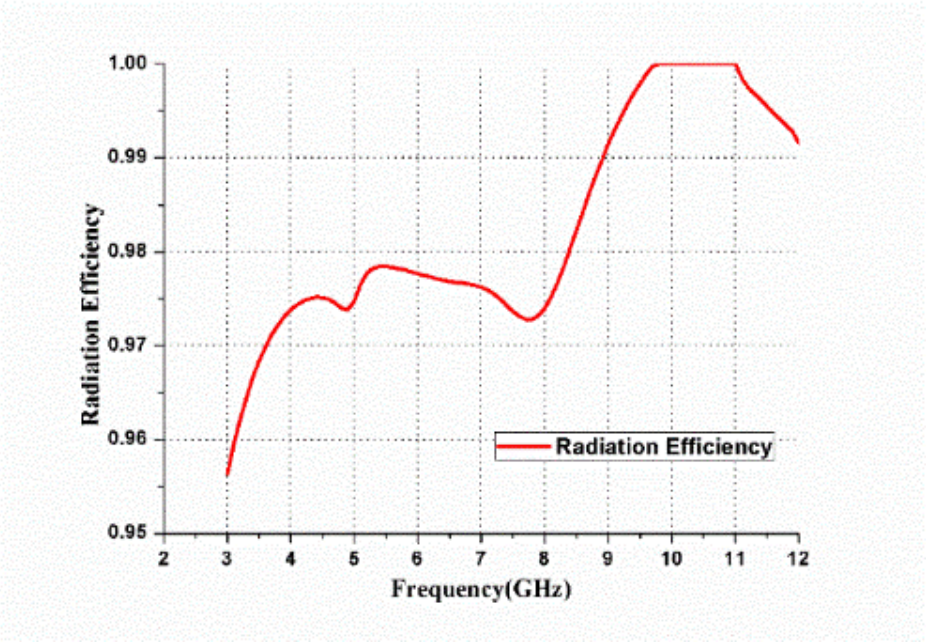

Fig. 5.20. The simulated radiation efficiency of the proposed antenna with superstrate.

The performance characteristics of the proposed prototype antenna are compared with some of the existing designs are tabulated in Table.5.4.

Table.5.4.Performance comparison of the proposed antenna with some of the existing designs

S.No	References	Resonant Frequency (GHz)	Impedance Bandwidth (MHz)	Gain (dBi)	Axial ratio Bandwidth (MHz)	Size of the antenna mm
1	[58]	8.6	980	3.4	-	50mmx30mm
2	[59]	9,11.35	612,351	8.2,10.1	-	30.26mmx33.06mm
3	[60]	5.8(5.725 GHz – 5.875 GHz)	150	17.5	-	-
4	[61]	2,2.1	54	5.0	26,23	20mmx20mm
5	[62]	1.625,1.75	100	7.0	19,21	30mmx30mm
6	[63]	3,3.6,3.7,4.5	100-180	2-4	-	30mmx40mm
7	[64]	2.27	265	6.8	56	-
8	[65]	10.8 (10.1 GHz –12.9 GHz)	2.8GHz	13.7	1.5	40mmx40mmx17.45mm
9	[86]	4.1, 5.8, and 6.7 GHz	450MHz (3.83–4.28GHz), 560MHz (5.41–5.97GHz) 830MHz (6.47–7.3GHz)	1-2 at all frequencies	200 370 230	29mm×26mm×1.6mm
10	[94]	3.1(2.84 GHz-3.24 GHz) 4.7 (4.44 GHz -4.92 GH)	400,480	5-6 at both frequencies	100,200	70mmx70mmx12mm
11	[95]	2.42,5,5.3	-	5.5,4.6,4	-	120mmx120mmx1.6mm
12	[96]	2.4,3.5,4.9	870,1170,400	2.73,2.08,3.04	300,100,200	40mmx40mmx1.6mm
13	[97]	6.95,7.93,8.9	5637	5.6,4,4	95,186,149	63mmx75mmx1.6mm
14	[98]	7.5,10.2,12.2	540,8000	1,1,4	152,161,112.5	35mmx30mmx1.6mm
15	**Proposed antenna**	**5.3,7.9,11.1**	**700,260,300**	**8.04,6.89,8.06**	**700,250,300**	**36mmx36mmx12.25mm**

5.3. Discussion on simulated and measured results.

Microstrip antennas are flexible, compatible to multiple circuitry, and need to be protected from ecological risk since it effects the performance characteristics of the antenna. One such technique to improve the performance as well as to protect it from environmental hazards is superstrate. The superstrate is placed at a height of $\lambda_o/4$ from the surface of the ground. When the patch is radiated, electric field waves get reflected and .transmitted towards the surface of the superstrate, and it acts as a partially reflecting surface, and the wave gets reflected towards the propagating wave and there by phase as well as the amplitude of the wave is increased.

By superstrate technique, the antenna performance characteristics are improved, but it lowers the resonant frequency, reduces impedance matching, and it effects the effective dielectric constant. These characteristics can be enhanced by the proper thickness of the superstrate chosen. The effective dielectric constant of the simple circular patch and change in effective dielectric constant with superstrate explain its effects briefly. Fig.5.9 illustrates the effect of effective dielectric constant, which lowers the resonant frequencies, as compared in simulated, measured, and theoretical results.

Due to slit formation on the circumference of the circular patch, which lengths the surface current distributions as shown in Fig.5, additional bands are obtained and are picturi zed in Fig.5.10. The performance and radiation characteristics of the proposed triple-band compact. Circularly polarized microstrip antenna is evaluated by the finite element method technique embedded in a solver called a high-frequency structure simulator (HFSS).

The superstrate is loaded on the various patch designs to improve the performance characteristics of the antenna, as illustrated in Table.5.4 and the proposed design shows better than other designs with respect to resonant frequencies (5.3GHz, 7.9Ghz, 11.1GHz), Impedance bandwidth (700MHz, 260MHz, 300MHz), gain (8.04dBi, 6.89dBi, 8.06dBi) and Axial ratio bandwidth (700MHz, 250MHz, 300MHz) and size of the antenna (36mmx36mmx12.25mm). With simple slits design on the patch and minimized ground the structure resonates at tri-frequencies.

The formation of slits onto the patch varies the results a lot since these depend on the patch's shape and the position of the slit. Superstrate is loaded on the patch at a distance of $\lambda_o/4$ from the surface of the ground to reflect the radiation from the patch, which improves the impedance bandwidth, axial ratio, and gain of the proposed triple-band compact circularly

polarized microstrip antenna. Compared to the literature of triple-band circularly polarized antenna with superstrate, the proposed design is compact, simple structure, easy fabrication; minimum return loss level, good radiation characteristics, and antenna gain characteristics are good at resonant frequencies.

5.4 Summary

In this chapter, a compact V-shaped slit microstrip circularly polarized antenna with superstrate for 5G WLAN and X-band application is fabricated. By changing length r_1 at one corner of the circular patch to form a V-shaped slit, the desired resonant frequencies with good circular polarization are achieved. A detailed description of how circular polarization is obtained with V-shaped slit formation at the corners is illustrated using the surface current distribution of the proposed antenna with superstrate. A comprehensive parametric analysis for various superstrate studied materials like RT Duroid 5880, FR-4, and RF-10 is discussed and tabulated. The measurement setup is described, and an antenna is connected after the ports are matched well.

The measured 10-dB impedance bandwidthsare13.2%(4.9GHz-5.6GHz),3.16%(7.74GHz-8GHz),2.7%(10.9GHz-11.2GHz), and gains of 8dBi,6.89dBi,8dBi at resonant frequencies 5.3GHz,7.9GHz, and 11.1GHz, and are in good agreement with simulated results using High-frequency structure simulator software v.13. The proposed triple-band compact circularly polarized microstrip antenna size is 36mmX 36mmX12.25mm and is better than literature reported antennas for 5G WLAN and X-band applications. The gain and the axial ratio bandwidth obtained in this work are superior compared to the designs reported in [58], [94], [95], [96], [97] and [98].Further the size of the proposed antenna is compact compared to the designs reported in [58], [94], [95], [96], [97] and [98]. The proposed circularly polarized compact antenna with superstrate possesses triple-band characteristics and is suitable for the 5G WLAN and X-band applications of satellite communications, air traffic control, wireless personal area network(WPN), remote sensing, vehicular applications, defense tracking, and modern radars.

- Swetha Ravikanti, L. Anjaneyulu “Triple band circularly polarized compact microstrip antenna with superstrate for 5G wireless local area network and X-band application”, International journal of communication systems (revision 3 Under Review SCI).

Chapter 6

Circularly polarized asymmetric U shape antenna with second-order bandpass frequency selective surface

This chapter introduces the concept of frequency selective surface and proposes an asymmetric U-shaped slit circularly polarized antenna with second-order bandpass frequency selective surface that is designed, compared theoretically, and evaluated. The performance of the proposed antennas is compared with the existing antennas.

Metamaterial is an artificial material that does not exist in nature, but the metallic elements' electrical properties will impact the antenna structure's properties. Meta surface is a periodic arrangement of metallic elements in a 2-D infinite array. Based on the sources, they are classified as passive and active arrays. In an active array, the incident plane wave is excited by individual generators connected to each element. Each generator has a uniform amplitude and a linear phase variation, so it produces two or more radiated waves. In a passive array, the incident plane wave is partly transmitted in the forward direction and partly reflected in the specular direction. A periodic surface is formed when identical elements are arranged in an infinite array of one or two dimensions [99].

Based on the material characteristics, periodic surfaces are classified and exhibit perfect reflection or transmission only at resonance. The use of two or more cascaded elements behind each other without dielectrics and the use of slabs sandwiched between cascading periodic surfaces lead to hybrid periodic surfaces. Applications of periodic surfaces are listed below

(i) Hybrid radomes
(ii) Bandstop filters
(iii) Dichroic sub reflectors
(iv) Circuit analog absorbers
(v) Meander line polarizers

Metamaterials are categorized into High impedance surface, Frequency selective surfaces (FSS), reactive impedance surface, and EBG structures. In Metasurface, based on the structure of the elements, antenna characteristics can be analyzed.

FSS is a periodic structure composed of a two-dimensional periodic array of different shapes embossed on a thin dielectric slab, exhibits frequency selectiveness in transmission/reflection characteristics, and shows electromagnetic wave filtering property(spatial filtering) as shown in Fig 6.1 and taxonomy of FSS as shown in Fig.6.2.

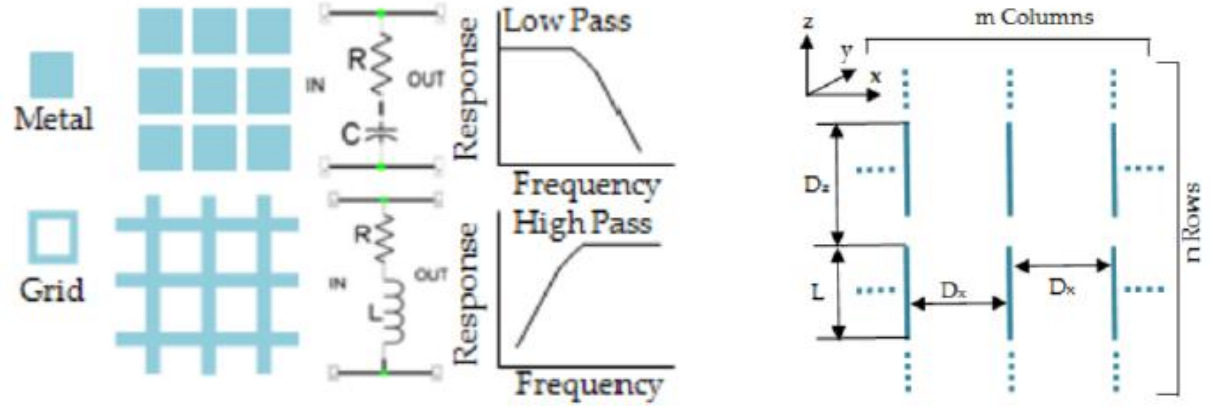

(a) (b)

Fig.6.1 (a) Equivalent circuit of FSS periodic structure with complementary array elements (b) 2-D periodic structure with element length L and element-spacing D_x and D_z.

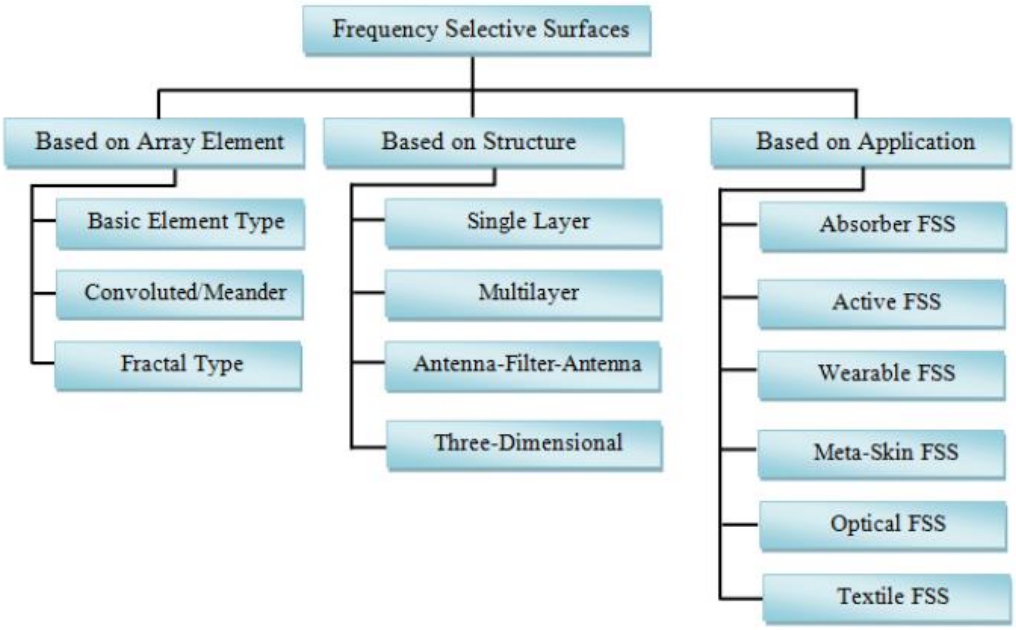

Fig.6.2 Taxonomy of FSS

Single layer FSSs are not able to provide adequate spatial filtering response, and its impedance bandwidth is narrow, so miniaturization of FSS is needed, and much importance is given for multilayer FSS to improve flexibility for varying parameters to achieve desired performance. In FSS elements are categorized in four groups as depicted in Fig.6.3.

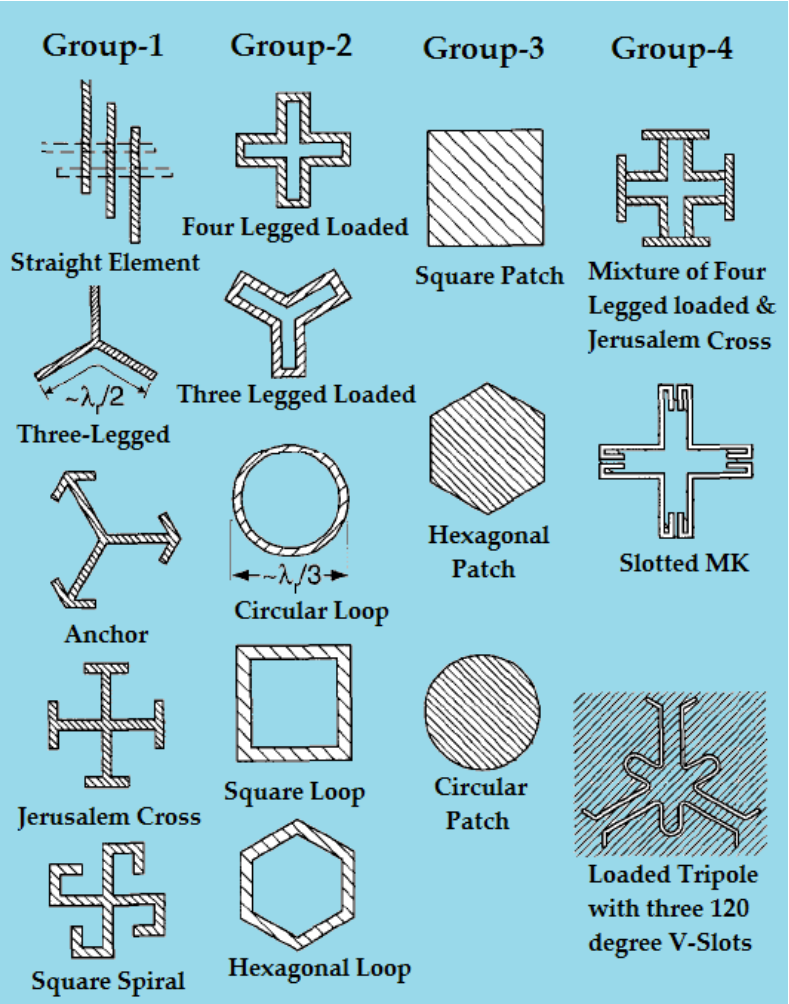

Fig.6.3 Classification of FSS Elements

The author's research focused on second-order bandpass frequency response for dual layer FSS and compared theoretical as well as measured performance characteristics of the proposed design. Parametric analysis is carried out for various parameters of the design with and without superstrate. The proposed design is simple with; high gain, wide bandwidth, and compact design are the attractive characteristics of the asymmetric U shape compact circularly polarized antenna with second-order bandpass frequency selective surface as the superstrate.

6.1 Analysis and configuration of asymmetric U-shape circularly polarized antenna with FSS layers.

The proposed composite structure consists of asymmetric U shaped patch antenna, minimized ground, and dual layer FSS superstrate is placed at a height H=10.7mm from the ground and is etched on RT Duroid 5880(ε_r=2.2) with thickness t=0.787mm and is depicted in Figs.6.4-6.5. The second-order response of FSS is achieved by cascading three FSS layers of patch-aperture-patch type with RT duroid as dielectric material in between them. The characteristics of unit cells of the wire grid and aperture type layers exhibit capacitive and inductive properties. The U shape asymmetric antenna resonates at 2GHz,2.7GHz, and 5.6GHz and the minimized ground structure at the bottom results in dual frequency. In the FSS technique, the design is low profile with second-order bandpass filter responses, and the unit cell of FSS are non-resonant structures. The overall response of the combined unit cell structures creates a second-order bandpass filter. The periodicity of FSS is less than the wavelength and thus reduces the sensitivity, with no grating lobe in accordance with the angle of incidence.

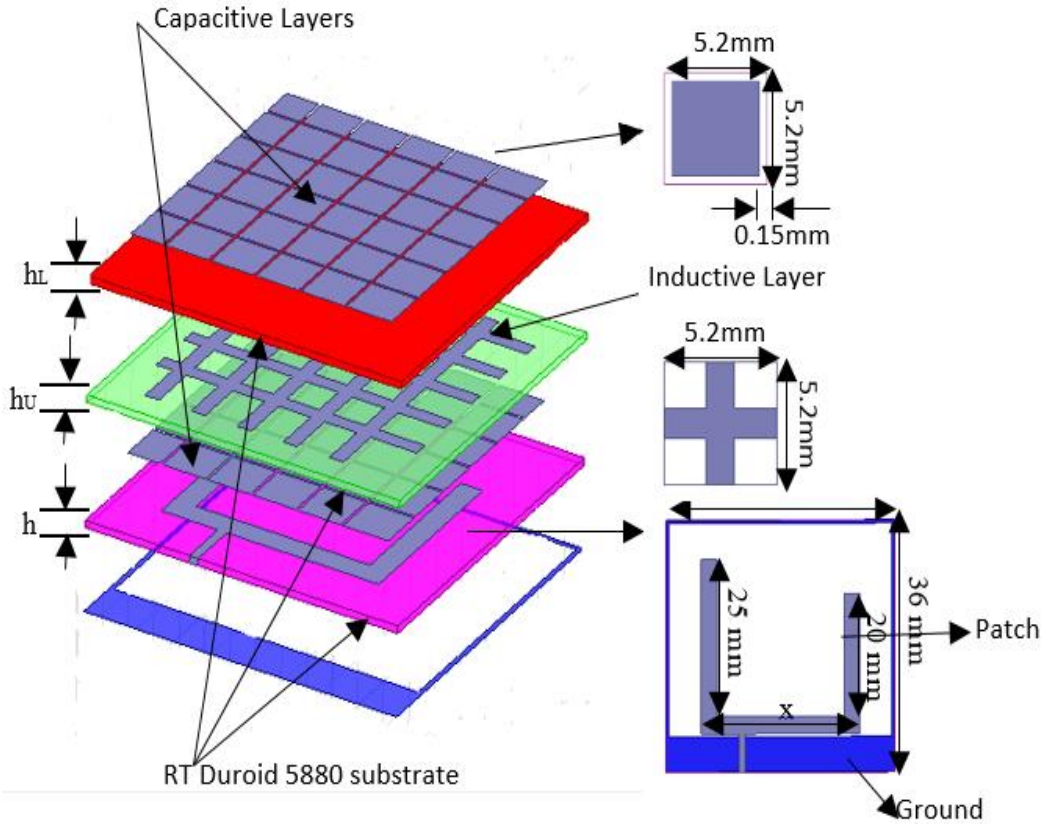

Fig.6.4 3-D view of the Asymmetric U shape antenna with dual layer FSS.

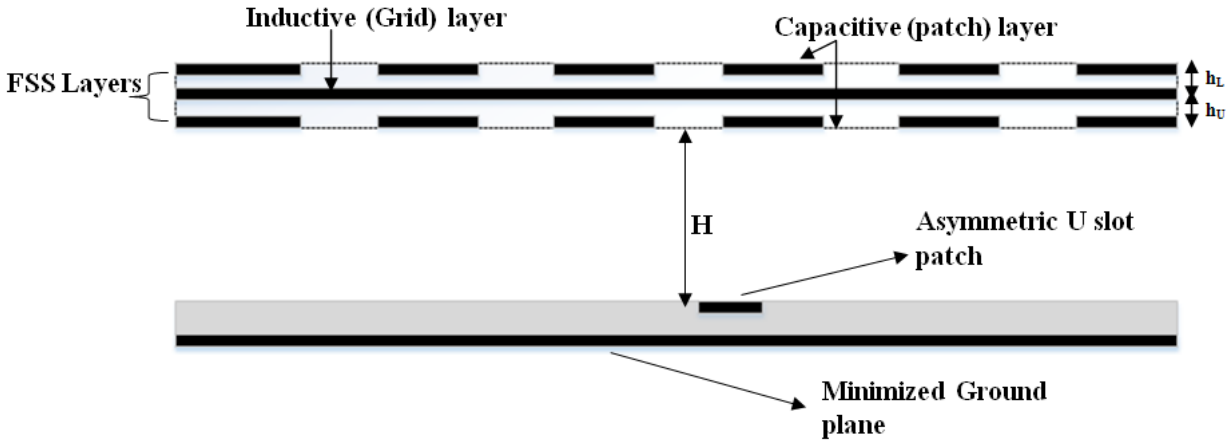

Fig.6.5 Side view of the FSS-antenna Geometry structure.

6.1.1 Parametric analysis

In U shaped asymmetric circularly polarized antenna, a parametric analysis is carried out for a parameter 'x' as shown in Figs.6.6-6.7 and tabulated in Table.6.1; x=25mm gives good results when compared to others. In general, uniform FSS has a uniform dimension of 2-D unit cell, but in order to produce circular polarization, asymmetry is created in the unit cell dimension.

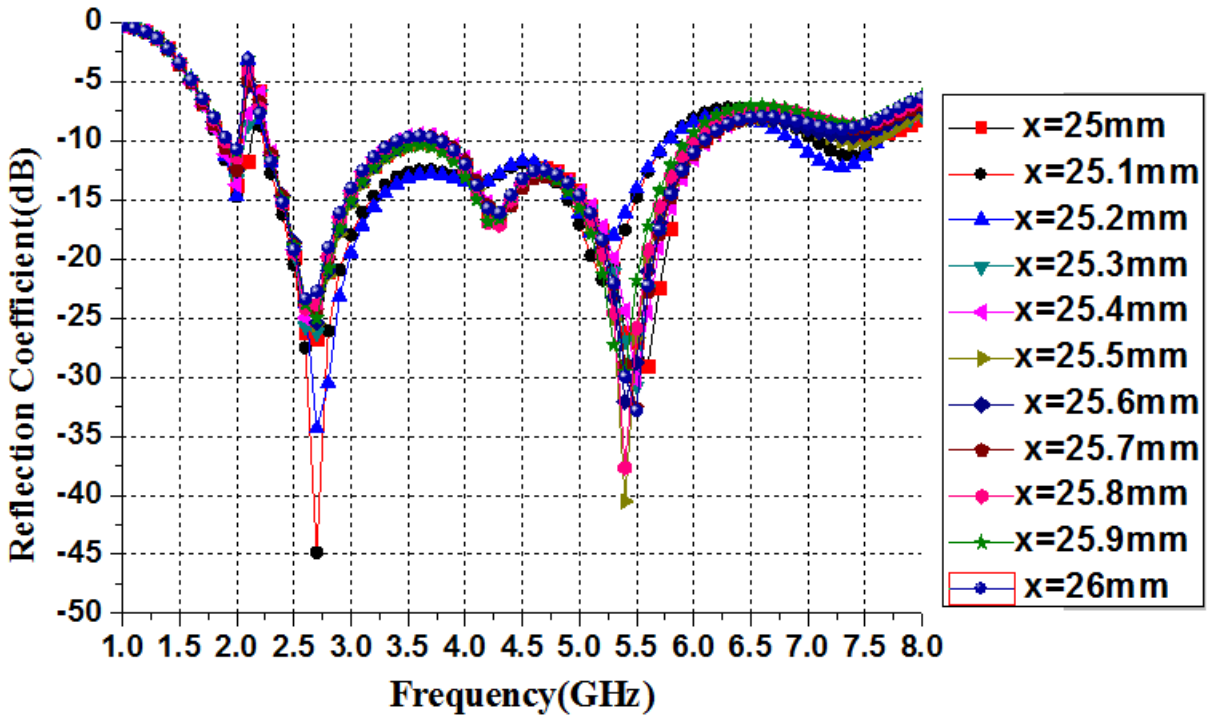

Fig 6.6 Reflection coefficient for various values of x

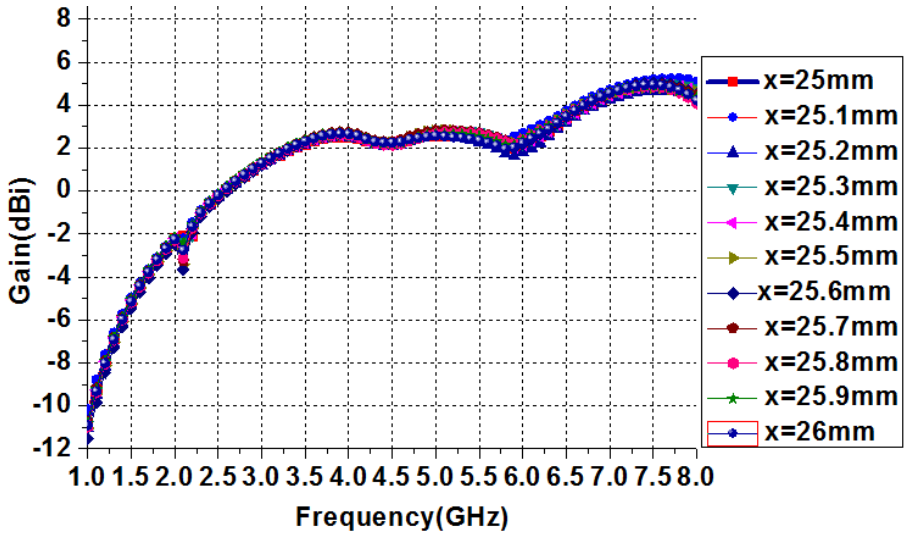

Fig 6.7 Gain for various values of x

Table.6.1 Performance of the antenna for various values of x.

Length of the patch(x in mm)	Resonant frequency(GHz)	Bandwidth(GHz)	Gain(dBi)
25	2,2.7,5.6	2.2-6.1=3.9GHz	0.43,2.47
25.1	2,2.7,5.2	2.2-5.8=3.6GHz	0.51,2.73
25.2	2,2.7,5.2	2.2-5.8=3.6GHz	0.35,2.55
25.3	2,2.7,5.5	2.3-6.1=3.8GHz	0.42,2.74
25.4	2,2.6,5.5	2.3-6.1=3.8GHz	0.14,2.62
25.5	2,2.7,5.4	2.3-6.1=3.8GHz	0.42,2.7
25.6	2,2.7,5.4	2.2-6.1=3.9GHz	0.32,2.66
25.7	2,2.7,5.5	4.9-6.1=1.2GHZ 2.2-3.4=1.2GHz	0.49,2.7
25.8	2,2.6,5.4	2.3-6=3.7GHz	0.11,2.69
25.9	2,2.7,5.4	2.3-5.9=3.6GHz	0.54,2.61
30	2,2.6,5.5	3.8-6.1=3.3Ghz 2.3-3.4=1.1Ghz	0.145,2.3,581

In FSS layers, as shown in Figs.6.8-6.9, the unit cell is of square shape of size Y_1 and Y_2. The unit cell size is varied for the desired frequency as shown in Table.6.2; better performance characteristics and are illustrated in Figs.6.10-6.11. In this geometry, two

capacitive layers and one inductive layer are present between two dielectric substrates RT Duriod 5880 in FSS. Y_1=5.2mm shows better performance, and Y_2=2.8mm is chosen to obtain the circular polarization.

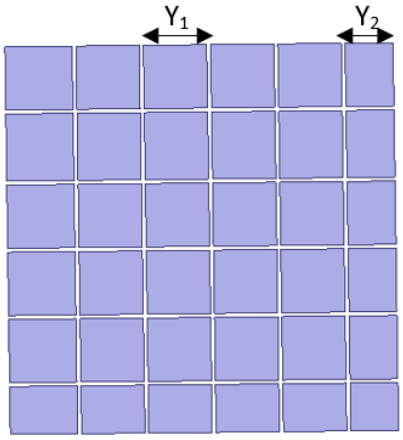

Fig.6.8 Capacitive layer on FSS

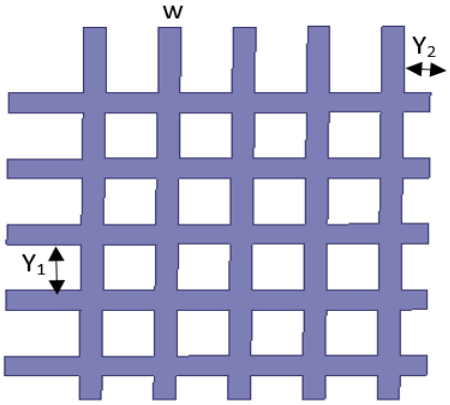

Fig.6.9 Inductive layer on FSS.

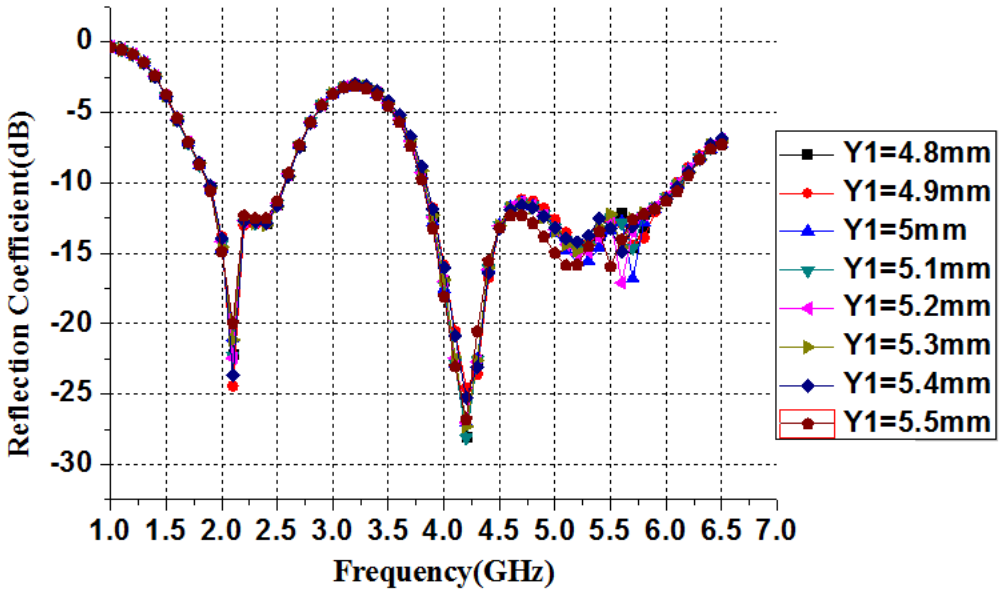

Fig.6.10 Reflection coefficient for various values of Y_1.

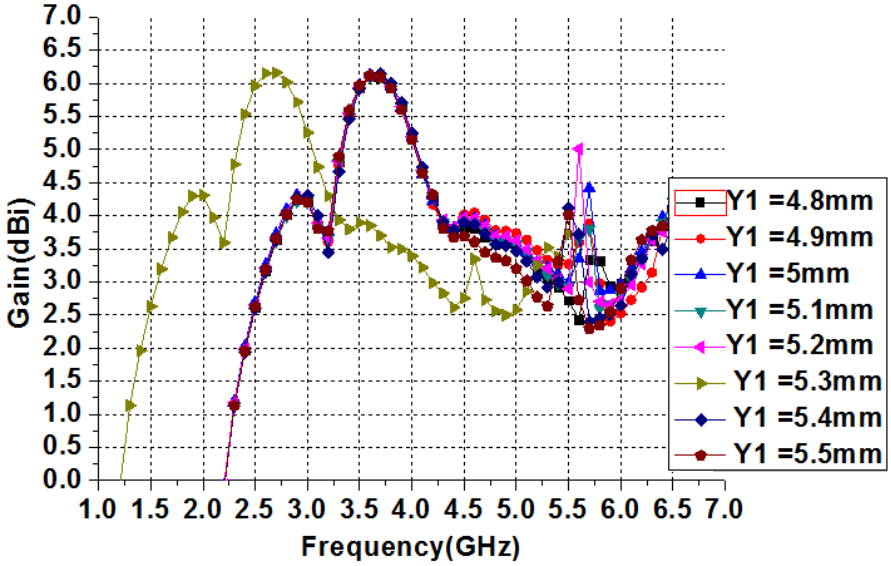

Fig.6.11 Gain for various values of Y_1.

Table.6.2 Performance of the antenna for various values of Y_1.

Cell size(Y_1 in mm)	Resonant frequency(GHz)	Bandwidth(GHz)	Gain(dBi)
4.8	2.1,4.2,5.2	3.8-6.1=2.3GHz 1.9-2.5=600MHz	-1.53,4.22,3.05
4.9	2.1,4.2,5.7	3.8-6.1=2.3GHz 1.9-2.6=700MHz	-1.47,4.17,3.87
5	2.1,4.2,5.7	3.8-6.1=2.3GHz 1.9-2.5=600MHz	-1.57,4.2,4.4
5.1	2.1,4.2,5.7	3.8-6.1=2.3GHz 1.9-2.6=700MHz	-1.56,4.25,3.79
5.2	2.1,4.2,5.6	3.8-6.1=2.3GHz 1.9-2.6=700MHz	-1.52,4.26,5
5.3	2.1,4.2,5.6	3.8-6.1=2.3GHz 1.9-2.6=700MHz	-1.52,4.29,3.34
5.4	2.1,4.2,5.6	3.8-6.1=2.3GHz 1.9-2.6=700MHz	-1.52,4.27,3.72
5.5	2.1,4.2,5.6	3.8-6.1=2.3GHz 1.9-2.6=700MHz	-1.67,4.31,4.07

6.1.2 Principle of operation for FSS layers

For the designed monopole asymmetric U shaped antenna has low gain, and to enhance it, an FSS with second-order bandpass filtering property is used. The second-order bandpass response is achieved by cascading three FSS layers, i.e., aperture patch type with RT duroid 5880(ε_r=2.2) as the dielectric material in between them, capacitive and inductive properties

are exhibited by unit cells of aperture type and patch layers. For the normal incidence of the electromagnetic wave, an equivalent circuit for FSS is shown in Fig.6.12. Fig.6.12 shows that parallel capacitors C_1, C3 are modeled as first and third patch type layers and inductor L as middle aperture type grid layer.Metallic FSS layers are separated from the substrate of height h_L and $h_{U,}$ having a characteristic impedance of $\frac{Z_0}{\sqrt{\varepsilon_{r1}}}, \frac{Z_0}{\sqrt{\varepsilon_{r2}}}$ for two small transmission lines. $Z_0, \varepsilon_{r1}, \varepsilon_{r2},$ are the characteristic impedance of 377Ω and dielectric constants of the substrate. Fig.6.12(b) shows the second-order filter nature; here the π network (L_1, L_m and L_3) is formed from the T network(L_{s1}, L_2 and L_{s2}), and its value can be found with the help of L_{s1}, L_{s2} and L_2 .

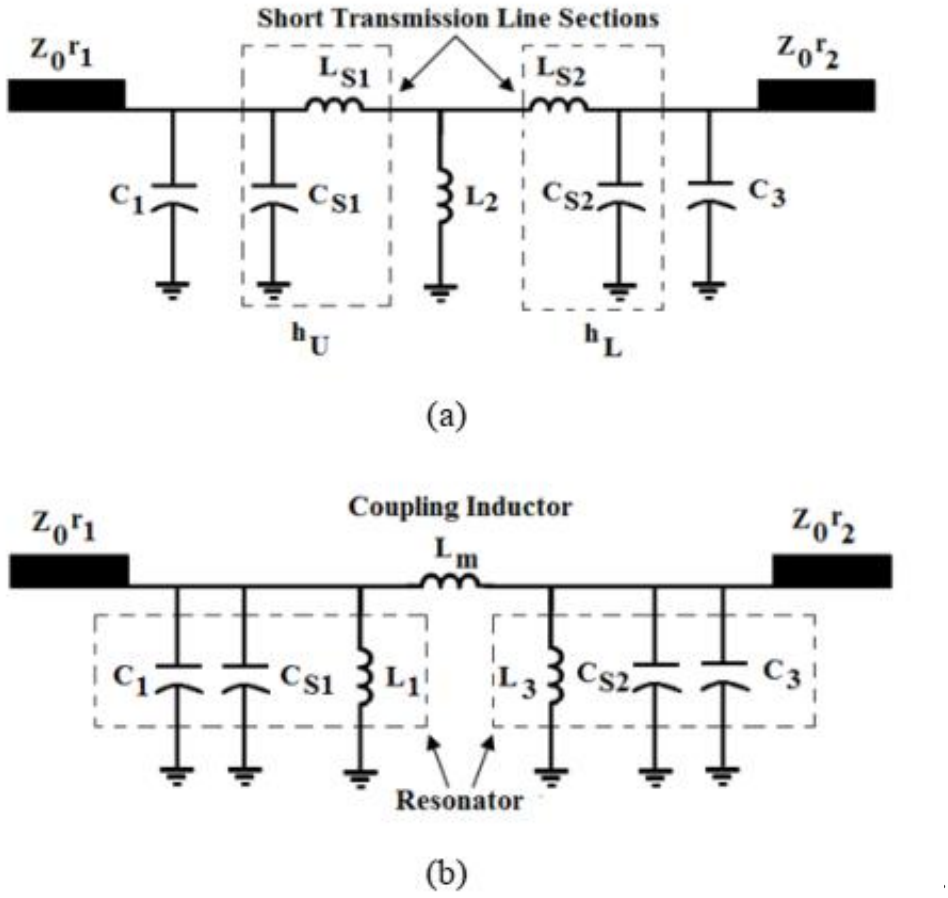

Fig.6.12 (a) Equivalent circuit model for FSS (b) Second-order coupled-resonator filter converted to π network from T network.

Second-order bandpass filtering response chosen for FSS for different parameters can be obtained from [100].

Table.6.3. Butter worth filter response for different parameters

Filter Type	Normalized loaded quality factor		Normalized coupling coefficient	Normalized impedances	
Butter worth	q_1	q_2	K_{12}	Source(r_1)	Load(r_2)
	1.4142	1.4142	0.70711	1	1

With the help of parameters provided in the table.6.3, the desired center frequency is 5.6GHz and fractional bandwidth δ, the value of inductor L_2 in the circuit can be known from the below equation [79].

$$L_2 = \frac{Z_0}{2\pi f_0 k_{12}} \cdot \frac{(k_{12}\,\delta)^2}{1-(k_{12}\,\delta)^2} \cdot \sqrt{\frac{r_1 r_2}{q_1 q_2}}\pi \tag{6.1}$$

In circuit short transmission line sections ($L_{s1,}$ Ls2) are calculated from the Telegraphers model as mentioned below.

$$L_{s1} = \mu_0 \mu_{r1} h_U \tag{6.2}$$

$$L_{s2} = \mu_0 \mu_{r1} h_L \tag{6.3}$$

In FSS, the capacitors C_1 and C_2 values are obtained from below equation [79]:

$$C_1 = \frac{q_1}{(2\pi f_0)\,Z_0\, r_1 \delta} - \frac{\varepsilon_0 \varepsilon_{r1} h_U}{2} \tag{6.4}$$

$$C_2 = \frac{q_2}{(2\pi f_0)\,Z_0\, r_2 \delta} - \frac{\varepsilon_0 \varepsilon_{r1} h_L}{2} \tag{6.5}$$

In the proposed design, the substrates are of the same material of RT Duroid 5880, for which $\varepsilon_{r1}=\varepsilon_{r2}=\varepsilon_r=2.2$ and $\mu_{r1}=\mu_{r2}=\mu_r=1$(Non-magnetic dielectric substrates). For the desired frequency f_0=5.6GHz (3.8GHz-6.2GHz), fractional bandwidth δ=0.41, $h_L=h_U$=0.787mm; and from these we have computed capacitor values $C_1=C_3$=252.49fF, L2=3.39nH .In FSS, the inductor and capacitor values are determined from the following equations [79]:

$$C_1 = C_2 = C = \varepsilon_0 \varepsilon_{eff}\, \frac{2Y}{\pi} \ln\left(\sin\frac{\pi s}{2Y}\right) \tag{6.6}$$

$$L_2 = \mu_0 \mu_{eff}\, \frac{Y}{2\pi} \ln\left(\sin\frac{\pi w}{2Y}\right) \tag{6.7}$$

With the help of these values C=252.49fF, L=3.39nH, s=0.3mm, ε_0=8.85x10 $^{-12}$ F/m and ε_{eff} (effective permittivity)= (ε_r+1/2) =1.6, μ_0=4πx10^{-7} H/m, μ_r=1 in Eq. (6.7) gives Y value and width of the inductive layer is found.

For simulation, HFSS is used, and the above values are considered initially, few successive simulations are performed to obtain optimal dimensions and are tabulated in Table.6.4 along with the circuit model of second-order bandpass response.

Table.6.4 Optimized dimensions of FSS unit cells for circuit model.

Parameter	**Y_1**	**W**	**S**	**h_U=h_L=0.787**
Circuit model	5.3mm	1.3mm	0.3mm	0.787mm
Optimized	5.2mm	1.6mm	0.3mm	0.787mm

6.1.3 Unit cell characteristics in FSS layers along with antenna

In HFSS software, the unit cells of three layered FSS are placed in a waveguide medium, i.e., PEC is placed at the sides and PMC at the bottom. Excitation is given along the x-axis, transmission and reflection coefficients of the unit cell are obtained along with transmission phase variation with respect to frequency as shown in Fig.6.13.

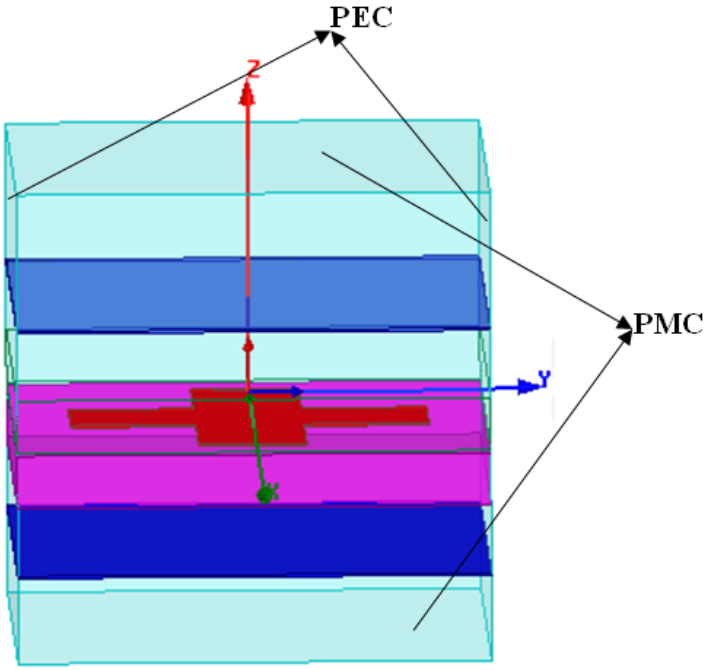

(a)

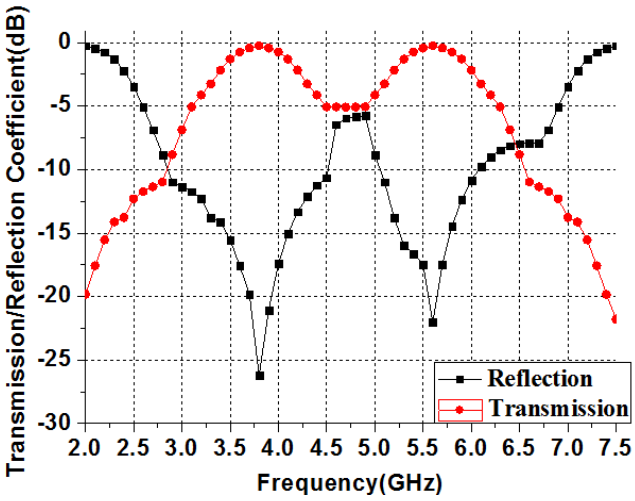

(b)

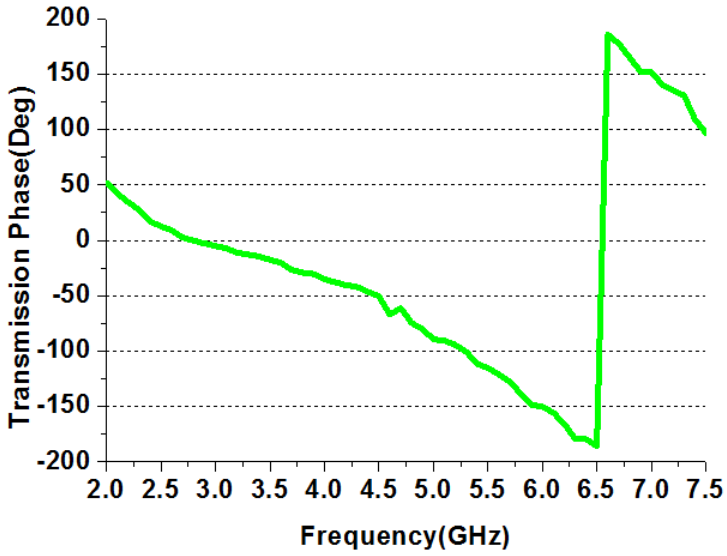

(c)

Fig.6.13. (a) Unit cell FSS configuration (b) Simulated reflection and transmission coefficient of FSS (c) Transmission Phase of FSS.

6.2 Measured and Simulated results

Fig.6.14. shows the fabricated prototype of antenna, FSS layers, and composite structure. Reflection coefficient for the composite structure along with the antenna is compared and shown in Fig.6.15. The superstrate antenna resonates at three frequencies, 2.1GHz, 4.2GHz, 5.6 GHz, with impedance bandwidth of 700MHz and 2.3GHz, respectively. It shows that the proposed design is suitable for 5G WLAN.

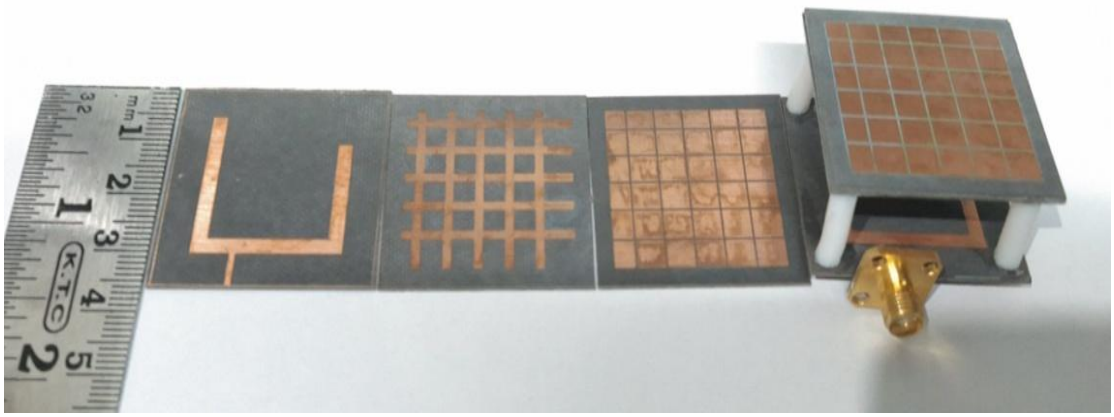

Fig.6.14. Fabricated proposed asymmetric U shape compact circularly polarized antenna with second-order bandpass FSS as the superstrate.

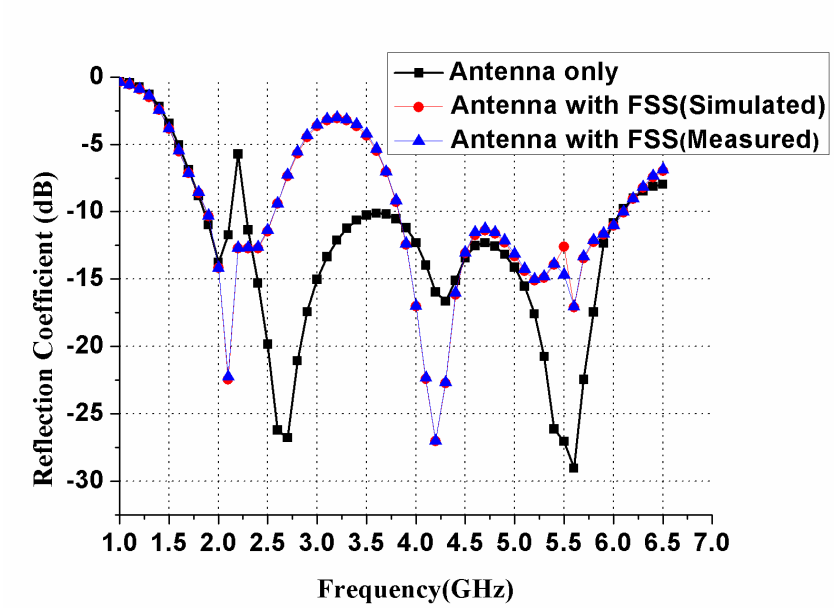

Fig.6.15. Reflection coefficient (simulated vs measured) with FSS of the antenna at the height of H=10.7mm.

It is noticed that the gain of the superstrate antenna is 5dBi at 5.6GHz, 4.26dBi at 4.26GHz, and the peak gain of the composite structure is 6.5dBi is shown in Fig.6.16. Axial ratio bandwidth of 2.1GHz is obtained at 5.6GHz as shown in Fig.6.17 and 200MHz at 2.1GHz frequency. Azimuth and elevation radiation patterns for all the resonant frequencies are shown in Figs.6.18-6.19.

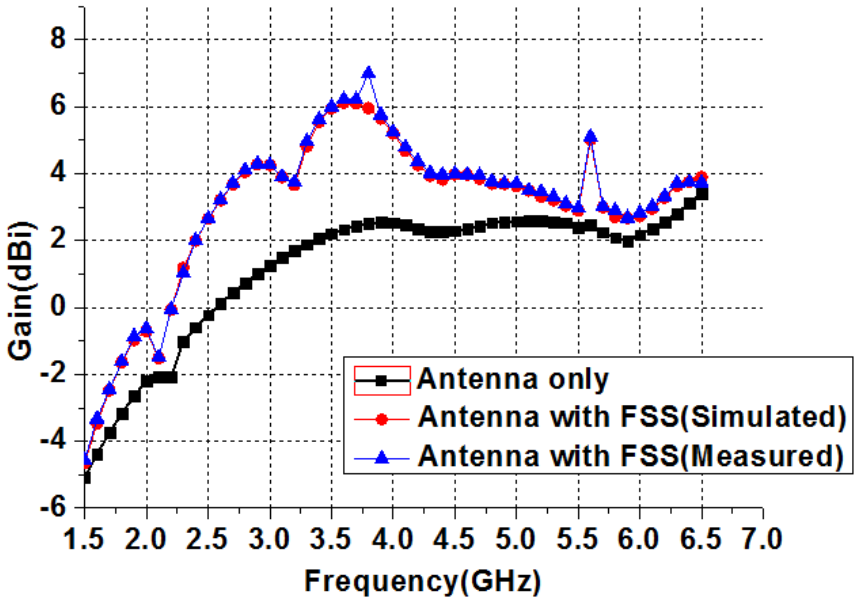

Fig.6.16. Gain of the antenna with FSS at height H=10.7mm.

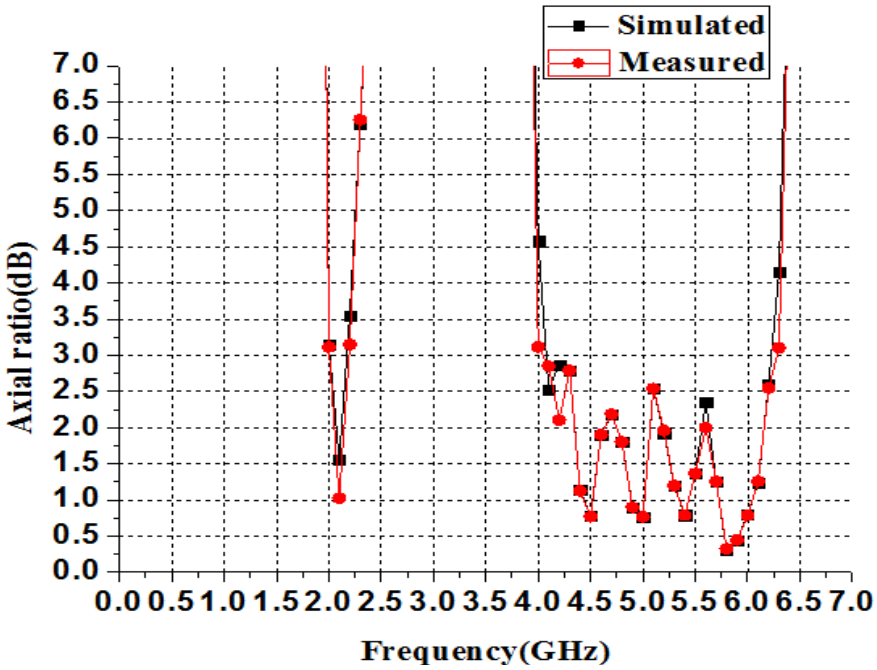

Fig.6.17.The axial ratio of the antenna with FSS

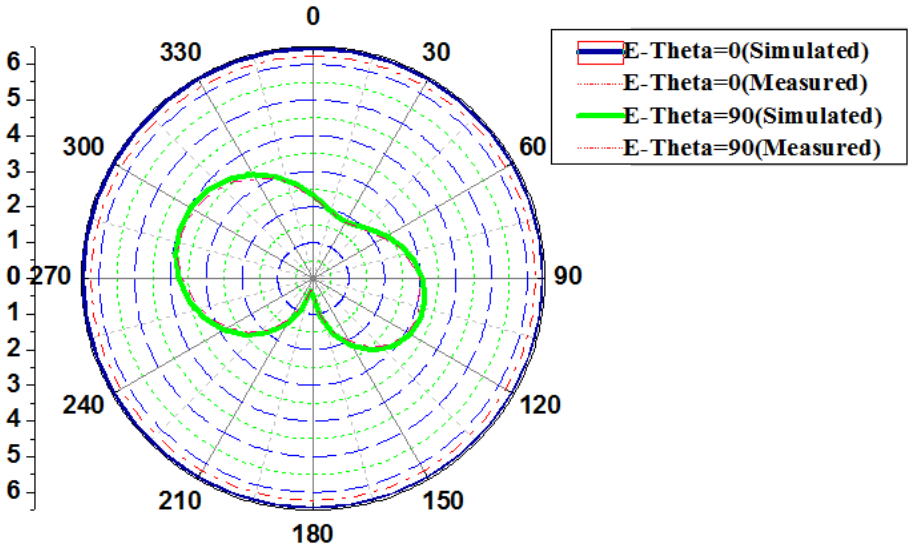

(a)

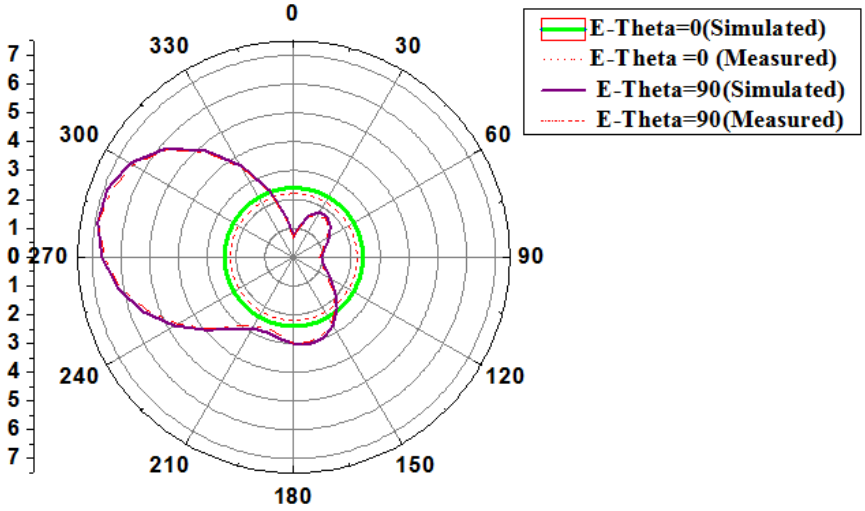

(b)

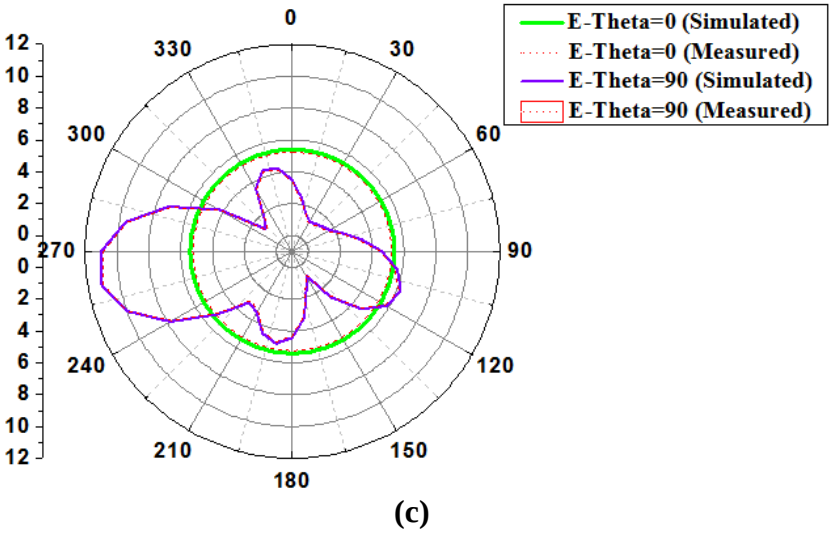

(c)

Fig.6.18.2-D Azimuth pattern at resonant frequency (a) 2.1GHz (b) 4.2GHz (c) 5.6GHz

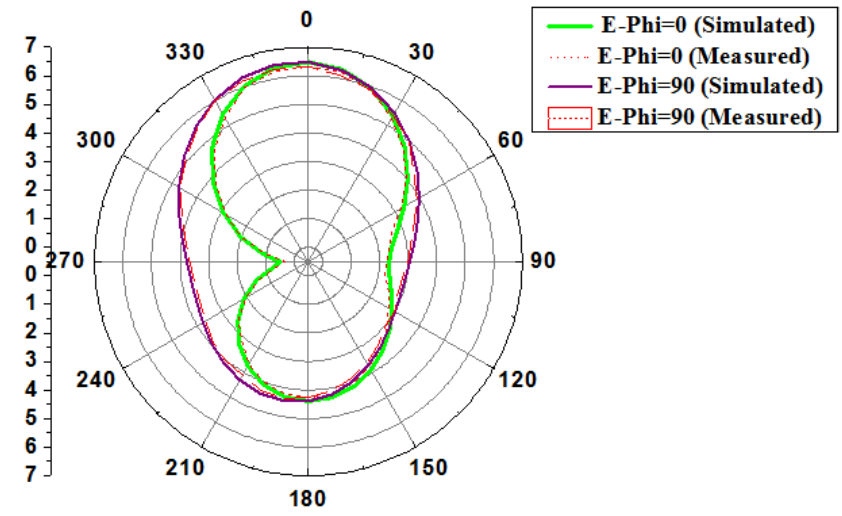

(a)

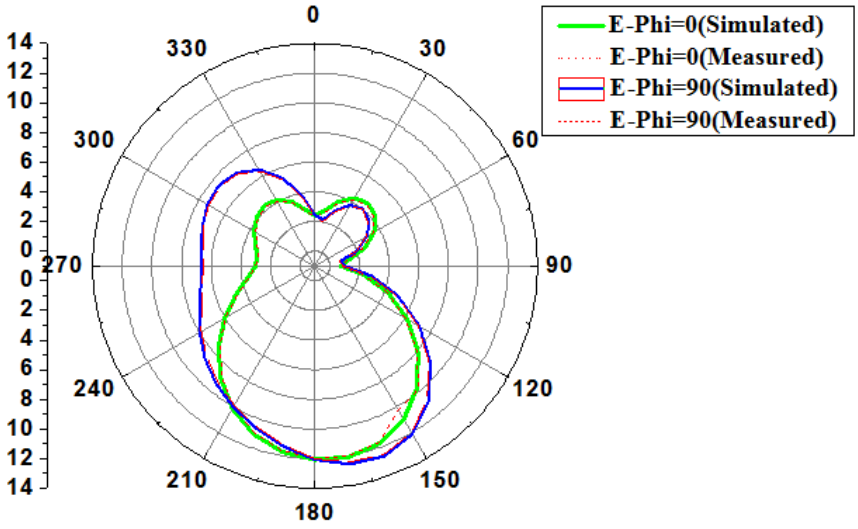

(b)

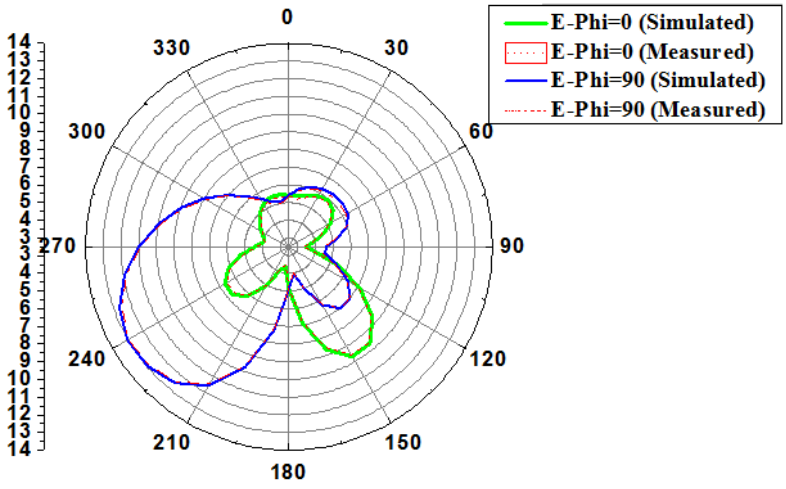

(c)

Fig.6.19.2-D Elevation pattern at resonant frequency (a) 2.1GHz (b) 4.2GHz (c) 5.6GHz

6.2.1 Measurement set up

The fabricated antenna consists of an asymmetric U shaped patch and dual layer FSS sandwiched between the dielectrics. The overall structure is supported by Teflon rods at the corners and excited through a line feed connector. The fabricated antenna is tested using a vector network analyzer, and measured results are compared with simulated results discussed above. The fabricated antenna and its measurement setup are shown in Fig.20. The fabricated antenna performances characteristics are compared with existing designs are shown in Table.6.5.

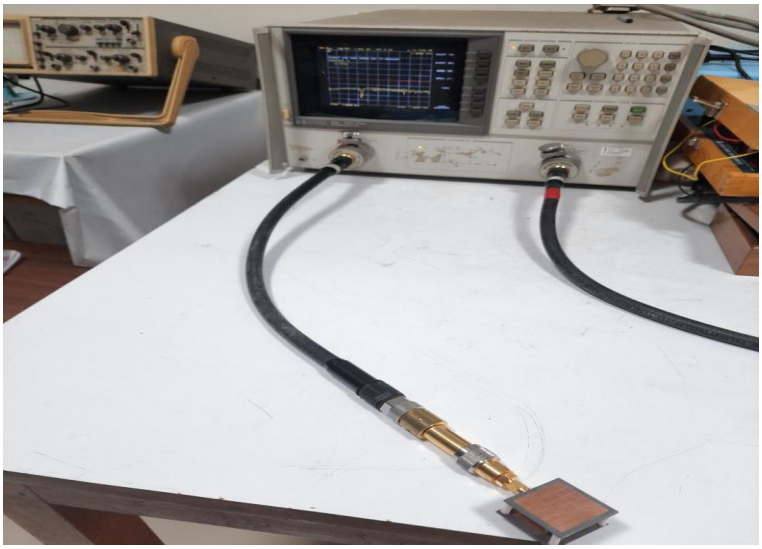

Fig.6.20. Measurement set up

Table.6.5 Comparison of the fabricated antenna with some of the existing antennas.

S.No	References	Resonant Frequency (GHz)	Impedance Bandwidth (%)	Gain (dBi)	Axial ratio Bandwidth (%)	Size of the antenna mm^3
1	[67]	2.5	14.8	8.5	11	45x45x8.3
2	[70]	5.81	73.67	5.6	18.93	100x100x32
3	[71]	2.4	4.95	3	11.6	84x84x17.5
4	[76]	8.5	20	16	20	120x120x14
5	[77]	7.66	55.7	15	47.7	36x36x26
6	**Proposed antenna**	**2.1,4.2,5.6**	**9.52,16,55**	**-0.15,4.6 ,6.5**	**9.5,4.7,3 7.5**	**36x36x12.27**

6.3 Discussion

FSS is a low profile structure because of non-resonant characteristics of the patch and grid layers and identified as a spatial filter. It allows or blocks electromagnetic waves in the band of interest. The incoming wave is propagated when the frequency matches with the resonance frequency, and the characteristics of the wave become smooth.

With the use of asymmetry in dimension of the unit cell in capacitive as well as inductive layers, circular polarization is achieved in the frequency of band of interest. With the designed superstrate dual layers, the gain is enhanced from 2.7dBic to 6.5 dBic in the desired frequency band.

It is observed that the radiation characteristics of the fabricated antenna with the superstrate layer become more directive due to its angular filtering property. The phase variation of the unit cell structure along broadside direction becomes zero in the 2GHz -6 GHz band due to the transmission and reflection waves phases being opposite in nature. This results in constructive interference of electromagnetic waves and efficiently enhances the performance characteristics along the broad side direction of propagation in an entire frequency band. The measurement set up for the proposed design is shown, and measured results are compared with the simulated results as discussed above.

6.4 Summary

In this chapter, gain enhancement of asymmetric U shaped antenna is attained with second-order bandpass frequency selective surface as the superstrate. Due to the asymmetry in U shape, antenna circular polarization is obtained, and further wave transmission is possible with asymmetric edge geometry in FSS. Compact geometry and with a minimum height between the antenna and superstrate achieved enhancement of 3dBi gain. The composite structure attains an impedance bandwidth of 55% and an axial ratio of 50% at the resonant frequencies 4.2GHz and 5.6GHz.It shows that the antenna is suitable for C-Band and 5G WIFI applications. The proposed design exhibits triple band, further it also provides better impedance bandwidth and compact size compared to existing designs reported in [67],[71],[76] and [77].

- Swetha Ravikanti , L. Anjaneyulu “Gain enhancement of Asymmetric U shape circularly polarized Antenna with second order bandpass Frequency selective surface as superstrate for C-Band and 5G WIFI Application”, in Progress in electromagnetic Research (Under Review SCI).

Chapter 7

Conclusions and Future work

7.1 Conclusions

The design and implementation of an optimized microstrip single antenna that demonstrates a circular polarization, with superstrate, aperture coupling feeding technique, and frequency selective surface and associated radiation pattern has been investigated. A systematic approach was taken for demonstrating this research. From the start, two main research interests were identified. Firstly a few designs to obtain circular polarization using various forms of slits, with the stacking of multiple layers and shorting pin antenna offering wideband with the use of aperture coupling feeding, are modeled and evaluated for their capabilities in connection with their operating characteristics. Secondly, a compact multi-layer frequency selective structure as a superstrate with monopole antenna that obtains multi-operating frequencies with broad performance characteristics is demonstrated with practical implementation. All the above fabricated antennas are useful for 5G wireless applications.

Circularly polarized antennas for 5G wireless applications require to operate in a determined changing environment keeping good electromagnetic characteristics. To start with, a few compact, coaxial probe feed microstrip antennas are designed for 5G WLAN applications. The core of the work presented in this thesis is the established methodology applicable for the realization of the circular polarization of the antennas. The concept of circular polarization is introduced by implementing various forms of slits mechanism.

A compact semicircular microstrip patch CP antenna for 5G WLAN application has been reported. The size of the compact microstrip patch antenna is 36 mm × 36 mm × 0.787 mm. By changing the radius r_2 at one corner of the semicircular slit, the desired resonant frequency band with circular polarization is achieved. A detailed description of how CP is obtained with slit formation at the corners is illustrated using surface current distribution at various time intervals. The specified fabricated design has been illustrated and compared with multiple existing models in terms of different performance parameters. The proposed structures give better return loss, axial ratio, gain, and omnidirectional pattern current designs. The resonant peak at 5.37 GHz falls in 5G WLAN (5.1–5.725 GHz) and is suitable for 5G WLAN

applications.

It is demonstrated that circular polarization is achieved by altering the antenna aperture structure that changes the direction of the current flow, which alters the direction of the E-field on the antenna, for the proof of concept, that changes the orientation of the surface electric currents on the patch. The basic principle implemented in this research for exciting circular polarization is introducing asymmetry in the aperture structure. Because of the quasi-symmetrical structure, the fundamental mode is split into two orthogonal degenerate modes generated only when the x-directed and y-directed currents have different electrical path lengths. The size of the compact microstrip patch antenna is 36 mm × 36 mm × 4 mm respectively.

The performance parameters of the designed antenna are impedance bandwidth of 29.10%, axial ratio bandwidth is 13.47%, and gain of 4.08dBic at the resonant frequency 3.47GHz and falls in the 5G radio band. These performance characteristics of hook-shaped aperture coupled circularly polarized antenna show better enhancement in impedance bandwidth and axial ratio. The simulated results are in good agreement with the measured results.

Using various materials, the concept of superstrate has been studied, and prototypes of the basic circular patches are fabricated with a single feed. It is shown that, by exciting the antenna with coaxial feed and superstrate, the surface electric current distribution on the basic patch alters its orientation, which changes the electrical distribution of radiation from the structure. This relationship between the source currents and the resulting radiation causes a slight shift in the operating frequency. With the compact size, the proposed antennas work for wideband applications; impedance bandwidths are 13.2% (4.9GHz-5.6GHz),3.16% (7.74GHz-8GHz),2.7%(10.9GHz-11.2GHz), and gains of 8dBi,6.89dBi,8dBi at resonant frequencies 5.3GHz,7.9GHz, and 11.1GHz, and are in good agreement with simulated results The size of the proposed triple-band compact circularly polarized microstrip antenna is 36mmX 36mmX12.25mm which is better than literature reported antennas for 5G WLAN and X-band application. The gain and the axial ratio bandwidth obtained in this work are superior compared to the designs reported in [58],[94],[95],[96],[97] and [98].Further the size of the proposed antenna is compact compared to the designs reported in [58], [94],[95],[96],[97] and [98].A circularly polarized compact antenna with superstrate possesses triple-band characteristics and

is suitable for the 5G WLAN and X-band applications of satellite communications, air traffic control, wireless personal area network(WPN), remote sensing, vehicular applications, defense tracking, and modern radars.

Finally,we designed a compact asymmetric U shape antenna with second-order bandpass frequency selective surface as superstrate and observed that radiation characteristics of the fabricated antenna with superstrate layer became more directive due to its angular filtering property. The phase variation of the unit cell structure along broadside direction becomes zero in the 2GHz -6 GHz band due to the transmission and reflection waves phases being opposite in nature. This results in constructive interference of electromagnetic waves and efficiently enhances the performance characteristics along the broadside direction of propagation in an entire frequency band. Compact geometry and with a minimum height between the antenna and superstrate achieved enhancement of 3dBi gain. The composite structure attains an impedance bandwidth of 55% and an axial ratio of 50% at the resonant frequencies 4.2GHz and 5.6GHz.It shows that the antenna is suitable for C-Band and 5G WIFI applications.

These antennas have been designed to operate on the most popular frequency ranges where a great number of 5G wireless communication applications exist. With circular polarization, the fading loss caused by multipath effects can be avoided and avails excellent frequency reuse properties. Aperture coupling technique and usage of shorting pin in stacked layers helps in strengthens the surface current distribution, Good co-polarization and cross-polarization for E and H-planes are observed. The experiment and simulation results prove the effectiveness of the proposed methods in the aspect of antenna size reduction, bandwidth enhancement, and multi-frequency operation. Furthermore, the antennas are completely planar, which makes them easy to be fabricated with a low cost. From this analysis, it has been concluded that a low cost, less complex, compact circularly polarized antenna design with broadband characteristics has been successfully introduced to the 5G wireless and radio frequency design community.

7.2 Future Scope

In the present thesis work, the co- and cross-polarization level of the aperture coupled circularly polarized antenna is improved by placing a reflector at the bottom of the antenna. The position of the reflector is placed at $\lambda_o/4$ behind the antenna, and the optimum size of the

reflector is to be chosen. So far in this research work, a conventional single feed port with circular polarization is used. Future research lines move towards the real implementation of a fully compound single antenna aperture with multiple ports for 5G wireless communication applications.

So far in the present research, parametric analysis is done using conventional microstrip feeding in FSS. In the future, FSS in two dimensions can be implemented on microstrip and can be extended to three dimensions. In FSS, the unit cells are capacitive and inductive in nature, so in the future, nano-scale cell metamaterials layers can be designed for 5G wireless applications.

List of Publications out of this research work

International Journals

[1]* Swetha Ravikanti and Anjaneyulu.Lokam, "A Survey on miniaturization of circularly polarized antennas for future wireless communications." published in Electronics and Communications Engineering: Applications and Innovations, Taylor and Francis CRC press (Scopus), p.63, ISBN no: 978-1-351-13682-2, 2019.

[2]* Swetha Ravikanti and L. Anjaneyulu, "Compact Circularly Polarized Patch Antenna for WiMAX Applications with Improved Impedance Bandwidth and Axial Ratio" published in Engineering, Technology & Applied Science Research Vol. 10, No. 1,p. 5104-5107, 2020 (ESCI),https://doi.org /10.48084 /etasr.3207.

[3]* Swetha Ravikanti and L. Anjaneyulu "A Novel And Compact Circularly Polarized Antenna for 5G Wireless Local Area Network Application ", published in Electrical, Control, and Communication Engineering Journal, Vol.16, no.1,p.44-50, November 2020. (ESCI), https://doi.org/10.2478/ecce-2020-0007.

[4]* Ravikanti Swetha and Lokam Anjaneyulu "Novel design and characterization of Wide Band Hook Shaped Aperture Coupled Circularly Polarized Antenna for 5G Application", Published in Progress In Electromagnetics Research C (Scopus), Vol. 113, p.161-175, 2021, doi:10.2528/PIERC21040202.

[5]* Swetha Ravikanti, L. Anjaneyulu "Triple band circularly polarized compact microstrip antenna with superstrate for 5G wireless local area network and X-band application", International journal of communication systems (Under Review revision 3 SCI).

[6]* Swetha Ravikanti, L. Anjaneyulu "Gain enhancement of Asymmetric U shape circularly polarized Antenna with second order bandpass Frequency selective surface as superstrate for C-Band and 5G WIFI Application", in Progress in electromagnetic Research (Under Review SCI).

International Conferences

[7]* Swetha Ravikanti and Anjaneyulu.Lokam," Single layer Asymmetric slit circularly polarized patch antenna for WLAN Application," Published in Advances in Communications, Signal Processing and VLSI, Select Proceedings of IC2SV (springer), p.219-225,2021.

[8]* Swetha Ravikanti and Anjaneyulu.Lokam, "A Circularly Polarized Patch Antenna for WiMAX Application," in IEEE International Conference on Innovative Technologies in Engineering 2018(ICITE OU) held in Osmania University, Hyderabad on 11-13th April 2018.

References

[1]. E. C. Jordan and K. G. Balmain, Electromagnetic waves and Radiating systems Second Edition, India: Prentice Hall , 2000.

[2]. *IEEE Transactions on Antennas and Propagation,* Vols. AP-17, no. 3; AP-22, no. 1 ; and AP-31, no. 6, Part II, May 1969; Jan 1974; Nov 1983.

[3]. C. A. Balanis, Antenna Theory Analysis and Design, New Jersy: John Wiley and Sons Inc., 2005.

[4]. G. Ramesh, P. Bhartia, I. Bahl and A. I, Microstrip antenna design handbook, Norwood, MA: Artech House Inc., 2001.

[5]. J. James and P. Hall, Handbook of Microstrip Antennas Vol-2, The Institution of Engineering and Technology, 1989.

[6]. R. F. Harrington, "Effect of Antenna Size on Gain, Bandwidth, and Efficiency," vol. 64D, no. 1, June 29, 1959.

[7]. L. J. Chu, "Physical limitations of omnidirectional antennas," *Journal of Applied Physics*, vol. 19, no. 12, pp. 1163-1175, Dec. 1948.

[8]. Pozar,D.M and D.Schaubert (eds). Microstrip antennas: The analysis and design of microstrip antennas and arrays, New York: John wiley and sons, Inc.,1995.

[9]. James, J.R and P.S Hall(eds.) Handbook of microstrip antennas, IEE Electromagnetic wave series,1989.

[10]. Balanis,C.A. Antenna theory : Analysis and design, Hoboken, NJ: John Wiley and sons, Inc.2005.

[11]. Steven (Shichang) Gao, Qi Luo, and Fuguo Zhu, Circularly polarized antennas, wiley publishers, 2014.

[12]. A. Osseiran, F. Boccardi, V. Braun, K. Kusume, P. Marsch, M. Maternia,O.Queseth, M. Schellmann, H. Schotten, H. Taokaet al., "Scenarios for 5g mobile and wireless communications: the vision of the metis project," IEEE Communications Magazine, vol. 52, no. 5, pp. 26–35, 2014.

[13]. Y. Niu, Y. Li, D. Jin, L. Su, and A. V. Vasilakos, "A survey of millimeter wave communications /(mmwave) for 5g: opportunities and challenges," Wireless Networks, vol. 21, no. 8, pp. 2657–2676, 2015.

[14]. M. M. Kassem and M. K. Marina, "Future wireless spectrum below 6 ghz: A uk perspective," in Dynamic Spectrum Access Networks (DySPAN),2015 IEEE International Symposium on. IEEE, 2015, pp. 59–70.

[15]. T. Wang, G. Li, B. Huang, Q. Miao, J. Fang, P. Li, H. Tan, W. Li,J. Ding, J. Li et al., "Spectrum analysis and regulations for 5g," in 5GMobile Communications. Springer, 2017, pp. 27–50.

[16]. "Federal Communications Commission," FCC, [Online]. Available: https://www.fcc.gov/.

[17]. Simon r. Saunders, Alejandro Aragon-Zavala. Antennas and propagation for wireless communication systems, John Wiley and sons, 2007.

[18]. Eldad Perahia and Robert Stacey. Next Generation Wireless LANs. Next Generation Wireless LANs, Cambridge University Press, 2008.

[19]. Yibo Wang, Zhinong Ying, Guangli Yang, "A Compact CPW-Fed Wideband Antenna Design for 5G/WLAN Wireless application," IEEE conference, 2017.

[20]. Braasch**,** M.S., Multipath effects, in Global positioning system: Theory and applications, edited by Parkinson, B.W.et al., American institute of aeronautics and astronautics (AIAA),1, pp. 547-568,1996.

[21]. Counselman, C.C., Multipath rejecting GPS antennas, Proceedings of IEEE,87(1), pp.86-91, January 1999.

[22]. Davies, K., Ionospheric radio propagation, NBS monograph 80,181, US government printing office Washington DC, 1965.

[23]. Brookner, E., W.M.Hall and R.H Westlake. Faraday laoss for L-band radar and communications systems, IEEE Transactions on aerospace and electronic systems, 21(4),459-469,1985.

[24]. Nakano, H. Helical and spiral antennas: A numerical approach, research studies press Ltd,1987.

[25]. K. C. Gupta and P. S. Hall, Analysis and Design of Integrated Circuit-Antenna Modules, NY: John Wiley & Sons, Inc., October 1999.

[26]. "An Introduction to HFSS: Fundamental Principles, Concepts and Use," Ansoft LLC, Pittsburgh, PA 15219, 2009.

[27]. "IE3D User Manual," Mentor Graphics Corporation, Fremont, CA, 2013.

[28]. K. Ming, H. W. Lai, K. M. Luk, and C. H. Chan, **"**Circularly polarized patch antenna for future 5G mobile phones," *IEEE Access*, vol. 2, pp. 1521–1529, 2014.

[29]. H. Wong, Q. W. Lin, H. W. Lai, and X. Y. Zhang, "Substrate Integrated Meandering Probe-Fed Patch Antennas for Wideband Wireless Devices," *IEEE Transactions on Components, Packaging and Manufacturing Technology*, vol. 5, no. 3 March 2015.

[30]. P. C. Sharma and K. C. Gupta, "Analysis and optimized design of single feed circularly polarized microstrip antennas," *IEEE transactions on Antennas and Propagation*, vol. AP-31, no. 6, November 1983. https://doi.org/10.1109/TAP.1983.1143162

[31]. W. S. Chen, C. K. Wu, and K. L. Wong, "Single-feed square-ring microstrip antenna with truncated corners for compact circular polarization operation," *Electron. Lett.* vol. 34, no. 11, pp. 1045–1047, May 1998. https://doi.org/10.1049/el:19980818

[32]. H. Wong, et al. "Virtually Shorted Patch Antenna for Circular Polarization," *IEEE Antennas and Wireless Propagation Letters*, vol. 9, 2010. https://doi.org/10.1109/LAWP.2010.2100361

[33]. Nasimuddin, X. Qing, and Z. N. Chen "Compact Asymmetric-Slit Microstrip Antennas for Circular Polarization," *IEEE Antennas Wireless Propag. Lett.* vol. 59, no 1, Jan. 2011.

[34]. A. Soltan, M. H. Neshati, "Development of Circularly Polarized Cavity Backed Slot Antennas Using SIW Structure," *3rd International Conference on Advances in Computational Tools for Engineering Applications* (ACTEA), 2016.

[35]. J. Liu, Y. Li, Z. Liang, and Y. Long, "A Planar Quasi Magnetic-Electric Circularly-Polarized Antenna," *IEEE Transactions on Antennas and Propagation*, vol. 64, no. 6, pp. 2108–2114, 2016.

[36]. Nasimuddin, X. Qing, and Z. N. Chen, "A Compact Circularly Polarized Slotted Patch Antenna for GNSS Applications," *IEEE Transactions on Antennas and Propagation*, vol. 62, no. 12, December 2014. https://doi.org/10.1109/TAP.2014.2360218

[37]. H. Iwasaki, "A Circularly Polarized Small-Size Microstrip Antenna with a Cross Slot," *IEEE Transactions on Antennas and Propagation*, vol. 44, no. 10, October 1996. https://doi.org/10.1109/8.537335

[38]. A. Ferchichi and A. Gharsallah, "A Circuit Model to a Directive Triangular EBG Antenna," *Int. Journal of Electronics and Telecommunications*, 2013, vol. 59, no. 2, pp. 125–130.

[39]. Jianxing Li, Bin He, Lumei Li, Anxue Zhang, Jiangang Liu, Qing Huo Liu, "Capacitor-Loaded Circularly Polarized Annular-Ring Slotted Microstrip Patch Antenna," IEEE International Symposium on Antennas, Propagation and EM Theory (ISAPE), china, 2016.

[40]. Xiao Zhang, *IEEE*, and Lei Zhu, "High-Gain Circularly Polarized Microstrip Patch Antenna With Loading of Shorting Pins," IEEE transactions on antennas and propagation, vol. 64, no. 6, June 2016.

[41]. Wen-Shyang Chen, Chun-Kun Wu Kin-Lu Wong, "A novel compact circularly polarized square microstrip antenna," IEEE Transactions on antennas and propagation, vol.49, no.3, 2001.

[42]. R. Sreemathy, Shahadev Hake, ShamaliSulakhe and SumitBehera, "Slit Loaded Textile MicrostripAntennas," IETE Journal of Research, 2020.

[43]. Dian Wang, Hang Wong, and Chi Hou chan**,** "Small Circularly Polarized Patch Antenna," in IEEE conference 2011.

[44]. Huang. H, Li. X, Liu. Y, "A Low-Profile, Single-Ended and Dual-Polarized Patch Antenna for 5G Application" *IEEE Transactions on Antennas and Propagation*, vol. 68, no. 5, p. 4048-4053. 2019.DOI: 10.1109/TAP.2019.2948743

[45]. Kirov.G. S and Mihaylova.D. P, "Circularly Polarized Aperture Coupled Microstrip Antenna with Resonant Slots and a Screen," *Radio Engineering*, 2010, vol. 19, no. 1, p. 111–116.

[46]. Ge. L, Yang. X, Zhang D, Li. M, Wong. H, " Polarization Reconfigurable Magneto-Electric Dipole Antenna for 5G Wi-Fi," *IEEE Antennas and Wireless Propagation Letters*, vol. 16, p. 1504-1507,2017. DOI: 10.1109/LAWP.2016.2647228

[47]. LAU. K. L, LUK. K. M, "Novel Wide-Band Circularly Polarized Patch Antenna Based on L-Probe and Aperture-Coupling Techniques," *IEEE transactions on antennas and propagation*, vol. 53, no. 1, p. 577–580,2005. DOI: 10.1109/TAP.2004.838796

[48]. Liu.J. C, Zeng. B. H, Badjie.I, Drammeh.S, Bor. S.S, Hung. T. F, Chang. D.C, " Single-Feed Circularly Polarized Aperture-Coupled Stack Antenna with Dual-Mode Square Loop Radiator," *IEEE antennas and wireless propagation letters*, vol. 9, p. 887–890,2010. DOI: 10.1109/LAWP.2010.2072980

[49]. Chen, Z. N, " Aperture-coupled asymmetrical C-shaped slot microstrip antenna for circular polarization," *IET Microwave and Antennas Propagation*, vol. 3, no. 3, p. 372-378, 2009. DOI: 10.1049/iet-map.2008.0126

[50]. Chang.T. N,Lin.J. M,Chen. Y. G, "A circularly polarized ring-antenna fed by a serially coupled square slot-ring," *IEEE Transactions on antennas and propagation*, 2012, vol. 60, no. 2, p. 1132–1135. DOI: 10.1109/TAP.2011.2173138

[51]. Liao.C. T, Lin.Y. F, Chen. C. H, Kao. S. Y, Chen. H. M. A, "Novel aperture-coupled circularly polarized square-ring patch antenna for wireless communication systems," *IEEE 5th Asia-Pacific Conference on Antennas and Propagation (APCAP)*, p. 57-58,2016. DOI:10.1109/APCAP.2016.7843097

[52]. Lai. H.W, Mak. K. M, Chan. K. F, " Novel aperture-coupled microstrip-line feed for circularly polarized patch antenna," *Progress in Electromagnetics Research*, vol. *144*, p. 1-9,2014. DOI: 10.2528/PIER13101803

[53]. Haraz. O, Ashraf. M. A, Ashraf. N, Alshebili. S. A, "Design and Characterization of Wideband Aperture-Coupled Circularly Polarized Antenna for Gigabits Per Second Wireless Communication System," *Wireless Personal Communications*, vol. 114. no. 1, p. 431-446,2020. DOI: 10.1007/s11277-020-07370-7

[54]. Gupta. A Gangwar. R. K, " Dual-Band circularly polarized aperture coupled rectangular dielectric resonator antenna for wireless applications," *IEEE Access*, vol. 6, p. 11388-11396,2018. DOI: 10.1109/ACCESS.2018.2791417

[55]. Dash.S. K.K, Cheng. Q. S, Khan. T, " A superstrate loaded aperture coupled dual-band circularly polarized dielectric resonator antenna for X-band communications, " *International Journal of Microwave and Wireless Technologies*, p. 1-8,2020. DOI: 10.1017/S1759078720001476

[56]. Wang, M., Wang, D. Y., Wu, W., Fang, D. G., Et Al. Single-Layer, Dual-Port, Dual-Band, and Orthogonal-Circularly Polarized Microstrip Antenna Array with Low Frequency Ratio. *Wireless Communications and Mobile Computing*, 2018, vol. 2018, p.1-10. DOI: 10.1155/2018/5391245

[57]. A. Buffi, R. Caso, M.R. Pino, P. Nepa, and G. Manara, "Single-feed circularly polarized aperture-coupled square ring slot microstrip antenna, "Electronics Letters, vol.46, no.4, 2010.

[58]. Shobhit K. Patela, Christos Argyropoulosa, Yogeshwar P. Kostab, " Broadband compact microstrip patch antenna design loaded by multiple split-ring resonator superstrate and substrate," *Waves in Random and Complex Media journal Taylor and Francis*, vol. 27,p.92-102,2017.

[59]. Chandrashekar K S, Chandramma S, HalappaGajera, Koushik Dutta, "Design of Microstrip Patch Antenna for Dual-band Operation using Metal Ring Superstrate," *Journal of Recent Technology and Engineering*, vol.5, issue 5, pp.4539-4543,2020.

[60]. R. K. Gupta, J. Mukherjee, "Effect of superstrate material on a high-gain antenna using array of parasitic patches," *Microwave and optical technology letters*, vol.52, No.1, pp.82-88,2010.

[61]. Sachin Kumar, B.K. Kanaujia, Mukesh Kumar. Khandelwal,a.k. Gautam, "Single-feed circularly polarized stacked patch antenna with small-frequency ratio for dual-band wireless applications," *Journal of Microwave and Wireless Technologies*, pp .1–6, 2015.

[62]. Sachin Kumar, B.K. Kanaujia, Mukesh Kumar.Khandelwal,a.k. Gautam, "Single-Feed Superstrate Loaded Circularly PolarizedMicrostrip Antenna for Wireless Application," *Wireless Pers Communication*, vol. 92, pp .1333–1346 , 2017.

[63]. PirSaadullah Shah, Shahryar Shafique Qureshi, Muhammad Haneef, Sohail Imran Saeed, "Size Reduction and Performance enhancement of PiShaped Patch Antenna using SuperstrateConfiguration," *Journal of Advanced Computer Science and Applications*, vo.10, No.5, pp.461-465,2019.

[64]. J.-S. Row, "Experimental study of circularly polarised microstrip antennas loaded with superstrate," *Electronicletters*, vol.41, No.21, 2005.

[65]. S.X. Ta and T.K. Nguyen. A.R. bandwidth and gain enhancements of patch antenna using single dielectric superstrate. *Electronic letters*, vol.53, pp.1015–1017, 2017.

[66]. Seyed Mohamad Amin Momeni Hasan Abadi and Nader Behdad, "A broadband, circular-polarization selective surface," inJournal of Applied Physics, June 2016.

[67]. S. Chaimool, K. L. Chung and P. Akkaraekthalin, "Simultaneous gain and bandwidths enhancement of a single-feed circularly polarized microstrip patch antenna using a metamaterial reflective surface," *Progress In Electromagnetics Research B, Vol. 22, 23-37, 2010.*

[68]. MoufidaBouslama, MoubarekTraii, Ali Gharsallah, and Tayeb A. Denidn, "High gain Patch Antenna using a FrequencySelective Surface (FSS)," International journal of communications, vol.8,2014.

[69]. Anurag Singh, Sandip Vijay, and Rudra Narayan Baral, "Low Cross-Polarization Improved-Gain RectangularPatch Antenna," *Electronics,v0l.8,*2019.

[70]. Deepak Gangwar, SushrutDas, R. L. Yadava, Binod Kumar Kanaujia, "Frequency Selective Surface as Superstrate on Wideband Dielectric Resonator Antenna for Circular Polarization and Gain Enhancement," Wireless PersCommun, vol. 97, pg.no:3149–3163, 2017.

[71]. SoumikDey, AnkitaIndu, SantanuMonda, and Partha P. Sarkar, "Diagonally Asymmetric CSRRs Loaded Circularly PolarizedAntenna with Frequency Selective Surface," *Progress In Electromagnetics Research M, Vol. 92, 43–54, 2020.*

[72]. Kalyanmondal, "Bandwidth and gain enhancement of microstrip antenna by frequencyselective surface for WLAN, WiMAX applications," in Sadhana, vol.44,2019.

[73]. PraphatArnmanee and ChuwongPhongcharoenpanich, "Improved Microstrip Antenna with HIS Elements and FSS Superstrate for 2.4GHz Band Applications", International Journal of Antennas and Propagation, 2018.

[74]. Hang Zhou, Shao-bo Qu, Bao-qin Lin, Jie-QiuZhang, ChaoGu, Hua Ma, ZhuoXu, Peng Bai and Wei-dong Peng, "Dual band frequency selective surface based on circular aperture-coupled patches," microwave and optical technology letters/vol. 53, pg. No. 8, August 2011.

[75]. O. Manoochehri, S. Abbasiniazare, A. TorabiandK. Forooraghi, "A Second-Order BPF Using A Miniaturizedelement Frequency Selective Surface," *Progress In Electromagnetics Research C, Vol. 31, pg.no:229-240, 2012.*

[76]. RasoulFakhte and Iman Aryanian, "Compact Fabry-Perot Antenna with Wide 3-dBAxial Ratio Bandwidth based on FSS and AMCStructures", IEEEAntennas and Wireless Propagation Letters,2020.

[77]. Nghia Nguyen-Trong, Huy Hung Tran, Truong Khang Nguyen, and Amin M. Abbosh, "A Compact Wideband Circular PolarizedFabry-Perot Antenna Using ResonanceStructure of Thin Dielectric Slabs," IEEE Acess, vol.6, 2018.

[78]. EsmaMutluer, Bora Döken, and Mesut Kartal, "A Novel Multi-Band Frequency Selective Surface for Ka-BandApplications," Conference ICTRS, Barcelona, Spain,2018.

[79]. Ayan Chatterjee and Susanta Kumar Parui, “Gain Enhancement of a Wide Slot Antenna Using a Second-Order Bandpass Frequency Selective Surface,” Radioengineering, vol. 24, pg.no. 2, June 2015.

[80]. Mudar Al-Joumaylyand Nader Behdad, “A New Technique for Design of Low-Profile,Second-Order, Bandpass FrequencySelective Surfaces,” IEEE transactions on antennas and propagation, vol. 57, pg.no. 2, February 2009.

[81]. Dubost G and Zisler S., "Antennas a Large Bande," Masson, New York, pp. 128–129, 1976.

[82]. Porath. R, “Theory of miniaturized shorting-post microstrip antennas,” *IEEE Transactions on Antennas and Propagation*, vol. 48, no. 1, p. 41-47,2000.DOI: 0018-926X (00) 01276-X.

[83]. Ansari.J. A, Singh. P, Yadav. N. P, Vishvakarma.B. R, “ Analysis of shorting pin loaded half disk patch antenna for wideband operation” *Progress in electromagnetics research*, vol. 6, p. 179-192,2009. DOI: 10.2528/PIERC09011203

[84]. Kumar. P, Singh. G, “Microstrip antennas loaded with shorting post,” *Engineering*, vol. 1, no. 1,p. 1-54,2009.DOI: 10.4236/eng. 2009.11006

[85]. Zhang. X, Zhu. L, “ Patch antennas with loading of a pair of shorting pins toward flexible impedance matching and low cross polarization,” *IEEE Transactions on Antennas and Propagation*, 2016, vol. 64.no. 4, p. 1226-1233. DOI: 10.1109/TAP.2016.2526079

[86]. Maharana Pratap Singh, Rahul Kumar Jaiswal, Kumar Vaibhav Srivastava & Saptarshi Ghosh. A miniaturized triple-band circularly polarized antenna using meander geometry. Journal of Electromagnetic Waves and Applications 2021;1-8.

[87]. Guha. D & Siddiqui. J. Y, “Resonant frequency of microstrip antenna covered with dielectric superstrate,” *IEEE Transactions on Antennas and Propagation*, vol.51, pp. 1649–1652, 2003.

[88]. Wong, K. L. Compact and broadband microstrip antennas, Wiley publishers,2002.

[89]. Krishna. D. D, Gopikrishna. M, Anandan. C. K, Mohanan. P,&Vasudevan. K, “ Compact dualband slot loaded circular microstrip antenna with a superstrate,” *Progress in Electromagnetics Research*, vol.*83*, pp.245–255,2002.

[90]. Lo YT, Lee SW. Antenna Handbook. Vol III Applications. Springer, New York, NY; 1993.

[91]. Krauss JD, Marhefka RJ. Antennas for All Applications. 3rd ed.McGraw-Hill, New York, NY, 2003.

[92]. Selvan KT, Sharma SK,Mishra G, George RR. A simpler reference antenna gain measurement method. Microw Opt Technol Lett. 2018;60:1937–1940.

[93]. Kieran J. Greene, Bruce Maca. Thoma.An Accurate Technique for Measuring the On-Axis Axial Ratio of Circularly Polarized Feed Systems. IEEE transactions on antennas and propagation. 1984; 32:12.

[94]. K. Kandasamy, B. Majumder, J. Mukherjee, and K. P. Ray, "Dual-Band Circularly Polarized Split Ring Resonators Loaded Square Slot Antenna," in *IEEE Transactions on Antennas and Propagation*, vol. 64,

[95]. Stefano, Giuseppe Pelosi, and Stefano Selleri. "A Tri-Band Circularly Polarized Patch Antenna for WiFi Applications in S-and C-band." *2020 IEEE International Symposium on Antennas and Propagation and North American Radio Science Meeting*. IEEE, 2020.

[96]. Kumari K, Jaiswal RK, Srivastava KV. A compact triple band circularly polarized planar antenna for wireless application. Microwave and Optical Technology Letters. 2020 Jul;62(7):2611-7.

[97]. Dhara R, Jana SK, Mitra M. Tri-band circularly polarized monopole antenna for wireless communication application. Radioelectronics and Communications Systems. 2020 Apr;63(4):213-22.

[98]. Dhara R, Mitra M. A triple-band circularly polarized annular ring antenna with asymmetric ground plane for wireless applications. Engineering Reports. 2020 Apr;2 (4):e12150.

[99]. Ben A Munk, " Frequency selective surface theory and design," John wiley and science, inc.,2000.

[100]. ZVEREV, A. I. *Handbook of Filter Synthesis*. New York: Wiley,1967.